NOTE TO USERS

Université d'Ottawa · University of Ottawa

Université d'Ottawa · University of Ottawa

FACULTÉ DES ÉTUDES SUPÉRIEURES ET POSTDOCTORALES

FACULTY OF GRADUATE AND POSTDOCTORAL STUDIES

Zdena HARDER

AUTEUR DE LA THÈSE - AUTHOR OF THESIS

M. Sc. (Biochemistry)

GRADE - DEGREE

Department of Biochemistry, Microbiology and Immunology

FACULTÉ, ÉCOLE, DÉPARTEMENT - FACULTY, SCHOOL, DEPARTMENT

TITRE DE LA THÈSE - TITLE OF THE THESIS

The Mechanism of Mitochondrial Fission : Dynamin-related Protein 1 and its Effectors

H. McBride

DIRECTEUR DE LA THÈSE - THESIS SUPERVISOR

CO-DIRECTEUR DE LA THÈSE - THESIS CO-SUPERVISOR

EXAMINATEURS DE LA THÈSE - THESIS EXAMINERS

J. Bell

B. McKay

J-M. De Koninck, Ph D

LE DOYEN DE LA FACULTÉ DES ÉTUDES SUPÉRIEURES ET POSTDOCTORALES

DEAN OF THE FACULTY OF GRADUATE AND POSTODORAL STUDIES

The Mechanism of Mitochondrial Fission: Dynamin-Related Protein 1 and its Effectors

Zdena Harder

Thesis submitted to the
Faculty of Graduate and Postdoctoral Studies
in partial fulfillment of the requirements for the degree of

Master of Science
in
Biochemistry

Department of Biochemistry, Microbiology and Immunology
Faculty of Medicine
University of Ottawa

April 2004

Your file Votre référence
ISBN: 0-494-01485-7
Our file Notre référence
ISBN: 0-494-01485-7

For Chris and Joshua

Abstract

Mitochondrial fission requires the evolutionarily conserved dynamin related GTPase (DRP1), which is recruited from the cytosol to the mitochondrial outer membrane (1-3) to co-ordinate membrane scission (see (4) for review). Currently, the mechanism of recruitment and assembly of DRP1 on the mitochondria is unclear. Here, using yeast two-hybrid, we identify Ubc9 and SUMO1 as novel DRP1 interacting proteins. We have determined that the interaction between DRP1 and SUMO1 requires SUMO1 conjugation and is nucleotide dependent. Pull-down experiments reveal that DRP1 is an authentic SUMO1 substrate and is likely modified by more than one SUMO1 molecule. Biochemical fractionation indicates that purified mitochondrial fractions contain a NEM-sensitive, SDS-resistant high molecular weight form of DRP1, consistent with the size of SUMOylated DRP1. Importantly, fluorescence microscopy reveals that a significant portion of cytosolic YFP:SUMO1 colocalizes with mitochondria. Video analysis further demonstrates that YFP:SUMO1 is often found at the site of mitochondrial fission and remains tightly associated to the tips of fragmented mitochondria. Surprisingly, immunofluorescence studies show that endogenous DRP1 only partially colocalizes with the many YFP: SUMO1 puncta seen on the mitochondria, suggesting that mitochondria contain other SUMOylated substrates. This is consistent with the presence of numerous unique SUMOylated products in the mitochondrial fraction. Finally, transient transfection of SUMO1 into cultured cells dramatically increases the level of mitochondrial fragmentation and protects DRP1 from protein degradation. Together, these data are the first to identify a function for SUMO1 on the

mitochondria and suggest a novel role for the participation of SUMO1 in mitochondrial fission.

Acknowledgements

I would like to give special thanks to Dr. Heidi McBride for accepting me in her lab at the University of Ottawa Heart Institute and for offering exceptional guidance, support, and encouragement throughout the course of my studies. I would also like to thank her for the continued interest and enthusiasm in the future direction of this project.

I would like to thank Dr. Johnny Ngsee and Dr. Doug Gray for their helpful advice during the development of this work.

I would like to thank Sandhya Gangaraju, Rodolfo Zunino, Liquin Xu and Margaret Neuspiel for their assistance and friendship during my graduate studies.

And finally, I would like to especially thank my wonderful husband Chris for his faith in me and for all his sacrifices (I couldn't have done it without you) and my adorable little munchkin Joshua, for allowing mommy to nurse in front of a computer screen. You both mean everything to me.

Table of Contents

Abstract iii

Acknowledgements v

Abbreviations x

List of figures xiii

List of tables xv

1. Introduction 1

1.1 MITOCHONDRIAL DYNAMICS: AN OVERVIEW. 2

1.2 MITOCHONDRIAL GTPASES: MFN (1 AND 2) AND DRP1 3

1.2.1. Mitofusins and mitochondrial fusion *3*

1.2.2. DRP1 and mitochondrial fission *6*

1.3 DYNAMIN FAMILY OF GTPASES 10

1.3.1. Dynamin 1 and the steps of clathrin-mediated endocytosis *10*

1.3.2. DRP1 and the steps of mitochondrial fission *13*

1.3.3. Domain organization of dynamins. *17*

1.3.4. GTP nucleotide cycle *20*

1.3.5. Recruitment and protein partners *24*

1.4 SUMO AND SUMOYLATION 28

1.4.1 Steps of SUMOylation *28*

1.4.2 Functions of SUMOylation *31*

1.4.3 ULPs and deSUMOylation *34*

Objectives. 36

2. Materials and Methods 37

2.1 CELL CULTURE 38

2.2 PREPARATION OF CONSTRUCTS 39

2.2.1. DRP1 and DRP1 mutants *39*

2.2.2. DRP1 interacting proteins: SUMO1, Ubc9 and TOPORS *40*

2.3 MITOCHONDRIAL FISSION: STEADY STATE VERSUS APOPTOSIS 41

2.3.1. Live cell video fluorescence microscopy *41*

2.3.2. Caspase-3 Activation Assay *42*

2.4 YEAST-TWO HYBRID SCREEN 43

2.4.1. Principle *43*

2.4.2. Yeast transformation of DRP1 bait *44*

2.4.3. Detection of LEXA2:DRP fusion protein expression in yeast *48*

2.4.4. Yeast transformation of HeLa library *49*

2.4.5. Reporter gene expression assays *51*

2.5 SPECIFICITY OF PROTEIN-PROTEIN INTERACTIONS 56

2.5.1. Yeast two-hybrid testing *56*

2.5.2. GST-pull down assays *57*

2.5.3. His6 pull-down assays *61*

2.6 SUBCELLULAR LOCALIZATION OF SUMO1, UBC9 AND TOPORS 62

2.6.1. Cellular fractionation *62*

2.6.2. Live cell video fluorescence microscopy *63*

2.7 FUNCTIONAL ANALYSIS OF SUMOYLATION IN MITOCHONDRIAL FISSION 65

2.7.1. Mitochondrial morphology with SUMO1 overexpression *65*

3. Results 66

3.1 MITOCHONDRIAL FISSION: STEADY STATE VERSUS APOPTOSIS 67

3.1.1. DRP1 recruitment to mitochondria is stimulated during apoptosis *67*

3.1.2. Over-expression of dominant negative DRP1(K38E) inhibits apoptosis *74*

3.2 YEAST TWO-HYBRID SCREEN 75

3.2.1. Identification of DRP1 interacting clones. *75*

3.3 SPECIFICITY OF PROTEIN-PROTEIN INTERACTIONS 87

3.3.1. Yeast two-hybrid testing and fluorescence microscopy *87*

3.3.2. Recombinant GST:DRP1 and GST:DRP1(K38E) pull down endogenous Ubc9 and SUMO1 from cytosol *97*

3.3.3. DRP1 is a SUMO1 substrate. *97*

3.4. SUBCELLULAR LOCALIZATION OF SUMO1 103

3.4.1. Endogenous SUMO1 associates with purified mitochondria *103*

3.4.2. Cytosolic SUMO1 YFP associates with dynamic mitochondria and localizes to the site of mitochondrial fission *106*

3.5 FUNCTIONAL ANALYSIS OF SUMOYLATION IN MITOCHONDRIAL FISSION 114

3.5.1. Overexpression of SUMO1 YFP causes increased mitochondrial fragmentation and protects DRP1 from degradation *114*

4. Discussion 119

4.1 MITOCHONDRIAL FISSION IS STIMULATED DURING APOPTOSIS 120

4.2 UBC9, SUMO1 AND TOPORS INTERACT WITH DRP1 IN A YEAST TWO-HYBRID SYSTEM 123

4.3 DRP1 IS REVERSIBLY MODIFIED BY SUMO1. 129

4.4 SUMO1 IS FOUND AT THE MITOCHONDRIA AND LOCALIZES TO THE SITE OF MITOCHONDRIAL FISSION. 133

4.5 SUMO1 OVER-EXPRESSION STIMULATES MITOCHONDRIAL FISSION AND PROTECTS DRP1 AGAINST DEGRADATION 134

5. Conclusions and Future Directions 137

6. Supplementary Movies 142

7. Reference List 143

Abbreviations

AD = activation domain

ALD1 = arabidopsis dynamin-like protein 1

AP-2 = adaptor protein 2

ATP = adenosine triphohsphate

BD = binding domain

BRD7 = bromodomain protein 7

CCB = clathrin-coated bud

CCV = clathrin-coated vesicle

CFP = cyan fluorescent protein

Cyt c = cytochrome c

DLP1 = dynamin-like protein 1

DMEM = Dulbecco's Modified Eagle Medium

DRP1 = dynamin related protein 1

DTT = dithiothreitol

DVLP = Dnm1p/Vsp like protein

EDTA = ethylene diamine tetra-acetic acid

FCS = fetal calf serum

Fis1p = Fission mutant 1

Fzo1 = Fuzzy Onion 1

GAP = GTPase activating protein

GDP = guanidine nucleotide diphosphate

GED = GTPase effector domain

GEF = GTP exchange factor

GST = glutathione- S transferase

GTP = guanidine nucleotide triphosphate

GTPγS = guanosine-5'-O-(3-thio)triphosphate

HEPES = N-[2-hydroxyethyl]piperazine-N'-[2-ethanesulfonic acid]

hGBP1 = human guanylate binding protein 1

IPTG = isopropyl-beta-D-thiogalactopyranoside

Mdvp1 = Mitochondrial division mutant 1

mtDNA = mitochondrial DNA

Mfn = mitofusin

ND10 = nuclear dots

NDK = nucleotide diphosphate kinase

NEM = N-ethyl maleimide

Oct = ornithine carboxyl transferase

OMP25 = outer membrane protein 25

ONPG = o-nitrophenyl b-D-galactopyranoside

OPA1 = optic atrophy 1

PFA = paraformaldehyde

PBS = phosphate buffered saline

PCR = polymerase chain reaction

PEG = polyethylene glycol

PH = pleckstrin homology

PIC1 = PML interacting clone 1

PI(4,5)P2 = phosphatidyl inositol 4,5 bisphosphate

PKC = protein kinase C

PML = promyelocytic leukaemia

POD= PML oncogenic domains

PRD = proline rich domain

LPAAT = lysophosphatidic acid acyl transferase

RanBP2 = Ran binding protein 2

RanGAP1 = Ran GTPase activating protein 1

SD = standard drop-out

SDS = sodium-dodecyl sulfate

SDS-PAGE = sodium dodecyl sulphate polyacrylamide gel electrophoresis

SENP = sentrin protease

SH3 = Scr homology 3

STS = staurosporine

SUMO = small ubiquitin-like modifier

TNF = tumor necrosis factor

TOM20 = translocase of the outer mitochondrial membrane 20

TOPORS = topoisomerase I-binding RING protein

UBL = ubiquitin like protein

UBC9 = ubiquitin conjugating enzyme 9

ULP = ubiquitin like proteases

X-Gal = 5-bromo-4-chloro-3-indolyl-b-D-galactopyranoside

YFP = yellow fluorescent protein

List of figures

Figure 1. 5
Mitochondrial morphology in mammalian cells is maintained by the antagonistic activity of fusion and fission.

Figure 2. 9
The dynamin family of proteins.

Figure 3. 12
Fission of clathrin-coated vesicles by Dynamin 1 during clathrin-mediated endocytosis in neurons.

Figure 4.....15
The steps of mitochondrial fission.

Figure 5. 19
Domain organization of DRP1 and Dynamin 1.

Figure 6A and B.....22
Domain arrangement of Dynamin 1 (ΔPRD) dimer and reconstruction of Dynamin 1 (ΔPRD) in the constricted state.

Figure 7. 30
The steps of SUMO1 conjugation.

Figure 8. 46
The principle of the yeast two-hybrid system.

Figure 9. 69
Mitochondrial fission occurs under steady state conditions in Cos7 cells.

Figure 10A and B.....71
Overexpressed DRP1 CFP is mainly cytosolic and does not alter mitochondrial morphology, while overexpressed DRP(K38E) forms large intracellular aggregates and is dominant interfering resulting in interconnected mitochondria.

Figure 11A and B.....73
Staurosporine induced apoptosis of Cos7 cells stimulates DRP1 recruitment and causes increased mitochondrial fragmentation.

Figure 12. 77
Overexpression of DRP (K38E) inhibits apoptosis.

Figure 13. 79
LEXA:DRP1 protein is highly expressed in L40 yeast.

Figure 14. 82
Relative β-Galactosidase activity of the 51 positive yeast two-hybrid clones.

Figure 15. 86
Comparison of the relative strength of select DRP1 protein-protein interactions from the yeast two-hybrid screen.

Figure 16A and B......90
SUMO1 conjugation is required for DRP1 interaction.

Figure 17A-D. 92
Specificity of DRP1 interactions.

Figure 18. 99
Recombinant GST:DRP1 and GST:DRP1 K38E pull-down endogenous Ubc9 and SUMO1 from cytosol.

Figure 19A and B......101
DRP1 is SUMO1 modified.

Figure 20. 105
Endogenous SUMO1 and an NEM-sensitive high molecular weight species of DRP1 are found on purified mitochondria.

Figure 21. 108
A fraction of SUMO1 YFP is found in the cytosol and often localizes to mitochondria.

Figure 22. 111
SUMO1 YFP localizes to the site of mitochondrial fission.

Figure 23A and B......113
Endogenous DRP1 partially colocalizes with mitochondrial YFP SUMO1.

Figure 24A-C......116
Overexpression of SUMO causes increased mitochondrial fragmentation and protects DRP1 from degradation.

List of tables

Table 1A-C.....53
Summary of constructs and cloning strategies.

Table 2. 84
Results of the yeast two-hybrid screen.

1. Introduction

1.1 Mitochondrial dynamics: An overview.

Mitochondria have long been perceived as immobile oval-shaped organelles dispersed in the cytosol, dutifully performing critical functions such as oxidative phosphorylation (5), steroidogenesis (6), amino acid synthesis (7) and regulation of apoptosis (8). Only recently, have our perceptions of the static mitochondria evolved. We now understand that mitochondria are rather dynamic, often reticular structures. This has sparked the emergence of a new field of study of mitochondrial dynamics; the primary interest of which is to dissect the molecular and genetic aspects governing the ability of mitochondria to move laterally within the cytoplasm, branch out, stretch, contract, fuse and divide. Initial work in this field focused on mitochondrial motility and provided insight into the means of mitochondrial travel along microtubules. This led to the discovery of the mitochondrial kinesins (9;10) and dyneins (11), the first proteins identified to be involved in mitochondrial dynamics. Subsequent mutagenesis and genetic studies performed in the yeast *Saccharomyces cerevisiae* by a number of different research groups were aimed at identifying key players responsible for defects in mitochondrial segregation into yeast buds, and for deficiencies in mtDNA segregation in dividing mitochondria. These works contributed many novel proteins to the growing list of molecules critical for the maintenance of mitochondrial morphology. Of the molecules identified, some were indirectly involved in mitochondrial dynamics through maintenance of cellular and cytoskeletal integrity (12;13). Others directly participated in modification of mitochondrial shape, such as the Dynamin 1 related mitochondrial GTPases (Dnm1p), critical for mitochondrial fission, and Fuzzy Onion 1 (Fzo1p) essential for mitochondrial fusion.

1.2 Mitochondrial GTPases: Mfn (1 and 2) and DRP1

Mitochondrial fusion and fission, mediated by Mfn (1 and 2) and DRP1 respectively, have been shown to function in an antagonistic fashion to regulate the steady state morphology of the mitochondria (**Figure 1 and supplementary movie 1**). Changes in the rates of fission or fusion lead to the dramatic alteration of mitochondrial morphology, distribution, and segregation into daughter cells during cell division.

1.2.1. Mitofusins and mitochondrial fusion

The outer mitochondrial membrane GTPase, Mitofusin, was originally identified as a protein involved in mitochondrial fusion in sterile *Drosophila melanogaster* males (14). Electron microscopy sections of the sperm tails of the flies lacking Fzo1 (Fuzzy Onion 1, mitofusin homologue in *D. Melanogaster*) revealed that the mitochondria were clustered together and could not fuse, giving rise to the appearance of onion layers and resulting in immobile sperm (15). A role for Fzo1 in mitochondrial fusion was further confirmed in *Saccharomyces cerevisiae* where budding yeast lacking Fzo1p had fragmented mitochondria and could not effectively segregate the mitochondrial DNA (mtDNA) (14). In mammalian systems, two isoforms of Fzo exist, termed mitofusin 1 (Mfn1) and mitofusin 2 (Mfn2) (16). Even though they are approximately 60% identical, the gene duplication of Mfn appears somewhat redundant since overexpression of Mfn1 in cultured embryonic cells of Mfn2 knockout mice partially rescues the fragmented mitochondrial phenotype (or vice versa)(17). Topologically, Mfn1 and Mfn2 span the mitochondrial outer membrane twice exposing both the N- (GTPase) and C- (coiled-coil) termini to the cytosol and trapping specific residues in

Figure 1. Mitochondrial morphology in mammalian cells is maintained by the antagonistic activity of fusion and fission. Mitochondria under steady state conditions appear as tubular organelles, a morphology that is maintained by the delicate balance between mitochondrial fission and fusion (center panel). However, when the rate of mitochondrial fission surpasses the rate of mitochondrial fusion, a fragmented phenotype is produced (right panel). Conversely, when the rate of mitochondrial fusion surpasses the rate of mitochondrial fission, an interconnected mitochondrial phenotype is produced. (left panel).

Figure 1.

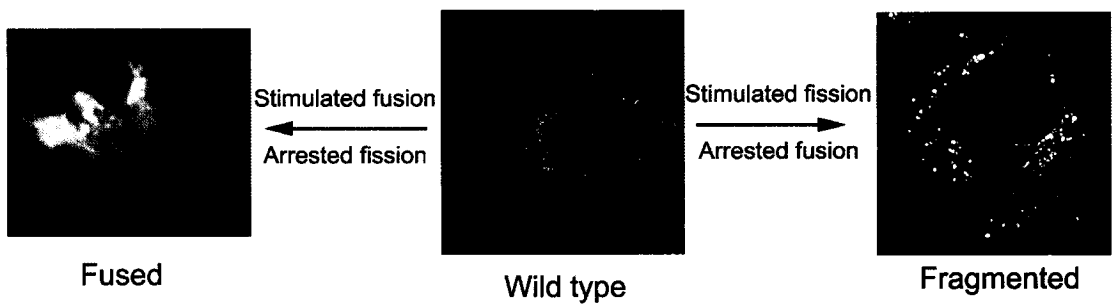
Stimulated fusion
Arrested fission
Stimulated fission
Arrested fusion
Fused
Wild type
Fragmented

the intermembrane space that are believed to be important in the creation of contact sites between the inner and outer membranes (18). The manner in which Mfn1 and Mfn2 mediate mitochondrial fusion is unknown. They may either behave as fusogens that directly merge the two sets of fusing mitochondrial bilayers or they may better resemble regulatory GTPases recruiting cytosolic effectors.

1.2.2. DRP1 and mitochondrial fission

The Dnm1p GTPase was first identified in 1995 in the yeast *Saccharomyces Cerevisiae* as the protein encoded by the dynamin related gene (DNM1)(19). This 85 kDa protein was shown to be involved in endosomal trafficking from the late Golgi compartment to vacuoles (19). It was later clarified by Ostuga et al. that Dnm1p actually controls mitochondrial morphology and distribution in yeast (20). They showed that disruption of the DNM1 gene resulted in mitochondria collapse into a perinuclear region while other organelles remained undisturbed. Dnm1p distribution was punctate along the mitochondrial network and cofractionated with mitochondrial membranes (20). Furthermore, interference with the GTPase domain resulted in an interconnected dominant negative mitochondrial phenotype (20). Shortly thereafter, the human homologue of yeast Dnm1p, DRP1 (Dynamin-Related Protein 1)(21) was cloned. Other groups also cloned mammalian DRP1 as Dnm1p/Vsp Like Protein (DVLP) (1), as Dymple (22) or as Dynamin-Like Protein 1(DLP1)(23). Similar to the results found in yeast, a mutation in the DRP1 GTPase domain caused retraction of the mitochondrial tubules into large perinuclear aggregates without affecting other pathways or organelles (1). Collectively, these early studies concluded that DRP1 is responsible for overall

mitochondrial distribution throughout the cell. It was not until 1999 that a direct function of DRP1 in mitochondrial fission was established. Yeast studies by Janet Shaw and colleagues (3) showed that Dnm1p mutations resulted in a network of interconnected mitochondrial tubules and prevented the mitochondrial fragmentation observed in Fzo1p mutant yeast strains. They found that Dnm1p localized along the outer mitochondrial membrane at the site of constriction of dividing tubules and at the tips of recently divided mitochondria. Similar observations were made with human DRP1 in mammalian cells in 2001 (1). Both these studies indicated, not only that DRP1 regulates mitochondrial fission, but also that DRP1 and Mfn (1 and 2) acted antagonistically to maintain proper mitochondrial morphology (**Figure 1**, right panel synonymous with mitochondrial phenotype seen in ΔFzo1p yeast, and left panel synonymous with mitochondrial phenotype seen in ΔDnm1p yeast). Corroborative work by RE Jensen highlighted the role of Dnm1p in mitochondrial fission and detailed the delicate balance of fission and fusion (24). The Dnm1p and Fzo1p double knockout mutants that he created had normal mitochondrial morphology. However, the balance was once again shifted towards mitochondrial fragmentation upon restoration of Dnm1p function in these yeast cells.

To date, it is clear that mitochondrial fission is essential for the maintenance of mitochondrial morphology and function. For example, fragmented mitochondria in yeast lacking Fzo1p eventually lose mtDNA and become respiratory incompetent (14). The focus of this thesis is to identify the molecular signals that regulate mammalian DRP1, and explore the functional consequences of steady state mitochondrial dynamics. To do this, it is helpful to compare DRP1 with the broader family of Dynamin GTPases. This

Figure 2. The dynamin family of proteins. Dynamins function in various regions of yeast, mammalian and plant cells to mediate membrane scission events. Dynamins 1,2 and 3 regulate the formation of clathrin-coated vesicles (CCVs) and participates in budding from the Golgi and the recycling endosome. DRP1 causes severance of the mitochondrial outer membrane, while OPA1 participates in mitochondrial inner membrane remodeling. Human Guanylate binding protein 1(hGBP1) and the Mx proteins have unique antiviral activity yet do not appear to participate in membrane scission. In plants, ADL1 and ADL2 are involved in membrane scission of chloroplasts and phragmoplastin participates in division of the cell wall. Figure adapted from (25).

Figure 2.

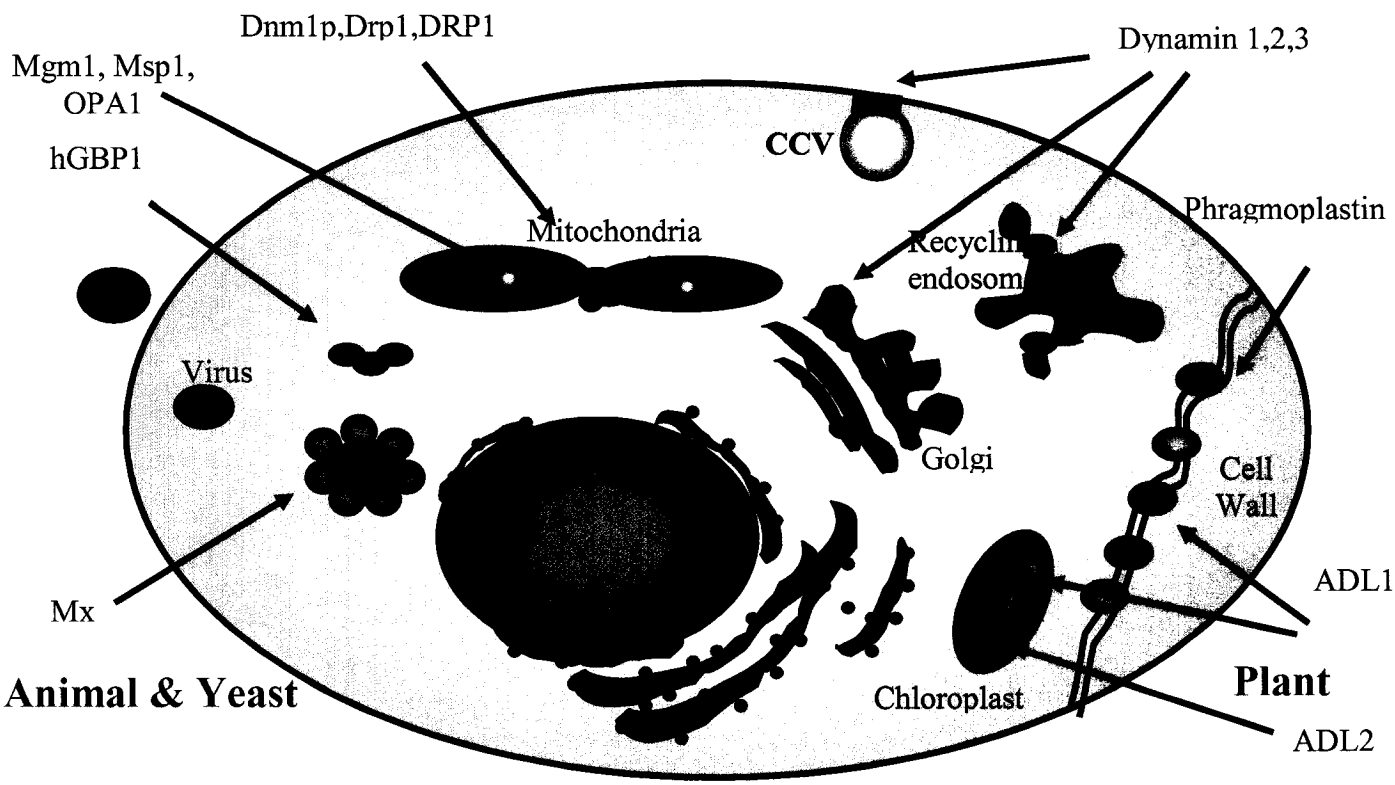
Dnm1p,Drp1,DRP1
Mgm1, Msp1,
OPA1
hGBP1
Dynamin 1,2,3
CCV
Phragmoplastin
Mitochondria
Recyclin
endosom
Virus
Golgi
Cell
Wall
ADL1
Mx
Animal & Yeast
Chloroplast
Plant
ADL2

may provide insights that will further our understanding of the mechanism of DRP1 recruitment to and activity at the mitochondria.

1.3 Dynamin family of GTPases

Membrane scission is critical for a number of cellular processes including clathrin-mediated endocytosis, budding of vesicles from the Golgi apparatus, and mitochondrial fission (see review (26)). Members of the Dynamin family of GTPases mediate these events. **Figure 2** is a schematic illustrating the various members of the dynamin family and their sites of action. David Suzuki pioneered the work on this family of proteins by discovering Dynamin 1(27). His studies of the *Drosophila melanogaster* temperature sentsitive mutant Dynamin1 homologue, *shibire*^{ts}, revealed impairment of clathrin-mediated endocytosis in neurons. The phenotype was characterized by elongated clathrin- coated invaginations of the plasma membrane unable to sever into clathrin-coated vesicles (CCVs). These observations prompted the functional characterization of this protein as the principal regulator of membrane division in the formation of CCVs. Since then, additional family members involved in numerous membrane division events throughout the cell have been identified (reviewed in (25)).

1.3.1. Dynamin 1 and the steps of clathrin-mediated endocytosis

The steps of Dynamin I dependent endocytosis serve as a template for membrane division events by all dynamins. Studies of Dynamin I in neuronal synapses have led to the following general model of dynamin-mediated membrane scission (also see review (28)). As illustrated in **Figure 3**, Dynamin I likely initially exists as a GDP bound, phosphorylated (29) tetramer (30;31) in cytosol. Upon membrane depolarization,

Figure 3. Fission of clathrin coated vesicles by Dynamin 1 during clathrin-mediated endocytosis in neurons. A diagram illustrating clathrin-coated vesicle formation by scission of clathrin -coated buds from the plasma membrane by Dynamin 1. Dynamin 1 exists as a phosphorylated GDP-bound tetramer in cytosol. Upon membrane depolarization in neurons, the membrane potential sensitive protein calcineurin dephosphorylates Dynamin 1, resulting in its recruitment to the clathrin cage of the forming bud. Encouraged by a local increase in GTP concentration and with the likely assistance of GTP exchange factors (GEFs), nucleotide exchange occurs on Dynamin 1. Dynamin 1 oligomerizes around the neck of the forming bud. Subsequent GTP hydrolysis is believed to provide the force necessary to generate a conformational change in the Dynamin 1 oligomer that results in scission of the clathrin-coated vesicle from the plasma membrane. The Dynamin 1 oligomer then disassembles and the GDP-bound form re-tetramerizes and is re-phosphorylated in cytosol by protein kinase C (PKC) or Cdk5/p35. The clathrin cage is uncoated and the vesicle enters the cell.

Figure 3.

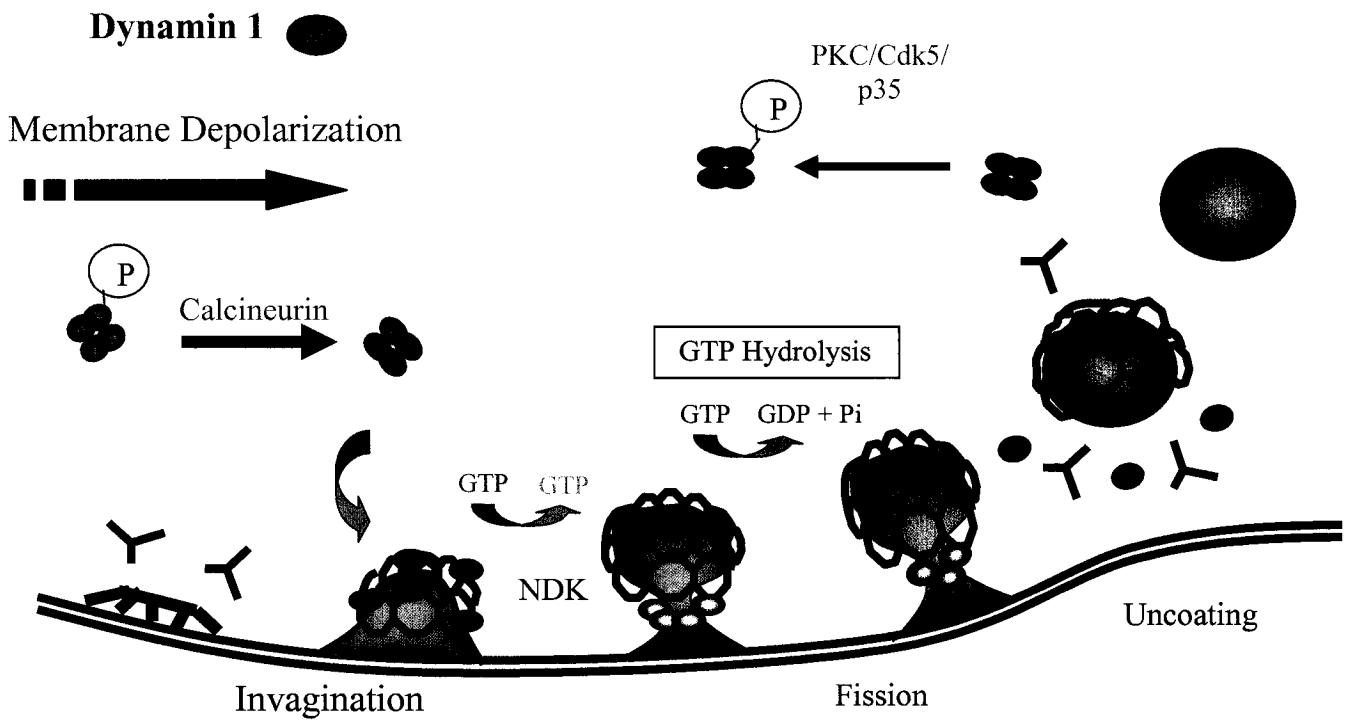
Dynamin 1
Membrane Depolarization
PKC/Cdk5/
p35
P
P
Calcineurin
GTP Hydrolysis
GTP GDP + Pi
GTP GTP
NDK
Uncoating
Invagination
Fission

dynamin I is dephosphorylated (32) by the calcium-sensitive phosphatase calcineurin (33;34). The tetramer is subsequently disassembled and Dynamin 1monomers are recruited to the plasma membrane at the site of clathrin-coated bud (CCB) formations (32). The nucleotide state of Dynamin 1 changes from GDP to GTP, a process facilitated by the excess of GTP over GDP in the cytosol. In addition, there is a GDP kinase specifically localized to the neck of the budding CCV that is thought to help facilitate GTP exchange on Dynamin 1 (35). Dynamin 1 oligomerization occurs around the neck of the budding vesicle (36), a process that does not appear to require nucleotide exchange but does require the proline rich domain (PRD) (28). Subsequent GTP hydrolysis and a conformational change in the Dynamin 1 oligomer (37;38) drives severing of the membrane, thereby releasing the CCV. Dynamin 1 oligomers are disassembled and the monomers are re-phosphorylated by protein kinase C and/or Cdk5/p35 (39). The original tetramer is reformed for a new cycle of membrane division. This entire procedure requires the participation of a number of accessory proteins. These include Dynamin 1 binding partners associated with the clathrin cage that are involved in the recruitment and specific localization of Dynamin 1, as well as proteins involved in GTP exchange. These accessory proteins and their regions of interaction with Dynamin 1 are discussed in further detail below.

1.3.2. DRP1 and the steps of mitochondrial fission

To date, the mechanism of DRP1 function in fission is still not fully understood. However, due to the domain conservation between DRP1 and Dynamin 1, the mechanism of DRP1 function at the mitochondria is likely to be analogous to Dynamin 1 function in

Figure 4. The steps of mitochondrial fission. A schematic illustrating four general steps in the process of division of a single mitochondrion. In step 1, a definite point of fission on the mitochondrion in identified by, as of yet, unknown means. Specific signaling mechanisms and/or cellular triggers likely initiate this process. This may also include reorganization of specific outer mitochondrial membrane proteins. Step 2 is defined by changes in membrane curvature (positive to negative membrane curvature) leading to constriction of the mitochondrion. Multiple factors/effectors such as lipid modifying protein, structural proteins, and critical players like DRP1, are likely recruited to the mitochondrion at this point to form functional fission complexes. Step 3 is characterized by actual scission of membranes, beginning with the inner mitochondrial membrane and causing substantial remodeling of the cristae. Finally, the outer membrane resulting in complete separation of one mitochondrion into two independent mitochondria.

Figure 4.

1. **Identification of point of fission**

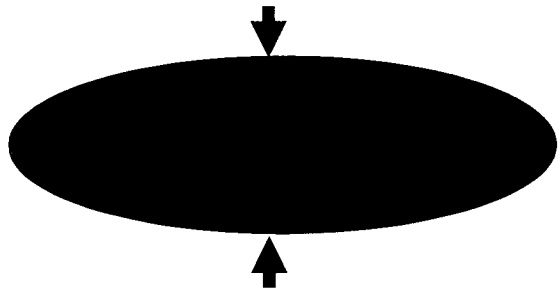

2. **Formation of negative membrane curvature**

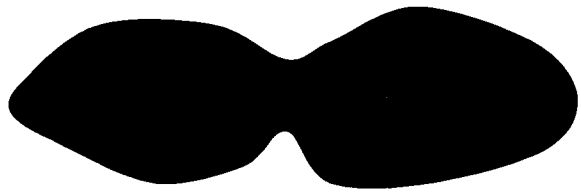

3. **Fission of *inner* mitochondrial membrane**

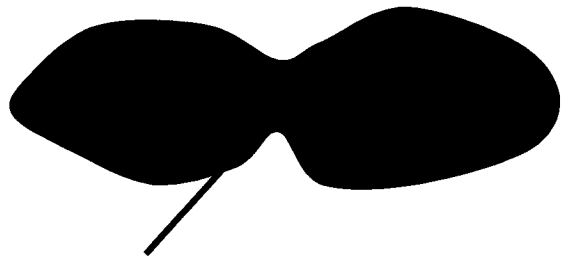

4. **Fission of *outer* mitochondrial membrane**

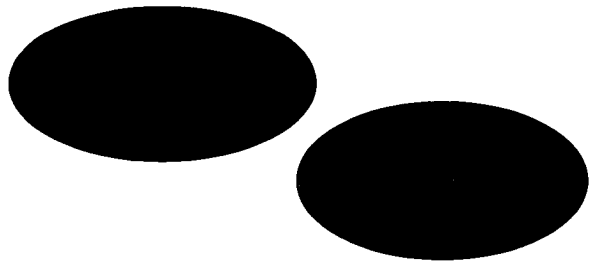

the formation of CCVs. As shown in **Figure 4**, the process of fission is complex. During a fission event, a single mitochondrion severs two sets of bilayers and then the four sets of bilayers must rejoin. Initially, a point of fission must be identified by a signal from within the mitochondria or from the extra-mitochondrial surroundings. DRP1, which is also known to form tetramers at low salt concentration (40), is likely found as a tetramer in cytosol. The phosphorylation state of DRP1 is unknown. However, algorithms (NetPhos2.0) suggest that there is a high probability of phosphorylation at numerous sites on the protein. A site of fission is then designated by specific protein factors and DRP1 is recruited to the outer mitochondrial membrane at that site. Many questions regarding the factors determining the recruitment of DRP1 to the mitochondria remain unanswered. In yeast studies, a few potential Dnm1p partners have been identified. However, their role in the fission process and Dnm1p recruitment are still unclear. These proteins are discussed in further detail below. At the mitochondria, DRP1 most likely self-assembles to form an oligomer around the outer membrane periphery. In vitro studies by Yoon et al. (41) have shown that recombinant DRP1 forms large sedimentable structures in the presence of the non-hydrolyzable GTP analogue guanosine-5'-O-(3-thio)triphosphate (GTPγS), which resemble stacks of helical rings by electron microscopy. Furthermore, recombinant DRP1 tubulates synthetic liposomes (41), an observation that was enhanced in the presence of GTPγS, suggesting that the GTP-bound form of DRP1 is preferentially oligomerized and membrane associated. Presumably, GTP hydrolysis and a change in the conformation of DRP1 would then force scission of the mitochondrial outer membrane. Importantly, since mitochondrial division requires scission of the two mitochondrial bilayers, communication between the inner and outer bilayers is

imperative. Studies in *Caenorhabditis Elegans* highlighted the independence of the inner and outer mitochondrial membrane fission machineries (2). When fission of the outer membrane was blocked by expressing the dominant interfering DRP1(K38E), the inner membrane still fragmented. Two important conclusions arose from this study. First, this work demonstrated that DRP1 mediates fission solely of the outer bilayer and, second, it implied the need for regulated interaction between the fission machineries of both bilayers for successful, complete mitochondrial division. In the final steps of fission, motility factors must laterally separate the two distinct mitochondrial entities. DRP1 would then disassemble and return to the cytosol.

1.3.3. Domain organization of dynamins.

Given that DRP1 and Dynamin 1 must both be recruited to the membrane, form oligomeric structures, bind and hydrolyze GTP and co-ordinate effector proteins (see below), it is not surprising that the amino acid sequence of the dynamins contain specific functional domains. The domain organization of Dynamin 1 (30) and DRP1 (42) are shown in **Figure 5**. Even though the overall sequence homology between Dynamin 1 and DRP1 is only 35%, they share a very similar domain organization. The GTPase domain, consisting of approximately the first 300 residues at the N-terminal region, is highly conserved in all dynamins and is characterized by four GTP binding elements G1-G4. The G1 motif (GxxxxGKS/T), also termed the P-loop binds the nucleotide phosphates (43). G2 (switch I region) consists of a conserved threonine and coordinates a Mg^{2+} ion when dynamin is GTP bound (43). This region undergoes significant

Figure 5. Domain organization of DRP1 and Dynamin 1. A schematic comparison of the domains of DRP1 and Dynamin 1, highlighting the functionally conserved domains and those that differ. DRP1 and Dynamin 1 both contain the highly conserved GTPase domain that contains four critical GTP binding elements (43) and mediates basal GTP hydrolysis. During protein oligomerization, the GTPase domain intermolecularly binds the GED domain, thereby substantially stimulating GTPase activity. The conserved middle domain also binds the GED domain during self-assembly. The middle domain is followed by the unique "insert B domain" in DRP1 and the pleckstrin homology (PH) domain in Dynamin 1. The function of the Insert B domain is currently unknown. However, the PH domain in the analogous position in Dynamin 1 is critical for the protein's recruitment to the plasma membrane. This domain specifically binds $PI_{4,5}P_2$ that is formed on the surface membrane of CCBs during invagination and, thereby, targets Dynamin 1 from the cytosol to the plasma membrane. The conserved GTPase Effector Domain (GED) is responsible for stimulated GTPase function by acting as a GTPase activating protein (GAP) during protein self-assembly. Dynamin 1 has an additional proline-rich domain (PRD) responsible for binding the Src homology-3 (SH3) domain of accessory proteins that participate in either regulation or execution of membrane scission. Notably, DRP1 lacks this domain.

Figure 5.

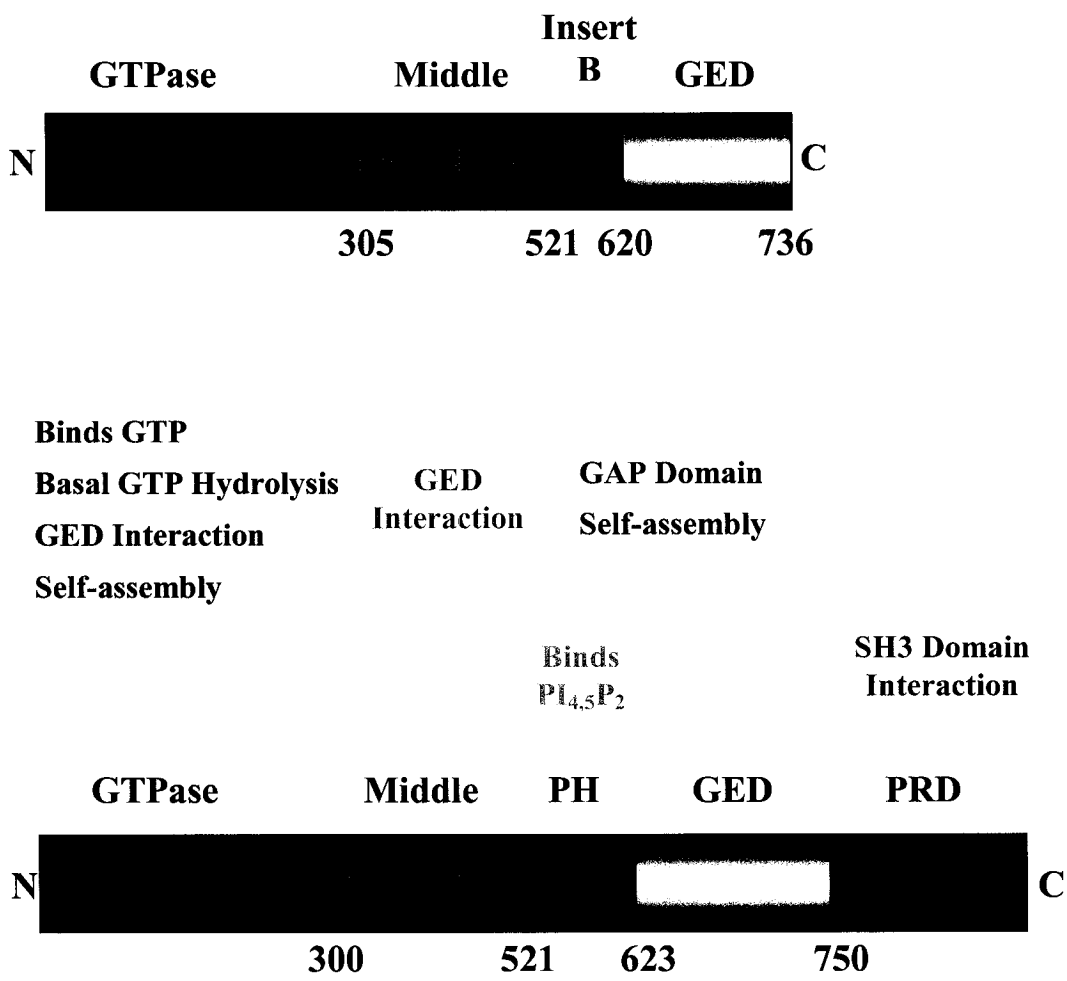
DRP1
Insert
B
GTPase
Middle
GED
N
C
305
521
620
736
Binds GTP
Basal GTP Hydrolysis
GED Interaction
Self-assembly
GED
Interaction
GAP Domain
Self-assembly
Binds
$PI_{4,5}P_2$
SH3 Domain
Interaction
GTPase
Middle
PH
GED
PRD
N
C
300
521
623
750
Dynamin 1

rearrangement (switch) when the nucleotide state of dynamin changes from GTP to GDP (43). The G3 (DxxG) motif also coordinates Mg^{2+} by "bridging [a] water molecule and a glycine whose amide nitrogen forms a hydrogen bond to the nucleotide[s] γ-phosphate"(43). Finally, the G4 (N/TKxD) motif associates with the nucleotide base (43). In addition to GTP binding, the GTPase domain is responsible for GTP hydrolysis and for Dynamin 1 self-assembly. These two aspects of the GTPase domain are described in detail below. The middle region of Dynamin 1, residues 300-521, also participates in self-assembly and the pleckstrin homology (PH) domain consisting of residues 522-623, has a critical role in Dynamin 1 recruitment to the plasma membrane through phosphatidyl inositol 4,5-bisphosphate ($PI_{4,5}P_2$) binding (44) (45)which leads to a subsequent activation of GTP hydrolysis (1000-fold) (37). A unique Insert B region of unknown function in DRP1 replaces these regions. The GTPase Effector Domain (GED), acting like an internal GTPase Activating Protein (GAP), stimulates the GTPase activity of Dynamin 1(46) and DRP1, and also partakes in self-assembly in Dynamin 1(47). Finally, the proline-rich domain (PRD), residues 751-864, interacts with the Src-homology 3 (SH3) domain of Dynamin 1 binding partners (28) and is critical for dynamin self-assembly (28). DRP1 lacks this final region suggesting that DRP1 binding partners interact through a different domain or by different means.

1.3.4. GTP nucleotide cycle

Dynamins possess an intrinsic GTP hydrolysis (48) capability as a function of their GTPase domains. However, if a GTPase Activating Protein (GAP) activates the GTPase, this hydrolysis rate can be substantially increased 10-fold (46). Dynamins supports their own GAP activity via their GTPase Effector Domains (GEDs).

Figure 6. Domain arrangement of Dynamin 1 (ΔPRD) dimer and reconstruction of Dynamin 1 (ΔPRD) in the constricted state. A. Domain arrangement of ΔPRD Dynamin 1 with proposed locations for the GTPase domain, middle domain, GED and PH domain. The blue contour lines indicate a central section through the T of the three dimensional map. The solid and dashed lines illustrate possible connections within and between two ΔPRD dynamin in the dimmer. **B. a,b)** Surface rendering of the constricted ΔPRD Dynamin 1 three-dimensional map viewed (a) perpendicular to the tube axis (b) and at a 45° angle. Three prominent domains (head, stalk, and leg) are coloured green, blue and gold, respectively; the inner lipid leaflet is coloured gray. Figures and legend taken directly from (49).

Figure 6.

A

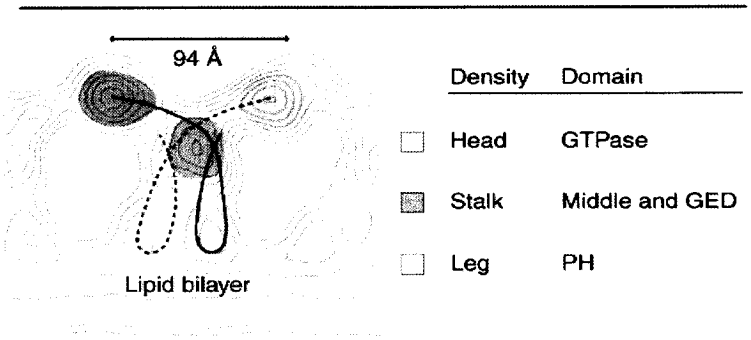
94 Å
Lipid bilayer
Density
Domain
Head
GTPase
Stalk
Middle and GED
Leg
PH

B

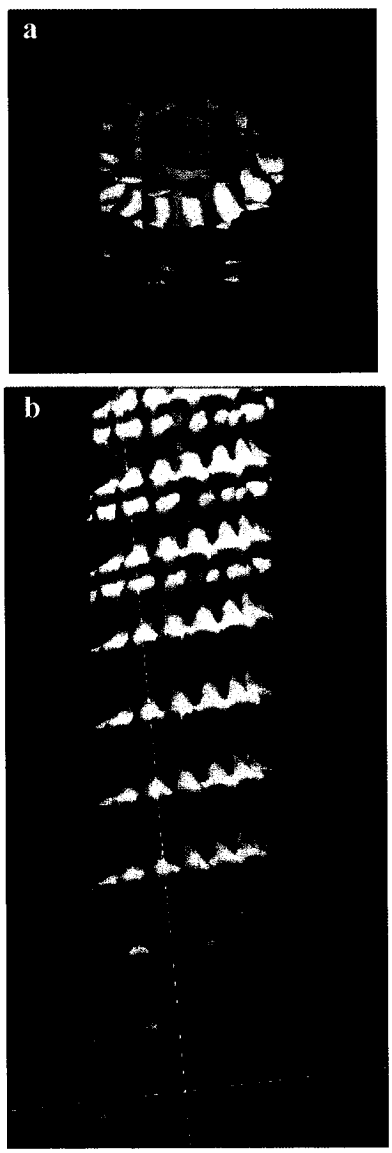
a
b

Oligomerization of dynamins enables the GTPase and GED domains of two individual dynamin proteins to come into close proximity and facilitate intermolecular interactions triggering a high rate of GTP hydrolysis (46;50). **Figure 6** illustrates a three-dimensional reconstruction of constricted Dynamin 1 (ΔPRD), its suspected orientation in the bilayer and highlights the regions of intermolecular interactions. DRP1 self-assembly might resemble that of Dynamin 1. It has been considered that GTP hydrolysis is required for membrane scission. However, the precise contribution of the hydrolysis event is still unknown. GTP hydrolysis can serve two purposes. First, it can act as a regulatory switch mediating protein-protein interactions. Or, it can serve as a force-generating event. Currently, two opposing theories exist regarding the role of GTP hydrolysis in dynamin function (see reviews (51;52)). Original studies of Dynamin 1 in nerve terminals by Pietro De Camilli in 1995 suggested that GTP hydrolysis is required for severance of the plasma membrane in the formation of synaptic vesicles. In his studies of synaptic vesicle recycling, he treated neurons with the non-hydrolyzable form of GTP, GTPγS (36). Electron microscopy studies revealed long tubular invaginations of the plasmalemma decorated with electron dense striations reminiscent of Dynamin 1 oligomers. As suspected, these striations were immunoreactive for Dynamin 1. The conclusion drawn from these studies was that GTP hydrolysis is critical for membrane fission and that Dynamin 1 functions as a mechanoenzyme. Similar elongated necks extending from the plasma membrane were observed in HeLa cells transfected with a GTPase deficient Dynamin1 (K44A) mutant (49). Conversely, research performed by Sandra Schmidt indicated that when the activated GTPase activity of Dynamin 1 was inhibited by mutation of critical residues in the GED domain (53), the rate of Dynamin-mediated

endocytosis of transferrin increased. These studies suggested that GTP hydrolysis is not required for membrane fission and, instead, suggested that Dynamin 1 behaves like a regulatory GTPase (54).

To date, this controversy has not yet been resolved. However, if Dynamin 1 is a regulatory GTPase, it is of a different class than the well-known Ras regulatory GTPase. The rate of GDP dissociation rates for Dynamin 1 (92 +/- 12 s^{-1}) (49) is relatively low in comparison to 3 x 10^5 s^{-1} for Ras . In addition, Dynamin 1 also has a much lower affinity for nucleotide at 7 x 10^5 M^{-1} s^{-1} (Ras = 1.4 x 10^8 M^{-1} s^{-1}). Dynamin 1 has a much higher rate of GTP hydrolysis at 8-30 x 10^{-3} s^{-1} (Ras = 3.4 x 10^{-4} s^{-1}) implying that its mechanism is unique from other regulatory GTPases, and possibly supports the idea that Dynamin 1 is a mechanoenzyme. The GTP affinity and GDP dissociation rates remain undetermined for DRP1. However, the GTP hydrolysis rate is also quite high at 80 x 10^{-3} s^{-1} further suggesting that it functions similar to Dynamin 1.

1.3.5. Recruitment and protein partners

Dynamin 1 and DRP1 are cytosolic proteins that cycle on and off the membrane. The recruitment of these proteins to their respective membranes is an important regulatory step. One major Dynamin 1 binding protein likely to be involved in its recruitment to the plasma membrane is amphiphysin 1. Originally found as a synaptic vesicle associated protein (55), subsequent studies showed that amphyphysin 1 interacts (56-58) and hetero-oligimerizes *in vitro* with Dynamin 1 through its SH3 domain. Further *in vitro* binding studies revealed that amphiphysin 1 simultaneously binds Dynamin 1 and α-adaptin, of the adaptor protein-2 (AP-2) complex found in clathrin-coated pits (58), implying a role for amphiphysin 1 in Dynamin 1 recruitment to the CCB. Since then, this

protein has proven to be a significant contributor in the regulation of clathrin-mediated endocytosis. Competitive inhibition of SH3 interactions with Dynamin 1 lead to a complete block in clathrin-mediated endocytosis (58;59). Furthermore, the function of both proteins is regulated by phosphorylation. Phosphorylation of each protein reduced their copolymerization into a ring formation and inhibited their overall interaction with each other (39). However, calcium entry into nerve cells upon membrane depolarization triggers their dephosphorylation by calcineurin and restores their copolymerization (60). Cdk5-dependent phosphorylation of amphiphysin 1 also inhibits its association with β-adaptin, thereby regulating Dynamin 1 recruitment to the plasma membrane (39). Dynamin 1 recruitment to the plasma membrane also partially depends on the formation of $PI_{(4,5)}P_2$ along the surface of the endocytic bud (61;62). The phosphoinositide 5'-phosphatase synaptojanin 1 (63) (substrate $PI_{(3,4,5,)}P_3$), is believed to be a lipid modifying enzyme involved in the creation of $PI_{(3,4)}P_2$ along the plasma membrane through the catabolism of polyphosphoinositides. Many studies have shown that failure to create these specific lipid domains results in inhibition of membrane fission and endocytosis (for example (64)). The interaction between Dynamin 1 and $PI_{(4,5)}P_2$ on the plasma membrane is then facilitated through its PH domain. Synaptojanin 1 has also been shown to interact with the PRD of amphiphysin 1 (65;66), which regulates its recruitment to the plasma membrane. Studies have shown that proper recruitment and stabilization of synaptojanin 1 is also regulated by another lipid modifying enzyme, endophilin (67;68). Recent work has demonstrated that phosphorylation of synaptojanin 1 by Cdk5 inhibits its association with endophilin (69) and, consequently, controls the turnover of

phosphoinositides on the membrane. Endophilin itself has also proven to be critical in the formation of CCVs. It possesses lysophosphatidic acid acyl transferase (LPAAT) activity that enables it to catalyze the formation of phosphatidic acid through the transfer of arachidonate to lysophosphatidic acid (70). Essentially, endophilin induces negative membrane curvature at the neck of the budding vesicle by converting an inverted-cone-shaped lipid into a cone-shaped lipid in the cytoplasmic leaflet of the bilayers (70). This change in membrane curvature promotes Dynamin 1 mediated constriction of the neck of the budding vesicle. This constriction occurs through the oligomerization of Dynamin 1 at the neck of the CCB. As mentioned earlier, subsequent GTP loading is encouraged by a local increase in GTP concentration. Recently, a nucleoside diphosphate kinase (NDK) has been shown to regulate Dynamin 1 dependent synaptic vesicle internalization. NDK generates nucleoside triphosphates from respective diphosphates and is believed to supply Dynamin 1 with a high local concentration of GTP (35).

In the case of DRP1, there has not been any direct evidence so far indicating that a change in lipid composition of the mitochondrial outer membrane is essential for DRP1 recruitment. However, a mitochondrial synaptojanin, synaptojanin 2A, has been shown to be important in determining mitochondrial distribution (71). Synaptojanin 2A binds a mitochondrial outer membrane protein 25, OMP25. Overexpression of OMP25 results in perinuclear clustering of mitochondria, a phenotype also observed by forced expression of synaptojanin 2A on the mitochondrial outer membrane. However, if the inositol 5'-phosphatase domain of synaptojanin 2A is removed, mitochondrial clustering is not seen. These findings suggest that modification of inositol phospholipids on the mitochondrial outer membrane may play a role in maintenance of mitochondrial

distribution. DRP1, though, is not equipped with a PH domain that would bind such modified lipids. Instead, its recruitment to such lipid domains on mitochondria must be facilitated through another domain or another protein. So far, there has not been any mitochondrial endophilin-like proteins identified that would be involved in the localization of synaptojanin 2A or in the modification of membrane lipids at the site of mitochondrial constriction. However, yeast genetic studies have identified a few proteins that associate with Dnm1p and may play a role in its function. Two groups identified yeast Fission mutant 1 (Fis1p) and Mitochondrial Division mutant 1 (Mdvp1) as proteins participating in mitochondrial fission (72;73).

Fis 1p is an integral membrane protein that is required for fission (72) of the mitochondrial outer membrane (74). However, yeast cells lacking Fis1p maintain Dnm1p recruited on the membrane in punctate structures. Therefore, Fis1p likely functions downstream of Dnm1p in yeast mitochondrial fission (72;73). Studies with the human homologue of Fis1 (hFis1) (75) suggest that it also interacts with DRP1 both biochemically and using fluorescence microscopy (76). Overexpression of hFis1 results in fragmented mitochondria and down regulation of hFis1 protein levels using antibodies or antisense oligonucleotides induces elongated and collapsed mitochondrial morphology. Together, these results suggest that Fis1 is required for mitochondrial fission in yeast and mammalian cells. However, the function for Fis1 in the process of fission remains undetermined.

Yeast Mdv1p is a soluble protein, containing a coiled-coil motif and seven C-terminal WD repeats (77). Mdv1p has been shown to interact with Dnm1p genetically and by yeast two-hybrid. Its localization to the mitochondrial outer membrane requires

Fis1p but not Dnm1p; however, its translocation to punctate fission complexes is Dnm1p dependent. Similar to Fis1p, Mdv1p is not required for the assembly of Dnm1p into fission puncta. Nonetheless, successful mitochondrial fission requires functional Mdv1p. To date, a mammalian Mdv1p homologue has not been identified.

Taken together, genetic screens in yeast have so far identified two novel proteins essential for mitochondrial fission. However, the specific function of these proteins has been difficult to elucidate. The work presented in this thesis describes the identification of a novel mammalian DRP1 interacting protein called SUMO1, which is an important regulatory factor in the function of DRP1.

1.4 SUMO and SUMOylation

SUMO (small ubiquitin-like modifier), also termed sentrin (78), is a small 18kDa protein involved in the reversible post-translational covalent modification of cellular substrates (see (79) for review). Highly conserved, SUMO is found as a single gene product in yeast (Smt3) and has three forms in humans: SUMO1 (also known as PIC-1 (80) and GMP1 (81)), SUMO-2 (82), and SUMO-3. These three forms share 50% sequence identity with each other and with the yeast Smt3 (79). SUMO is classified as a member of one of the two families of ubiquitin-like proteins (UBLs) that share many similarities with ubiquitin (Ub), namely protein structure and mode of modification. However, there are functional differences between modification by SUMO and Ub.

1.4.1 Steps of SUMOylation

The addition of a molecule of SUMO to a substrate, termed SUMOylation, requires a number of steps each of which is regulated by distinct enzymes. The steps of

Figure 7. The steps of SUMO1 conjugation. SUMO1 is synthesized as an inactive precursor that is proteolytically cleaved at the C-terminus to reveal a critical glycine doublet of the mature protein. SUMO1 is then transferred, in an ATP dependent manner, to a specific cysteine residue of its E1 activating enzyme, which subsequently transfers SUMO1 to another specific cysteine residue of its E2 conjugating enzyme. Finally, SUMO1 is ligated to its substrate via an E3 ligating enzyme. The E3 ligating enzymes likely catalyze SUMO1 conjugation to a subset of substrates (not necessarily functionally related). Figure adapted from (79).

Figure 7.

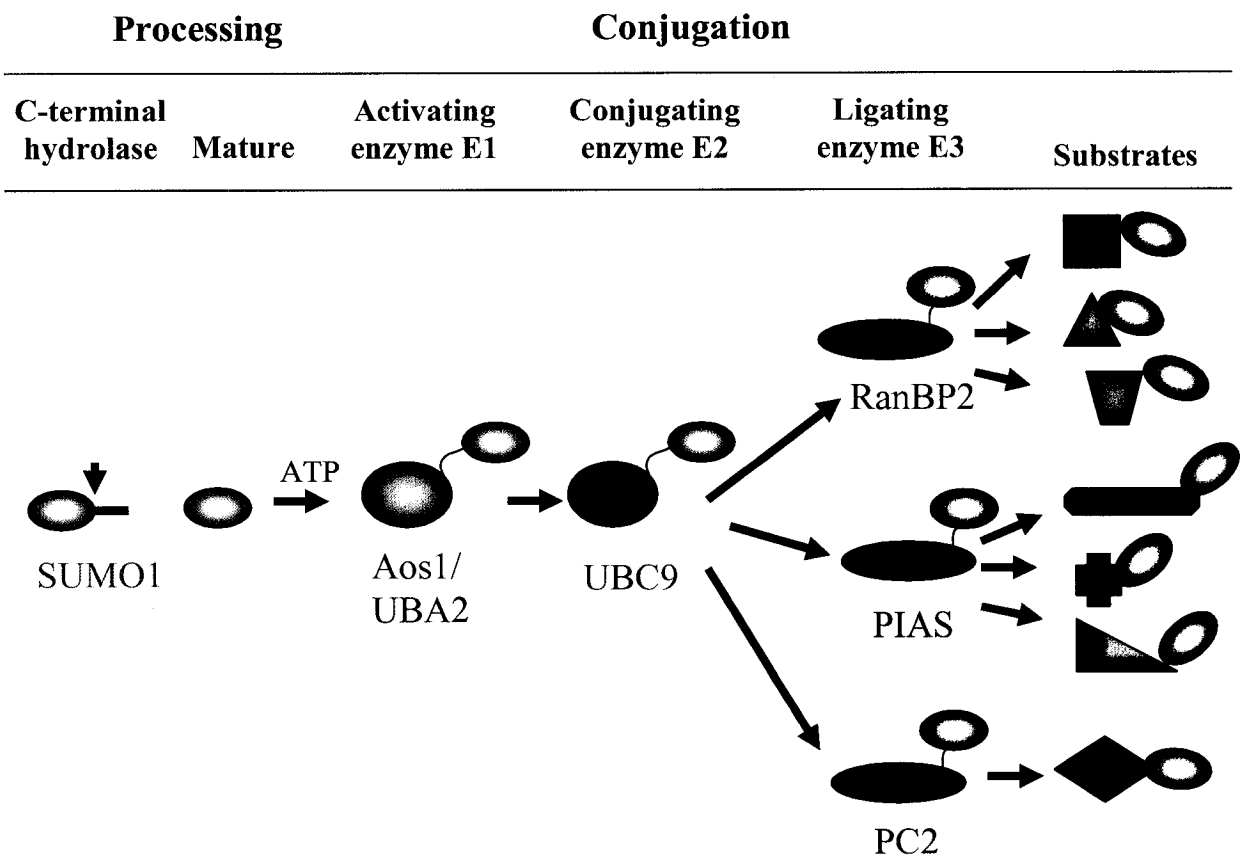
Processing
Conjugation
C-terminal hydrolase
Mature
Activating enzyme E1
Conjugating enzyme E2
Ligating enzyme E3
Substrates
ATP
SUMO1
Aos1/
UBA2
UBC9
RanBP2
PIAS
PC2

SUMOylation are analogous to those of ubiquitination. **Figure 7** illustrates the activation, conjugation and ligation steps of SUMOylation and highlights the function of their corresponding E1, E2 and E3 enzymes (also see (79)). SUMO1 is initially formed as an immature precursor that must be proteolytically processed for activation. Specific hydrolases cleave carboxyl-terminal amino acids of SUMO1 to reveal a glycine doublet critical for covalent attachment. The number of amino acids cleaved depends on the SUMO isoform. A heterodimeric E1 enzyme, Aos1/Uba2 (83), then activates the mature SUMO1 in an ATP dependent manner (84). This involves the formation of both a thioester bond between SUMO1 and E1 and a SUMO1-adenylate intermediate (84). The activated SUMO1 molecule is then transferred to a specific cysteine residue of the conjugating E2 enzyme, Ubc9 (ubiquitin conjugating enzyme 9), the only known E2 conjugating enzyme specific to SUMOylation (85-87). SUMO1 is then attached to the substrate via an isopeptide bond between the carboxy-terminal glycine of SUMO1 and the ε- amino group of a specific lysine on the substrate (79). This conjugation is facilitated by an E3 ligating enzyme (88). The E3 enzyme confers substrate specificity to SUMOylation and may be key in the regulation of SUMOylation. Substrates can be modified by multiple SUMO molecules at a number of distinct sites. SUMOylation of more than one lysine residue is more common than SUMO-SUMO chains on a single lysine (89). These multi-SUMO chains do not occur with SUMO1 but have been observed with SUMO2 and SUMO3 (90).

1.4.2 Functions of SUMOylation

A number of functions for SUMO1 have been described for its various modified substrates. Unlike ubiquitin, SUMO1 does not target proteins for proteosomal

degradation. Instead, SUMOylation has been shown to compete for sites of ubiquitination and inhibit protein degradation (91;92), as well as mediate subcellular targeting (93) and protein-protein interactions (94;95). Since the majority of SUMO1 substrates are resident nuclear proteins, most of the research has been focused on SUMO1 function in the nucleus. However, SUMOylation has an important role in modification of a limited number of cytosolic proteins. The following section describes the most prominent roles for SUMO1.

1.4.2.1. Regulation of intracellular targeting

The translocation or recruitment of proteins to specific subcellular destinations is a critical step in regulation of protein function. The classic example of SUMO1 regulated protein translocation is the Ran GTPase activating protein, RanGAP 1 (81). This protein is central to the control of nuclear-cytoplasmic transport and monitors which proteins are permitted to pass through the nuclear pore (see (96) for review). RanGAP 1 is targeted to the nuclear pore complex where it interacts, and is conjugated by, the SUMO E3 ligase, RanBP2 (Ran binding protein 2) (97). Once at the nuclear pore complex, it performs its function to stimulate hydrolysis of GTP by the nucleo-cytoplasmic shuttling GTPase, Ran. Therefore, it is the SUMO E3 ligase, RanBP2, a protein resident to the cytosolic side of the nuclear envelope that determines the subcellular localization of the SUMO1 substrate RanGAP. SUMOylation also plays a role in the formation of PML nuclear bodies (98) (also called PODs, PML oncogenic domains or ND10, nuclear dots (10)). PML bodies form puncta of varying size and number inside the nucleus. The formation and disassembly of these PML bodies appears to be dependant on the SUMOylation of its main component PML, the promyelocytic leukaemia protein (99). Once formed, PML

bodies are preferential sites for the recruitment of a number of SUMOylated nuclear substrates including Sp100 (100), Daxx (101), p53 (102) and various other transcription factors. The function of PML bodies remains elusive. However, SUMO1-mediated translocation of these proteins into PML bodies appears to affect their functional properties. For example, the transcriptional activity of p53 is increased upon SUMOylation and translocation to PML bodies (103). In contrast, movement of the SUMO1-modified form of the transcriptional co-repressor Daxx into PML bodies, appears to inhibit its activity (104).

1.4.2.2. Regulation of protein-protein interactions

Protein-protein interactions are known to be regulated by factors such as phosphorylation and nucleotide state. SUMOylation has now proven to be an additional means of such regulation. For example, disassembly of the oligomerized yeast septins is dependent on Smt3 (yeast SUMO1) modification (94). Septins are GTPases that self-assemble to form 10 nm filaments around the necks of budding yeast and are believed to be involved in the final stages of cytokinesis in the formation of the daughter yeast bud (see review (105)). Work performed by Gunter Blobel and colleagues demonstrate that SUMOylation regulates the cell cycle dependent recruitment and oligomerization of septins around the neck of budding yeast (94). Immunofluorescence experiments reveal that Smt3 is associated only with the mother side of the septin ring. Yeast strains harboring point mutations that obliterate all septin Smt3 sites have a striking phenotype that the septin rings are unable to disassemble and remain attached to the mother bud

after cytokinesis. In this case, it is not uncommon that a mother bud is decorated with remnants of numerous septin rings from previous cell divisions.

1.4.2.3. Regulation of protein stability

A unique regulatory link exists between the ubiquitination and SUMOylation systems. A prime example of this relationship is the regulation of NF-κB activity (91). NF-κB function is mediated through protein degradation of its inhibitor IκBα. Normally, NF-κB is maintained inactive in cytosol by complex formation with IκBα. Upon stimulation by specific factors like tumor necrosis factor (TNF), IκBα is phosphorylated leading to its ubiquitination and subsequent degradation. Once freed from its inhibitor, NF-κB translocates to the nucleus where it transcribes target genes. Competition of SUMO1 for the ubiquitination site on IκBα prevents the degradation of IκBα, allowing it to inhibit NF-κB activity. In this case, SUMOylation and ubiquitination act antagonistically to regulate protein stability and function.

1.4.3 ULPs and deSUMOylation

SUMOylation is a reversible process. The removal of SUMO from substrates, termed deSUMOylation, is highly regulated and requires a unique set of cysteine proteases termed ubiquitin-like protease (ULPs). These ULPs contain a conserved His/Asp/Cys catalytic triad responsible for their enzymatic activity. In *Saccharomyces Cerevisiae*, two such ULPs, Ulp1 and Ulp2 (106), (107;108)mediate the cleavage of the isopeptide bond between yeast Smt3 and the substrate, and are responsible for the maturation of Smt3 into its conjugatable form. DeSUMOylation is essential for yeast viability (108) as indicated by the lethality of yeast lacking Ulp1. Interestingly, Ulp2 is

not essential for yeast viability and cannot rescue the Ulp1 deletion, indicating that the two ULPs modify unique independent substrates (106-108). This is further supported by the different pattern of Smt3 conjugates observed when each ULP is deleted. In humans, a greater number of ULPs exist to accommodate the increased number of substrates and, potentially, the three isoforms of SUMO. The regulation of substrate specificity of ULPs is evident but not well understood. Studies suggest that a determining factor may be subcellular localization of the ULP and accessibility of the substrate. For example, SENP-2 (sentrin protease) appears to reside at the nuclear face of nuclear pores (109), SMT3IP1 is found in the nucleolus (110), and SENP-1 localizes primarily to the nucleus with a small amount observed in the cytoplasm (483). The N-terminal region of these ULPs appears to be responsible for their targeting to distinct regions within the cell, which consequently restricts their deconjugating activity to a specific subset of substrates (111). For example, SENP-1 cannot deSUMOylate cytosolic SUMO1-RanGAP1 but removes SUMO1 from PML. Evidently, regulation of SUMO1 function is as dependent on removal of SUMO1 as it is the addition of SUMO1. Protein activity stimulated by SUMO1-mediated translocation or protein-protein interaction is then terminated by deSUMOylation.

In this thesis, we identify SUMOylation as an authetic post-translational modification of DRP1, and as a common mode of protein modification of mitochondrial substates. We also present a novel role for SUMO1 on the mitochondria and in the process of mitochondrial fission. These findings implicate the participation of additional unidentified molecules in the regulation of mitochondrial morphology such as a specific SUMO1 E3 ligase and ULPs.

Objectives.

The goal of this research is to understand the regulation of DRP1 function in mitochondrial fission. Therefore, the three objectives outlined below are aimed at addressing this problem and, ultimately, providing insight into the mechanism and physiological role of mitochondrial fission in mammalian cells. These are:

1. Examination of the role of DRP1 mediated mitochondrial fission in the progression of programmed cell death.

2. Identification and characterization of DRP1 interacting proteins. A yeast two-hybrid system is used to identify proteins that interact with DRP1. This system enables identification of potential effectors and regulators that may either directly participate in mitochondrial fission or mediate the event.

3. Analysis of the functional roles of DRP1 interacting proteins by overexpression experiments of wild-type and mutant proteins.

2. Materials and Methods

2.1 Cell culture

Adherent COS-7 (African green monkey kidney cells) obtained from the American Type Culture Collection (ATCC, Rockville, MD) were cultured in 10 cm polystyrene dishes (Becton Dickinson Labware, Franklin Lakes, NJ) in Dulbecco's Modified Eagle Medium (DMEM) (Sigma, St.Louis, MO) supplemented with 10% fetal calf serum (FCS), 100 U/ml penicillin, 100 μg/ml streptomycin and 2mM glutamine (Invitrogen, NY), and incubated in a humidified atmosphere at 37°C and 5.0% CO_2. Cells were subcultured at a ratio of 1:5-1:8, 2 times per week. The growth media was aspirated, the cells were washed once with 1 mL of cold 1X phosphate buffered saline (PBS) (136mM NaCl, 2mM KCl, 16mM Na_2HPO_4, 0.017mM KH_2PO_4, pH 7.4), 1 mL 0.25% Trypsin/0.03% EDTA (Invitrogen, NY) solution was then added to the cells and they were incubated at 37° C for approximately 5 min to promote detachment. Once detached, fresh complete media, prewarmed at 37°C, was added to the cells and they were split at the desired ratio. For general transfection of mammalian expression vectors, the cells were seeded at a density of $8x10^4$ cells/well in regular growth media the day before transfection on glass coverslips (Fisher Scientific) placed in the wells of 24-well plates (Becton Dickinson Labware, Franklin Lakes, NJ). 0.2-1.5 μg of the desired constructs were transfected the following day using Lipofectamine 2000 (Invitrogen, Carlsbad, CA) according to the manufacturers' protocol. Transfection media was replaced with regular growth media after 3-4 hours. Cells were analyzed accordingly 24-48 hours post-transfection.

2.2 Preparation of constructs

2.2.1. DRP1 and DRP1 mutants

Full-length DRP1 and the dominant negative mutant DRP1 K38E cDNAs in the form of the constructs pcDNA3-HAN-DVLP and pGEX-4T2-DVLP (K38E) were generous gifts from K. Nakayama (Institute of Biological Sciences, University of Tsukuba, Tsukuba Science City, Ibaraki). For yeast-two hybrid screening, DRP1 was subcloned into pFASTBac GSTb (for future baculovirus protein expression) (Clontech, Palo Alto, CA) using the restriction sites BamH1 and Not1 to generate pFASTBac GSTb:DRP1. DRP1 was subsequently cloned into pLEXA2 (Marino Zerial, Dresden, Germany) using the restriction sites BamH1 and Pst1. For mammalian fluorescent protein fusion construct expression, DRP1 and DRP1 (K38E) were each cloned directly from pFASTBacb:DRP1 and pGEX-4T2:DRP1 (K38E) respectively into both pECFP-C1 (Clontech, Palo Alto, CA) and pEYFP-C1 using the restriction sites BamH1/BglII and Xho1/Sal1. For His6 pull-down experiments, pcDNA4:DRP1:His was created by isolation of DRP1 from pcDNA3-HAN-DVLP using BamHI and XhoI and insertion into pcDNA4:HisC. At each cloning step for all constructs, the isolation of the DRP1 insert was verified by visualization of a 2.2 kb band when the restriction digests were run on a 0.7% agarose electrophoresis gel. The DRP1 inserts were then ligated into the appropriate vector using T4 DNA Ligase and the completed construct was transformed into XL-Blue chemically competent E. Coli (Stratagene, La Jolla, CA), using heat shock (15 min ice, 45 sec at 42°C, 2 min ice). The bacteria were streaked on LB agar plates containing 50 μg/ml ampicillin (pLEXA2) or 30 μg/ml kanamycin (pECFP/pEYFP) and grown overnight at 37°C. Plasmid DNA was isolated from the bacteria by alkaline lysis methods and

positive colonies for each construct were verified using restriction digestion. A large preparation of pure construct DNA was obtained from 150mL of bacterial culture lysed and purified using QIAGEN midiprep chromatography columns (QIAGEN, Mississauga, ON) according to manufacturers' specifications. Various DRP1 point mutants and domain constructs for yeast two-hybrid testing, fluorescence microscopy and bacterial protein expression were made using the Quikchange Mutagenesis Kit (Stratagene, Cedar Creek, TX) according to the manufacturers protocol or were subcloned from constructs provided by K. Nakayama. PCR primers (Sigma Aldrich) designed for each mutation are listed in Table 1B,C (shown with the template, the new restriction site introduced for screening and the final mutant constructs). Final constructs were similarly transformed into XL-Blue chemically competent *E. Coli* using heat shock. Positive bacterial colonies were screened by restriction digests and a high quality preparative batch of construct DNA was obtained using QIAGEN midiprep kits. Additional constructs used in this research are listed in Table 1A with their sources, cloning strategy and derivative plasmids

2.2.2. DRP1 interacting proteins: SUMO1, Ubc9 and TOPORS

Full length SUMO1 and Ubc9 were pulled out of the yeast two-hybrid screen (described in section 3.2.1) in the pGAD vector (Marino Zerial, Dresden, Germany), whereas only the C-terminal amino acids 873-1020 of TOPORS were isolated. SUMO1, Ubc9 and the TOPORS terminal fragment were all subcloned from pGAD into pLEXA for reciprocal yeast two- hybrid experiments using the restriction sites SmaI and XhoI/SalI and the isolation of all inserts from restriction digests was verified by visualization of a ~1 kb band on a 0.7% agarose electrophoresis gel. SUMO1 and Ubc9 were also PCR amplified

from pGAD with primers carrying new 5' BamH1 and 3' Xho1 sites and new 5' EcoR1 and 3' Xho1 sites respectively (Table 1B). Both PCR fragments were confirmed by restriction digests with the introduced sites and visualization of a ~300 bp band on 0.7% agarose electrophoresis gel. These fragments were then used to clone SUMO1 into pEYFP-C3 using BamH1 and Xho1/Sal1 and Ubc9 into pEYFP-C1 using EcoR1 and Xho1/Sal1. General procedures for cloning, screening and final construct DNA preparation were similar to those described above for DRP1. Constructs carrying a mutant form of SUMO1 lacking its two terminal glycines (SUMO1 ΔC5) were also produced for yeast two-hybrid testing and fluorescence microscopy with the Quikchange Mutagenesis Kit using primers that introduce a stop codon upstream of these two amino acids (Table 1C).

2.3 Mitochondrial fission: steady state versus apoptosis

2.3.1. Live cell video fluorescence microscopy

To visualize mitochondria, the mitochondrial targeting signal from the mitochondrial matrix protein ornithine carboxyl transferase (OCT) was attached to the N-terminus of fluorescent proteins (CFP, YFP or DsRed2) (Clontech, Palto Alto,CA) creating an inert mitochondrial marker. Cos7 cells were then transfected with the plasmid encoding the matrix targeted fluorescent protein as described in section 2.1. To prepare the cells for visualization, the glass coverslips were mounted in a live cell metal slide containing regular growth media supplemented with 20mM HEPES, pH 7.4. The cells were maintained at 37°C during analysis in an enclosed Olympus 1X70 inverted microscope operated using TILLvisION v4.0 software (T.I.L.L Photonics GmbH, Martinsried,

Germany). The dynamics of mitochondria are captured using a 100X objective (Uplan APOA) by recording images of successive excitation of the cells at an appropriate wavelength (434nm for CFP, 514nm for YFP, 558nm for DsRed2) through an appropriate filter (CFP/YFP dual pass filter, CFP/YFP/DsRed triple pass filter (Chroma)) at a given exposure time (usually 100-400ms) for each frame. The number of frames ranges between 50-200 and the time between frames ranges from 2-4 seconds. The TILLvisION software then compiles the frames into a movie.

2.3.1.2 DRP1 recruitment during apoptosis

Cos7 cells seeded on glass coverslips in 24-well plates were grown to 80% confluence and co-transfected with 1μg pECFP:DRP1 and 0.5μg pOCT-YFP as described in section 2.1. The next day, 1.2 μM staurosporine (112) was added to the growth media for 2.5 hours to induce apoptosis. The live cells were then mounted and analyzed by microscopy using the CFP/YFP dual pass filter (see section 2.3.1).

2.3.2. Caspase-3 Activation Assay

Cos7 cells seeded in 6-well dishes in normal growth media were grown to 80% confluence and transfected with either pECFP:DRP1 or pECFP:DRP1 (K38E) as described in section 2.1. The following day, the cells were washed twice with cold PBS to remove floating cells and apoptosis was induced by incubating the cells for 2.5 hours with 1.2 μM staurosporine in regular growth media at 37°C. The cells were then harvested (suspended and adherent cells) by centrifugation at 16 000 x g at 4°C for 5 minutes, washed with cold PBS and reharvested. Cold lysis buffer (50 mM Tris-HCL pH

7.5, 1% NP-40, 0.25% sodium deoxycholate, 150 mM NaCl, 1mM EGTA) was added to the cells, they were lysed on ice for 15 minutes and the cell debris was pelleted at 16 000 x g at 4°C for 15 minutes. The supernatant was collected, the protein concentration was determined (BioRad Protein Assay Kit, Mississauga, Ontario) and the protein concentrations of the lysates were equalized with lysis buffer. An equivalent amount of lysate was placed in triplicate into a black opaque 96 well plate (Costar, Acton, MA) and dithiothreitol (DTT) was added to a final concentration of 2 mM per well. A final concentration of 0.05 μM of a Caspase-3 fluorometric substrate (Ac-Asp-Glu-Val-Asp-amino-AMC) (Upstate Biotechnology, Lake Placid, NY) was then incubated with the samples for 10 minutes at room temperature. The fluorescence of the Caspase-3 fluorometric substrate (excitation= 380nM and emission=460nm) was read in a plate reader (POLARstar Galaxy, BMG-Labtechnology GmbH, Offenburg, Germany).

2.4 Yeast-two hybrid screen

2.4.1. Principle

The yeast two-hybrid method, developed by Fields and Song, is based on the ability of two fusion proteins to interact in the yeast nucleus and form a transcriptionally active unit whose function is detectable by in vitro assay (113). The two fusion proteins are encoded by two independent plasmids that are co-introduced into yeast. One plasmid codes for a fusion product between the LEXA protein DNA-binding domain and the two-hybrid bait (full-length DRP1). The other plasmid encodes a fusion product between the GAL4 activation domain and a protein from the gene library (HeLa cell library). Yeast are transformed with both plasmids and the resulting fusion proteins are expressed in the

yeast nuclei. Should an interaction occur between the bait (DRP1) and a library protein, these two proteins come into close proximity. Consequently, their fusion partners, the DNA-binding domain from LexA and the activation domain from GAL4, are also brought together and thus combine to form a functional transcription factor that then transcribes reporter genes present in a particular yeast strain (see also (114) for review) (two reporter genes in the L40 yeast strain used are: β-galactosidase and an enzyme for the synthesis of histidine). **Figure 10** is a schematic diagram summarizing the principle of the yeast two-hybrid system.

2.4.2. Yeast transformation of DRP1 bait

Full length DRP1 cloned into pLEXA2 (pLEXA2: DRP1) (see section 2.2.1) was used as bait for the yeast two-hybrid screen. The L40 yeast strain used for the screen (kindly provided by Johnny Ngsee, Loeb Research Institute, Ottawa) was initially streaked on fermentable YPD agar plates (1% yeast extract, 2% peptone, and 2% dextrose) (Clontech, Palo Alto, CA), made according to the supplier's protocol, and incubated at 30°C for 3-5 days until the appearance of colonies. The general growth curve and doubling time of the yeast was determined by inoculating liquid YPD media with approximately 5.5 x 10^5 cells/ml yeast (determined by counting the density of a starter 5ml YPD yeast culture grown overnight from a single yeast colony). The density of yeast was monitored over time using spectrophotometry (Beckman DU 640) by determining absorbance of the culture at 600nm. Once the viability of the L40 yeast was determined, the pLEXA2:DRP construct was transformed. Approximately 25 µl of yeast freshly grown on YPD plates for 3-5 days was resuspended in double distilled water, pelleted at 16 100

Figure 8. The principle of the yeast two-hybrid system. Full-length DRP1 is cloned in frame into the pLEXA2 vector, encoding a DNA binding domain (BD), resulting in a BD:DRP1 fusion protein. Proteins of the DNA library (X) are cloned into the pGAD GH vector (not necessarily in frame), encoding an activation domain (AD), and resulting in a AD:X fusion protein. The two constructs are co-transformed into yeast where the resulting fusion proteins meet in the nucleus. Should an interaction occur between DRP1 and a protein X of the library, the BD and AD come into close proximity to form a function transcription factor and drive transcription of reporters. These reporters are previously introduced into the yeast genome. TRP=synthesis of tryptophan allowing growth on media lacking this amino acid. LEU=synthesis of leucine allowing growth on media lacking this amino acid. HIS= synthesis of histidine allowing growth on media lacking this amino acid. LacZ= expression of the lacZ gene resulting in activity of β-galactosidase. P=yeast promoter. Note: not all vector components are shown.

Figure 8.

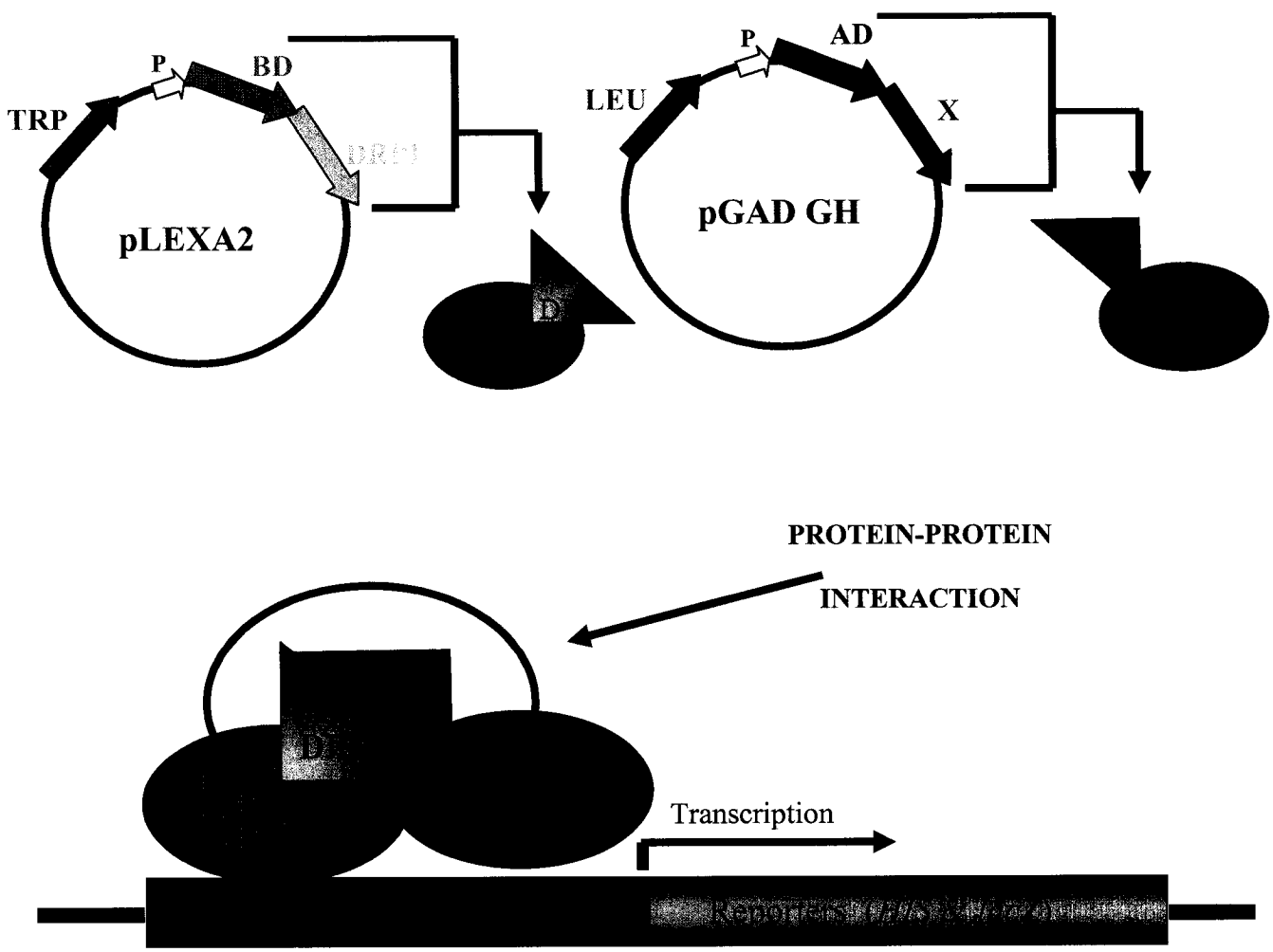
TRP
P
BD
pLEXA2
LEU
P
AD
X
pGAD GH
PROTEIN-PROTEIN
INTERACTION
Transcription

x g (Eppendorf centrifuge 5415 D) and briefly incubated at 30°C for 5 minutes in 0.1 M lithium Acetate (LiAc) (Sigma, Oakville, ON). The following transformation reaction mix was then added: 240 µl polyethylene glycol 50% w/v (PEG), 36 µl 1M LiAc, 50 µl 2mg/ml of boiled single stranded salmon sperm carrier DNA (ss-DNA), and 2µg plasmid DNA (pLEXA2:DRP) (as well as 2µg each of pLEXA2 and pLEXA-Rab5Q79L in parallel). The reactions were vortexed and incubated at 42°C for 20 minutes. The transformed yeast were pelleted again 16 100 x g, resuspended in double distilled water and streaked on plates selective for the plasmid (made from standard drop-out agar (SD agar) (Clontech, Palo Alto, CA) supplemented with essential amino acids except tryptophan (-Trp) (Clontech, Palo Alto, CA) according to suppliers specifications) and incubated at 30°C for 3-5 days (see section 2.4.5.1 for details on yeast growth selection). The resulting colonies were re-streaked on control SD agar plates lacking leucine (-Leu) (Clontech, Palo Alto, CA), SD agar plates lacking histidine (-His) (Clontech, Palo Alto, CA), and SD agar plates lacking combinations of these amino acids (-Trp, -Leu), (-Leu, -His), (-Trp, -His) and (-Trp, -Leu, -His) (Clontech, Palo Alto, CA) to test for auto-activation of reporter genes that may potentially allow growth on these plates.

Doubling time for the pLEXA2:DRP transformed yeast was then determined to assess potential yeast toxicity of the bait DNA, by inoculating liquid SD (-Trp) media with 2.16 x 10^6 cells/ml of transformed yeast and monitoring yeast density over time in a similar manner as described above.

2.4.3. Detection of LEXA2:DRP fusion protein expression in yeast

LexA2: DRP1 fusion protein expression in yeast was determined by Western Blot analysis. pLexA2:DRP and pLexA2 alone negative control yeast cultures were grown overnight at 30°C in liquid SD (-Trp) media from fresh single colonies. The following day, the yeast were diluted 1:5 into liquid YPD media and allowed to incubate at 30°C to reach an OD_{600} of 0.4-0.6. At this density, the yeast were harvested at 1000 x g (Sorvall RT 6000D centrifuge) for 5 minutes at 4°C, washed in double distilled water, repelleted at 1000 x g, and broken by snap freezing and thawing in liquid nitrogen and subsequent incubation at 60°C. The yeast cells were solubilized using prewarmed cracking buffer (8M Urea, 5% w/v SDS, 40mM Tris-HCL pH 6.8, 0.1 mM EDTA, 0.4mg/ml bromophenol blue, deionized water), containing a protease inhibitor cocktail (0.1 mg/ml pepstatin A (Sigma,Oakville,ON), 0.03mM leupepin (Sigma,Oakville,ON), 145 mM benzamidine (Sigma,Oakville,ON), 0.37mg/ml aprotinin (Sigma,Oakville,ON), and 0.1M phenylmethyl-sulfonyl fluoride (PMSF) Sigma,Oakville,ON), heated at 70°C for 10 min, vortexed vigorously in the presence of acid-washed glass beads (425-600 micron) (Sigma, ST. Louis, MO) and centrifuged at 16 100 x g (Eppendorf centrifuge 5415 D). The supernatants were then briefly boiled at 100°C, re-vortexed, and re-centrifuged. The final supernatants were prepared in 2X sodium-dodecyl sulfate (SDS) sample loading buffer containing 1mM DTT, boiled briefly, run on a 10% SDS-PAGE gel and subsequently transferred onto nitrocellulose membrane. Non-specific protein binding to the membrane was blocked by incubation with PBS/Tween/ 5% milk for 1hour shaking at room temperature. The membrane was probed with monoclonal anti-LexA antibodies (Clontech, Palo Alto, CA), diluted 1:10000 in 5mg/ml bovine serum albumin (BSA)

with 0.25% azide, for 30 minutes at room temperature then washed 5 times for 5 minutes each in blocking solution. The membrane was then probed with secondary goat anti-mouse antibodies conjugated to horseradish peroxidase (HRP) (anti-mouse HRP) (Jackson Immuno research laboratories, Westgrove,PA), diluted 1:5000 in blocking solution, for 30 minutes at room temperature then washed 5 times for 5 minutes each in PBS/Tween. The membrane was briefly incubated with a chemiluminescent HRP substrate (Supersignal, Biolynx INC, Brockville, Ontario), exposed to film (Kodak, X-Omat Blue XB-1, Perkin Elmer) and developed.

2.4.4. Yeast transformation of HeLa library

A HeLa cDNA library (a generous gift from Marino Zerial, EMBL, Heidelberg) was used as a target protein gene source for the yeast two-hybrid screen. Once the pLEXA2:DRP transformed yeast were deemed viable and fusion protein expression was confirmed, the efficiency of transformation of this yeast with the library cDNA was determined, so that proper scaled up procedures to obtain the desired number of transformants (6×10^6 transformants = full library) can be performed. A 10X protocol was followed where a starter 25 mL liquid SD (-Trp) culture of pLEXA2:DRP yeast was grown overnight at 30°C. The following day, the cell titre was calculated and 2.5×10^8 transformed yeast cells were washed in liquid YPD media, pelleted at 3000 x g, then resuspended in 50ml pre-warmed (30°C) liquid YPD media. The yeast culture was allowed to incubate at 30°C until the yeast were in log phase growth and the density reached 2×10^7 cells/ml. The yeast were then harvested at 3000 x g and resuspended in 0.1M LiAc for 15 min at 30°C. They were again repelleted and incubated at 30 min at 30°C with the same transformation mix as described above in section 2.4.2 scaled up ten times, except

plasmid DNA was replaced with 0.1, 0.5, 2 and 10 μg library DNA in parallel reactions. The reactions were incubated at 42°C for 30 min with inversion, after which the cells were harvested, resupended in double distilled water, plated at various dilutions of 1:10000, 1:1000 and 1:100 on SD agar plates (-Trp, -Leu) and incubated at 30°C until the appearance of colonies. After calculation of transformation efficiency, the final yeast two-hybrid screen was performed using the same protocol as above scaled up to 60X and using 60 μg library DNA. The transformed yeast were plated on SD agar (-Trp, -Leu, -His) plates with the remainder being plated on SD agar (-Trp, -Leu) to assess transformation efficiency. Colonies that grew on SD agar (-Trp, -Leu, -His) plates were then tested for the expression of the second reporter gene, β-galactosidase, as described below (section 2.4.5.2 and 2.4.5.3). Colonies positive for both reporters were streaked on SD agar (-Leu) plates to select strictly for the library plasmid. Colonies from these plates were then grown in liquid SD (-Leu) media overnight and the library plasmid DNA was isolated using QIAPREP chromatography columns (QIAGEN, Mississauga, ON) following the protocol provided by the manufacturer for yeast DNA extraction. The purified library plasmid DNAs were subsequently transformed into XL-Blue chemically competent *E.Coli* using heat shock and cultures from the resulting colonies were screened for presence of the library plasmid using restriction digestion. Large preparative cultures of the positive clones were grown and the plasmid DNA was purified using the QIAGEN midiprep kit (QIAGEN, Mississauga, ON) and sent for sequencing (Canadian Molecular Research Services, CMRS, Ottawa, ON). The identities of the clones were determined by comparing the resulting sequences against a sequence database (BLAST, NCBI).

2.4.5. Reporter gene expression assays

2.4.5.1. Yeast Growth

The expression of yeast genes encoding enzymes that synthesize specific amino acids, allows growth on media lacking these amino acids. This expression enables selection of efficiently transformed yeast and allows detection of protein-protein interactions (bait and target). The plasmid source of these genes and the significance of growth on specific plates are outlined below:

Tryptophan: Synthesis is due to (*TRP*) genes present on pLEXA2. Growth on SD agar plates lacking tryptophan reflects successful transfection of yeast with the bait.

Leucine: Synthesis is due to (*LEU*) genes present on pGAD. Growth on SD agar plates lacking leucine reflects successful transfection of yeast with the library.

Histidine: Synthesis is due to transactivation of (*HIS*) genes present in the L40 yeast strain. Growth on SD agar plates lacking histidine is indicative of a protein-protein interaction between bait and a library protein.

Table 1. Summary of constructs and cloning strategies. Listed are all the constructs used in these studies as well as their sources, cloning strategy and purpose.

Table 1.

A

Construct	Source	Restriction sites used for cloning	Experiment
pFASTBacGSTb:DRP	pcDNA3:HAN:DRP1 (K. Nakayama)	BamHI, Not1	Subcloning, baculoviral protein expression
pLexA2:DRP	pFASTBacGSTb:DRP	BamHI, PstI	Yeast two-hybrid
pLexA2:DRP(K38E)	pGEX-4T2:DRP(K38E) (K. Nakayama)	BamHI,XhoI/SalI	Yeast two-hybrid
pECFP-C1:DRP	pFASTBacGSTb:DRP	BamHI/BglII, XhoI/SalI	Fluorescence microscopy
pEYFP-C1:DRP	pFASTBacGSTb:DRP	BamHI/BglII, XhoI/SalI	Fluorescence microscopy
pECFP-C1:DRP(K38E)	pGEX-4T2:DRP(K38E) (K. Nakayama)	BamHI/BglII, XhoI/SalI	Fluorescence microscopy
pEYFP-C1:DRP(K38E)	pGEX-4T2:DRP(K38E) (K. Nakayama)	BamHI/BglII, XhoI/SalI	Fluorescence microscopy
pLexA:SUMO	pGAD:SUMO	SmaI,XhoI/SalI	Yeast two-hybrid
pLexA:Ubc9	pGAD:Ubc9	SmaI,XhoI/SalI	Yeast two-hybrid
pLexA:TOPORS (873-1020)	pGAD:TOPORS (873-1020)	SmaI,XhoI/SalI	Yeast two-hybrid
pEYFP-C1:Ubc9	pcDNA3-myc:Ubc9	EcoRI,XhoI	Fluorescence microscopy
pcDNA4:DRP1:His	pcDNA3:HAN:DRP1	BanHI/XhoI	His6 pull-down
pcDNA4:SUMO1:His	pcDNA3:SUMO1	BamHI/XhoI	His6 pull-down

B

Primer name	Primer sequence	Restriction sites introduced	Template DNA	Constructs created
SUMO top	gtg gat ccc atg tct gac cag gag gca aa	BamHI	pGAD:SUMO	pEYFP-C3:SUMO
SUMO bot	ggc ctc gag cta aac tgt tga atg acc cc	XhoI		
Ubc9 top	gcg aat tcc atg tcg ggg atc gcc ctc ag	EcoRI	pGAD:Ubc9	pcDNA3-myc:Ubc9
Ubc9 bot	ggc ctc gag tta tga ggg cgc aaa ctt ctt	XhoI		

C

Primer name	Primer Sequence	New restriction site	Template DNA	Constructs created
DRP K216G top	aga acc cta gct gta atc aca ggc ctt gat ctc atg gat gcg ggt	Stu1	pLexA2:DRP, pLexA2:DRP (K579A)	pLexA2:DRP (K216G), pLexA2:DRP (K216G, K579A),
DRP K216G bot	acc cgc atc cat gag atc aag gcc tgt gat tac agc tag ggt tct	Stu1		
DRP K497V top	ctg gct tat atc aac aca gtg cac cca gac ttt gct gat gct	ApaL1	pLexA2:DRP, pECFP-C1:DRP	pLexA2:DRP (K497V), pECFP-C1:DRP (K497V)
DRP K497V bot	agc atc agc aaa gtc tgg gtg cac tgt gtt gat ata agc cag	ApaL1		
DRP K597A top	aga gga atg ctg aaa act tct gca gct gaa gag tta tta gca	Pst1	pLexA2:DRP, pECFP-C1:DRP, pGEX-4T2:DRP	pLexA2:DRP (K579A), pECFP-C1:DRP (K579A), pGEX-4T2:DRP (K579A)
DRP K597A bot	tgc taa taa ctc ttc agc tgc aga agt ttt cag cat tcc tct	Pst1		
DRP K679V top	ttt ttg gtt aat cat gtg gtc gac act ctt cag agt gag ct	Sal1	pLexA2:DRP, pECFP-C1:DRP	pLexA2:DRP (K679V), pECFP-C1:DRP (K679V)
DRP K679V bot	ag ctc act ctg aag agt gtc gac cac atg att aac caa aaa	Sal1		
DRP 1-260 top	aag aag agt gta act gat taa gtc gac gat gag tat	Sal1	pLexA2:DRP	pLexA2:DRP (1-260),
DRP 1-260 bot	aag aaa agc ata ctc atc gtc gac tta atc agt tac	Sal1		
DRP 254-525 top	c gga tcc cca gtc aaa ctt gga ata att	BamH1	pLexA2:DRP	pLexA2:DRP (254-525), pLexA2:DRP (254-575),
DRP 254-525 bot	gc gaa ttc tca tcc aac ccc acc acc tcc aga	EcoR1		
DRP 254-575 bot	gc gaa ttc tca tcc aac ccc acc acc tcc aga	EcoR1		
SUMOΔC5 top	tat cag gaa caa acg ggg tga tat cca aca gtt tag ata ttc ttt	EcoRV	pGAD:SUMO pEYFP:SUMO	pGAD: SUMOΔC5, pEYFP-C3: SUMOΔC5
SUMOΔC5 bot	aaa gaa tat cta aac tgt tgg ata tca ccc cgt ttg ttc ctg ata	EcoRV		

2.4.5.2. Qualitative β-Galactosidase Assay: X-Gal colony filter lift

To further verify the presence of a protein-protein interaction between DRP1 and a library protein, the expression of a second reporter gene, *LacZ*, was tested on all yeast colonies that survived growth on SD agar (-Trp, -Leu, -His) plates. The colony filter-lift assay is strictly qualitative and is a relatively sensitive way of simultaneously screening many yeast colonies. Circular filter paper (12.5 cm VWR 410 filter paper, West Chester, PA) was placed directly onto the colonies to be assayed such that they were partially transferred onto the paper. The filter paper was then submerged in liquid nitrogen (to break open the yeast cells), thawed at room temperature and placed on top of another piece of filter paper pre-soaked in Z buffer/X-Gal solution (60mM Na_2HPO_4, 30mM NaH_2PO_4, 10mM KCl and 1mM $MgSO_4$, 0.8mM X-Gal (5-bromo-4-chloro-3-indolyl-b-D-galactopyranoside, colorimetric β-galactosidase substrate, (Sigma)). The filter papers were incubated at 30°C until the appearance of blue colonies. These blue yeast colonies were subsequently restreaked on a Master plate and allowed to regrow for quantitative analysis.

2.4.5.3. Quantitative β-Galactosidase Assay: ONPG liquid culture

The relative strength of the protein-protein interaction between DRP1 and the library proteins was assessed quantitatively using a liquid culture assay. Colonies positive for the filter-lift assay were grown in liquid SD (-Trp, -Leu) media overnight. The following day, the cultures were diluted 1:4 in liquid YPD media at 30°C and allowed to reach mid-log phase growth (determined by an OD_{600} 0.5-0.8). At this point, the exact OD of the culture was recorded. The yeast cells were harvested in triplicate at 10 000 x g, the

supernatant was removed and the cells were washed in Z buffer. The final yeast pellet was resuspended in Z buffer and the samples underwent three 1 min freeze/thaw cycles of liquid nitrogen/37°C. Once the cells were permebealized, 4mg/ml of ONPG colorimetric substrate (o-nitrophenyl b-D-galactopyranoside; Sigma) in Z buffer was added to the samples and the reaction was incubated at 30°C until the appearance of a yellow colour. At this point, the reaction was terminated with 1M Na_2CO_3 and the endtime was noted. The yeast cell debris was cleared at 16 100 x g and the absorbance of the reaction at 420nm was recorded. The activity of the β-galactosidase enzyme was calculated in terms of β-gal units (1 unit refers to the amount of enzyme that hydrolyzes 1μmol of ONPG per minute per cell), and this value was used as a relative indication of the strength of the different protein-protein interactions.

2.5 Specificity of protein-protein interactions

2.5.1. Yeast two-hybrid testing

Various DRP1 domain constructs and point mutants (**Table 1**) were tested for their interactions with three proteins pulled out of the screen, SUMO1, Ubc9 and TOPORS. L40 yeast were co-transformed with these DRP1 constructs and each of SUMO1, Ubc9 and TOPORS. A number of positive controls (DRP1 + DRP1, Rab5Q79L + Rabaptin) and negative controls (DRP1 $_{(\text{various constructs})}$ + Rabaptin) were cotransformed in parallel. The yeast transformation protocol used was the same as the one described in section 2.4.2 except that two plasmids were transformed (pLEXA2: DRP1 $_{(\text{various mutants})}$ and either pGAD: SUMO1, Ubc9 or TOPORS $_{(873\text{-}1020)}$). The final transformed yeast were streaked on SD agar (-Trp, -Leu) plates, to select for both plasmids, and incubated at 30°C until

the appearance of colonies. These colonies were then picked and grown in liquid SD (-Trp,-Leu) media for quantitative β-galactosidase assays as described in section 2..4.5.3 to compare the relative strengths of protein-protein interactions.

2.5.2. GST-pull down assays

The interactions between DRP1, SUMO1 and Ubc9 were verified biochemically using GST-pull down assays.

2.5.2.1. Purification of recombinant GST:DRP1 and GST:DRP1(K38E)

pGEX-4T2:DRP1 and pGEX-4T2:DRP1(K38E) constructs coding for GST:DRP1 and GST:DRP1(K38E) fusion proteins respectively, were transformed using heat shock into BL21 chemically competent *E.Coli* for bacterial protein expression. 3 L cultures of each of GST:DRP1, GST:DRP1(K38E) and GST alone were grown from overnight starter cultures in liquid media (LB + 50μg/mL ampicillin) first for 2 hours at 30°C and then at room temperature until the OD_{600} reached 0.6-0.9. Protein expression was induced with 100 μM IPTG (isopropyl-beta-D-thiogalactopyranoside) for 16-18 hours at 30°C, then the cultures were harvested at 4 000 rpm (Sorvall Legend RT) for 10 min and resuspended in ice-cold buffer (50mM Tris, pH 8.0, 100mM NaCl, 2mM $MgCl_2$, 5mM β-mercaptoethanol, 1% Triton X-100 and a protease inhibitor cocktail consiting of 60μg/ml chymotrypsin, 1.1×10^{-6} M leupeptin, 2μg/ml aprotinin, 25μg/ml antipain, and 1×10^{-3} M pepstatinA). The bacteria were broken by passing twice through a pre-cooled French pressure cell press (ThermSpectronic) at approximately 2000-2500 psi and the bacterial lysate was cleared at 90 000-100 000 x g (Beckman L8-80M Ultracentrifuge) for 30

minutes at 4°C. The supernatant was added to pre-equilibrated (50mM Tris, pH 8.0, 100mM NaCl, 2mM $MgCl_2$, 0.1% Triton X-100) glutathione-sepharose beads (Amersham Pharmacia Biotech Inc, Piscataway, NJ) and incubated for 2 hours at 4°C with rotation. The beads were collected at 3000rpm (Sorvall RT 6000D), washed 4 times with buffer (50mM Tris, pH 8.0, 100mM NaCl, 2mM $MgCl_2$, 2mM β-mercaptoethanol, 0.1% Triton X-100) and loaded into a column at 4°C. The beads were re-washed once with buffer and ¼ of the bead volume was eluted with 15 mM reduced glutathione in buffer (50mM Tris, pH 8.0, 100mM NaCl, 2mM $MgCl_2$) to check protein concentration. The remainder of the bead-bound protein was used for the GST pull-down assay.

2.5.2.2. Preparation of bovine heart and rat liver mitochondria and cytosol

Rat liver preparation

12-16 week old Wistar rats were anesthetized in a CO_2 chamber for 10 minutes. The neck was dislocated and a 10 cm incision was made down the abdomen. The liver was extracted and placed in ice cold buffer (20mM Hepes pH 7.4, 220 mM mannitol, 68mM sucrose, 80mM KCl, 0.5 mM EGTA, 2mM $Mg(Ac)_2$, 1mM DTT). The tissue was divided in half and 20mM N-ethyl maleimide (NEM) was added to the buffer for one of the samples. The tissue was thoroughly homogenized in a Dounce homogenizer and centrifuged at 1500 x g at 4°C for 20 minutes. The supernatant was transferred to another tube and the pellet was washed in 2 volumes of buffer. Both samples were then re-centrifuged at 1500 x g at 4°C for 20 minutes. The final pellet was collected as the nuclear/unbroken cell fraction and the cleared supernatant was centrifuged to isolate mitochondria at 8000 x g 4°C for 30 minutes. The supernatant from this spin was

transferred to another tube and the mitochondrial pellet was washed again in buffer and re-centrifuged at 8000 x g 4°C for 30 minutes. This final pellet was resuspended in a minimal volume of buffer as the mitochondrial fraction. Finally, the supernatant from the first high speed spin was cleared at 100 000 x g at 4°C for 45 minutes and collected as the cytosolic fraction. All unused fractions were frozen in liquid nitrogen and placed at -80°C.

Bovine heart preparation

Bovine heart was obtained fresh from a slaughterhouse and immediately placed on ice in ice cold 1XPBS without protease inhibitors. The heart was cut into small pieces and washed by decanting with 1X PBS. The total weight of the heart was determined and 2X volumes of mitochondrial isolation buffer (20mM HEPES, pH 7.4, 220mM mannitol, 68 mM sucrose, 80mM KCL, 0.5 mM EGTA, 2mM Mg(Ac)2, 1mM DTT, 1X protease inhibitor cocktail mentioned above) was added to the tissue. The heart was placed in a Waring blender and homogenated until smooth at high speed. The lysate was centrifuged at 3000 rpm (Sorvall Legend RT) at 4°C for 20 minutes. The supernatant was transferred to a fresh tube and spun at 6500 x g (Sorvall RC-5) for 15 minutes. The supernatant was saved and the mitochondrial pellet was washed three times in mitochondrial isolation buffer and recentrifuged at 6500 x g. The final mitochondrial pellet was resuspended in isolation buffer without DTT and protease inhibitors. The cytosolic fraction was obtained by centrifugation of the saved supernatant at 100 000 x g at 4°C for 40 minutes.

2.5.2.3. GST pull-down of SUMO1 and Ubc9

The rat liver and bovine heart cytosols obtained without NEM (section 2.5.2.2) were pre-cleared with pre-equilibrated glutathione-sepharose beads (100µl beads per 1mL cytosol) for 2 hours at 4 °C with rotation. 40 µg of recombinant GST:DRP1, GST:DRP1(K38E) and GST alone proteins bound to glutathione-sepharose beads were added to each of three samples of 1mg pre-cleared rat liver cytosol and bovine heart cytosol supplemented with 20mM ATP. The six reactions were incubated overnight at 4 °C with rotation. The following day, 20 mM NEM was added to the samples for an additional 2-hour incubation at 4 °C with rotation to inhibit deSUMOylation enzymes. Next, the beads were collected at 800 x g and washed 3 times with 5 bead volumes of cold wash buffer (20 mM Hepes 250 mM NaCl, 5mM $MgCl_2$, 1 mM DTT, 10 µM GDP and 20mM NEM). One bead volume of SDS-PAGE sample buffer (with 100mM DTT) was added to the samples and they were boiled for 10 min at 95°C. The samples were briefly centrifuged and the supernatant was loaded and run on a 4-20% gradient gel (Tris-Glycine Precast gels, Invitrogen). After sufficient protein separation, the proteins were transferred to nitrocellulose membrane and analyzed by Western Blot. The membranes were blocked with PBS/Tween/5%milk for 1 hour. The rat liver cytosol pull-down was probed with a monoclonal anti-SUMO1 antibody (Zymed Laboratories, San Fransisco, CA)(1:200 dilution) and the bovine heart cytosol pull-down was probed with a monoclonal anti-Ubc9 antibody (Transduction Laboratories, Lexington, KY) (1:300 dilution) for 30 minutes. The membranes were washed in blocking solution for 5 times 5 minutes and then incubated with a goat anti-mouse-HRP secondary antibody (Upstate Biotechology, Lake Placid, NY) (1:5000 dilution) for 30 minutes. The membranes were washed in

PBS/Tween for 5 times 5 minutes and incubated for 1 minute with ECL chemiluminescent substrate. The membranes were exposed to film and developed.

2.5.3. His6 pull-down assays

Cos7 cells were grown to confluence in 3 x 10 cm_2 dishes in regular growth media. The cells were transiently cotransfected (Lipofectamine 2000, Invitrogen) with either DRP1:YFP/His6:SUMO1, His6:DRP1/ YFP:SUMO1 or His6:LacZ/DRP1:YFP. Following 16 hours transfection, the media was aspirated, the cells were scraped and washed 3 times in ice-cold 1 X PBS, and solubilized in buffer containing 1%Tx-100, 10 mM HEPES, pH 7.4, 150 mM NaCl, 0.5 mM EDTA, 2 mM $MgCl_2$, and protease inhibitor cocktail +/- 20 mM NEM for 30 minutes at 4 °C. Solubilized lysates were precleared at 13,000 x g for 30 minutes and incubated with Nickel-agarose beads (QIAGEN, Mississauga, ON) for 1.5 hours at 4 °C with rotation. The beads were centrifuged at 800 x g and the unbound, flow-through material was collected. The beads were subsequently washed 5 times with 10 bead volumes of lysis buffer containing 10 mM imidazole (QIAGEN, Mississauga, ON). The proteins bound to the column were eluted 100 mM imidazole in lysis buffer. For both experiments, SDS sample buffer was added to the samples (whole cell lysates, flow-throughs and bound proteins) and they were boiled for 5 minutes. The samples were then loaded and run on a 4-20% SDS-PAGE, transferred onto nitrocellulose, analyzed by Western Blot (as previously described for the GST pull-down) and probed with anti-DRP1 (1:500 dilution), polyclonal anti-SUMO1 (1:200 dilution) and anti-FP (fluorescent protein) (1:300 dilution) antibodies.

2.6 Subcellular localization of SUMO1, Ubc9 and TOPORS

2.6.1. Cellular fractionation

Nuclear, cytosolic and mitochondrial levels of SUMO1 were determined biochemically using subcellular fractionation. Twenty 10 cm dishes of Cos7 cells were grown to 80% confluence. The growth media was aspirated and the cells were washed once with ice-cold 1XPBS, scraped, pooled into 2 samples and harvested at 1000 rpm (Sorvall RT 6000D). The cell pellets were washed once with 100 volumes of mitochondrial isolation buffer (220 mM mannitol, 68 mM sucrose, 80 mM KCl, 0.5 mM EGTA, 2 mM Mg(Ac)2, 10 mM HEPES pH 7.4, and 1X CLAAAP). The two samples were collected by centifugation at 1000 rpm (Sorvall RT 6000D) and resuspended in 5 volumes of isolation buffer (with one sample containing 20mM NEM in the buffer). The cells were broken by 10-15 passages through a pre-cooled cell cracker (EMBL, Germany) using ball bearing size 8.002 mm. The samples were spun at 1500 x g at 4°C for 20 minutes and the post-nuclear supernatant (PNS) was collected. The pellet was washed again with ten volumes of buffer and both the pellet and supernatant were respun at 1500 x g at 4°C for 20 minutes. The final washed pellet was collected as the nuclear/unbroken cells fraction. The cleared PNS was centrifuged at 8000 x g at 4°C for 30 minutes to collect the mitochondrial fraction. The mitochondrial pellet was washed with 10 volumes of mitochondrial isolation buffer and recentifuged at 8000 x g at 4°C for 30 minutes to ensure a pure mitochondrial fraction. Finally, the post-mitochondrial supernatant was cleared at 100 000 x g at 4 °C for 30 minutes and collected as the cytosolic fraction. Nuclear, cytosolic and mitochondrial samples (with and without NEM) were resuspended in SDS sample buffer, boiled for 15 minutes and run on a 4-20% gradient gel (pre-cast

gel, Invitrogen). The proteins were transferred to nitocellulose membrane and probed with polyclonal anti- SUMO1, monoclonal anti-DRP1, and polyclonal TOM 20 as a mitochondrial control (a generous gift from Gordon Shore, McGill University, Montreal). Unfortunately, the fractionation could not be probed for TOPORS due to poor antibodies.

2.6.2. Live cell video fluorescence microscopy

To visualize the subcellular localization of Ubc9, TOPORS and SUMO1 and to study their dynamics with the mitochondria, they were analyzed as fluorescent fusion proteins with a mitochondrial matrix marker. Cos 7 cells seeded on glass coverslips in the wells of 24-well plates were co-transfected with each of pEYFP:SUMO1, pEYFP:Ubc9 and pEGFP:TOPORS (kindly provided by Eric Ruben, New Jersey) along with either pOCT:CFP (in combination with YFP) or pOCT:DsRed2 (in combination with GFP) as described in section 2.1. 24 hours post-transfection, the coverslips were mounted in live cell metal chambers in regular growth media supplemented with 20mM HEPES pH 7.4. The subcellular localization of Ubc9 was visualized using the CFP/YFP dual pass filter by excitation of Ubc9-YFP at 514nm and excitation of the OCT-CFP with 434nm. The intracellular localization of TOPORS was assessed by excitation of TOPORS-GFP and OCT-DsRed at 489nm and 558nm respectively through a GFP/DsRed beam splitter (Optical Insights, Santa Fe, NM). Finally, SUMO1 localization was determined by excitation of YFP:SUMO1 and OCT:CFP at 514nm and 434nm respectively through the CFP/YFP dual pass filter. High exposure levels of YFP:SUMO1 were used to better resolve cytosolic staining. To understand cytosolic SUMO1 dynamics, movies were recorded of YFP:SUMO1 and OCT:CFP cotransfected cells by excitation of the CFP at

434nm for 500ms, followed by excitation of the YFP at 514nmm for 150ms with a 4000ms delay between frames.

2.6.3. Immunofluorescence microscopy

Cos 7 cells seeded on glass coverslips in the wells of 24-well plates were grown to 80% confluence in regular growth media. Cells were transiently cotransfected with YFP:SUMO1 and OCT:DsRED2 (Lipofectamine 2000, Invitrogen). 24 hours post-transfection, cells were immunolabeled for endogenous DRP1. Growth media was aspirated and cells were washed twice with 1X ice-cold PBS. Cells were fixed with 3% paraformaldehyde (PFA) for 10 minutes at room temperature, then washed twice with PBS. Residual PFA was quenched with 50mM ammonium chloride for 30 minutes and the cells were again washed twice in PBS. Cells were permeablized with 0.1% TX-100 for 2 minutes and subsequently washed in PBS and incubated with 10% fetal bovine serum (FBS) for 60 minutes at room temperature. The cells were incubated with primary antibodies, anti-DRP1 (1:250 dilution in 5% FBS) for 20 minutes at room temperature and then washed times 5 minutes each with 10% FBS. They were then incubated with using Alexa 350 conjugated secondary anti-mouse antibodies for 20 minutes at room temperature and washed 5 times 5 minutes each with 10% FBS. The coverslips were rinsed with water, mounted on glass slides and sealed with Movial. The triple labeled cells were visualized using a Fura filter (Chroma, Rockingham, VT) (excitation of 350nm for DRP1), and a CFP/YFP/DsRED triple pass filter (Chroma, Rockingham, VT) (excitation of 514nm for YFP and 558 for DsRED2).

2.7 Functional analysis of SUMOylation in mitochondrial fission

2.7.1. Mitochondrial morphology with SUMO1 overexpression

Cos7 cells transiently co-transfected with 1μg of pOCT-CFP and each of YFP vector alone, SUMO1-YFP and SUMO1ΔC5-YFP were mounted in live cell metal chambers, 24 hours post-transfection, with regular growth media supplemented with 20mM HEPES pH 7.4 and prepared for quantification of mitochondrial phenotype. For unbiased analysis of mitochondrial morphology, transfected cells were first found by searching in the YFP channel for expression. Once YFP, SUMO1-YFP and SUMO1ΔC5-YFP expressing cells were located, mitochondrial phenotype was noted, after switching to the CFP channel, as tubular, rod-like or fragmented. A total of 552, 576 and 357 transfected cells were analyzed for YFP, SUMO1-YFP and SUMO1ΔC5-YFP over-expressing cells respectively.

2.7.2. Changes in DRP1 protein expression with SUMO1 overexpression

Three 175cm2 flasks of Cos7 cells were grown to confluence and transiently transfected with each of YFP:DRP as control , YFP:SUMO1 and YFP:SUMO1ΔC5 (Lipofectamine 2000, Invitrogen). 16 hours post-transfrection, the cells were harvested by centrifugation at 3000 rpm and resuspended in solubilization buffer (1%Tx-100, 10 mM HEPES, pH 7.4, 150 mM NaCl, 0.5 mM EDTA, 2 mM $MgCl_2$, and protease inhibitor cocktail mentioned above) in the presence and absence of 20 mM NEM. The cells were incubated on ice for 1.5 hours and the lysates were cleared 13 100 x g. 50 μg of total extracts were loaded on a 6% SDS-PAGE, transferred to nitrocellulose and analyzed by Western blot using anti-DRP1 antibodies (1:500 dilution). Ponceau Red (BioRAD, Mississauga, ON) staining was used to determined total protein content of the samples.

3. Results

3.1 Mitochondrial fission: steady state versus apoptosis

Under normal growth conditions in all cells, mitochondrial fission and fusion are in dynamic equilibrium. **Figure 9** shows a steady state Cos 7 cell transfected with OCT YFP to label the mitochondrial matrix. The mitochondria are tubular and well distributed throughout the cytosol (top panel). The series of bottom panels illustrates a mitochondrial fission event occurring in this cell. It is clear that this process involves a degree of mitochondrial elongation and membrane stretching. Yet, the entire process of fission is relatively rapid, taking approximately 1 minute (panels 150-210 sec.) to complete full membrane separation (**Supplementary movie 2**). At any given moment, approximately 2-3 fission events can be seen in an entire cell. However, the number of fission events occurring at a particular moment depends on the status of the cell and can change in response to stimuli. For example, induction of apoptosis causes clustering and increased fragmentation of mitochondria (data not shown and see section 3.1.1). This was initially observed when cell death was triggered in KB cells using Fas antigen and the dynamics of the cell was monitored by video microscopy for 3 hours. These observations prompted additional studies aimed at addressing the possibility that mitochondrial fission, and DRP1 recruitment, is stimulated during apoptosis and that mitochondrial fission may play a role in the progression of apoptosis. To examine these issues, two experiments were performed.

3.1.1. DRP1 recruitment to mitochondria is stimulated during apoptosis

DRP1 recruitment to mitochondria was studied during programmed cell death. When Cos7 cells over-express DRP1 CFP under normal conditions, the DRP1 CFP protein is mainly cytosolic and very little is recruited to mitochondria, consistent with

Figure 9. Mitochondrial fission occurs under steady state conditions in Cos7 cells. African green monkey kidney (Cos7) cells were transiently transfected with pOCT-YFP to label the mitochondrial matrix and analyzed 24 hours after transfection. The cells were mounted in a metal chamber in regular growth media supplemented with 20mM HEPES pH 7.4 and maintained at 37°C during analysis. A movie of the dynamics of the mitochondria (**Supplementary movie 2**) was recorded by excitation of the cells at 514nm for 200ms through a CFP/YFP dual pass filter for 74 frames with a 2 second delay between frames. Shown is the 4 minutes of the movie highlighting a single mitochondrion undergoing a fission event.

Figure 9.

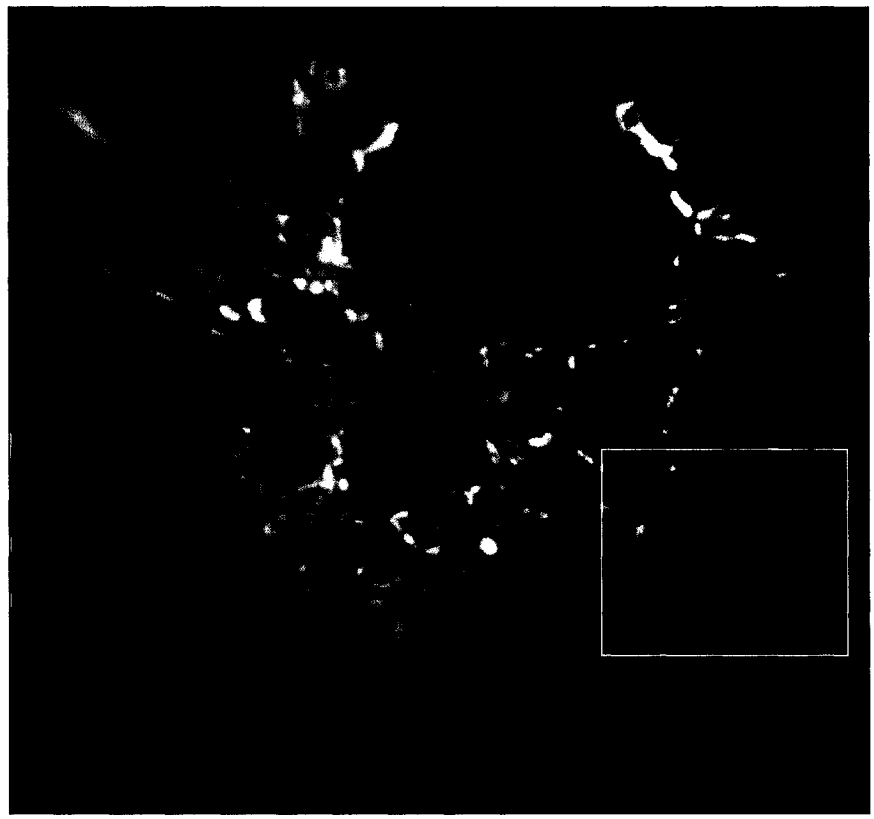

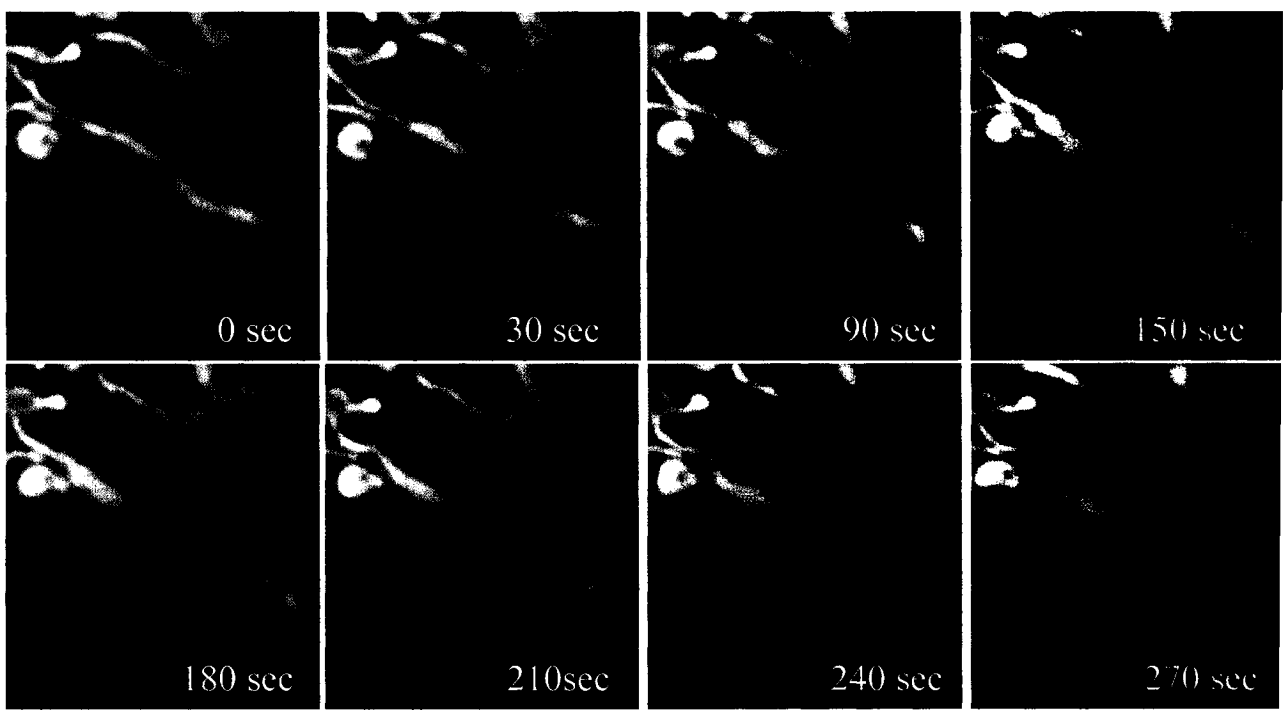

Figure 10. Overexpressed DRP1 CFP is mainly cytosolic and does not alter mitochondrial morphology, while overexpressed DRP(K38E) forms large intracellular aggregates and is dominant interfering resulting in interconnected mitochondria. Cos7 cells were transiently co-transfected with either pECFP:DRP1 and pOCT:YFP or pECFP:DRP1(K38E) and OCT:YFP. 24 hours post-transfection, the cells were mounted in a metal chamber in regular growth media supplemented with 20mM HEPES pH 7.4 and maintained at 37°C during analysis. DRP1 distribution (Ai and Bi) and mitochondrial morphology (Aii and Bii) were visualized by excitation of the sample at 434nm and 514nm respectively. Notably, DRP1 CFP has mainly a cytosolic distribution (Ai) while DRP1(K38E) aggregates (Bi). The mitochondrial morphology is unchanged form wild-type cells upon overexpression of DRP1 CFP (compare Aii, with Figure 9 top panel). However, overexpression of DRP1(K38E) results in a network of mitochondrial tubules (Bii) that eventually collapse in a perinuclear region (see also **Supplementary movie 3**).

Figure 10.

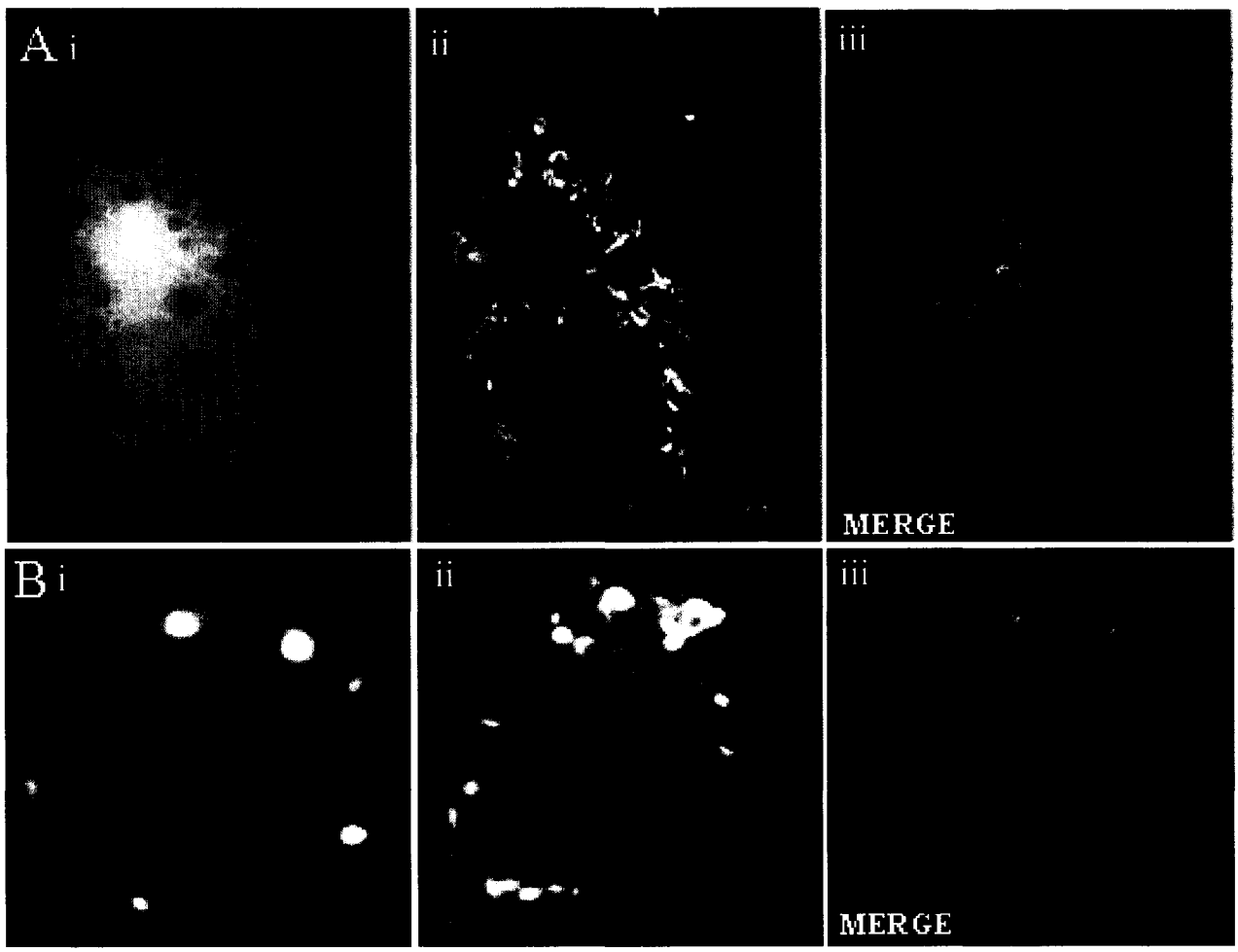

Figure 11. Staurosporine induced apoptosis of Cos7 cells stimulates DRP1 recruitment and causes increased mitochondrial fragmentation. Cos7 cells were transiently co-transfected with pECFP:DRP1 and pOCT:YFP. After 24 hours, apoptosis was triggered with 1.2 μM STS, the cells were mounted in a metal chamber in the STS containing media supplemented with 20mM HEPES pH 7.4 and the cells were maintained at 37°C during analysis. In panel A, an image of a single cell approximately 30 minutes following induction of apoptosis shows substantial DRP1 recruitment to and oligomerization on the mitochondria. The same cell 2.5 hours later is shown in panel B with completely fragmented mitochondria. The insert illustrates the localization of DRP1 to the site of fission.

Figure 11.

A

B

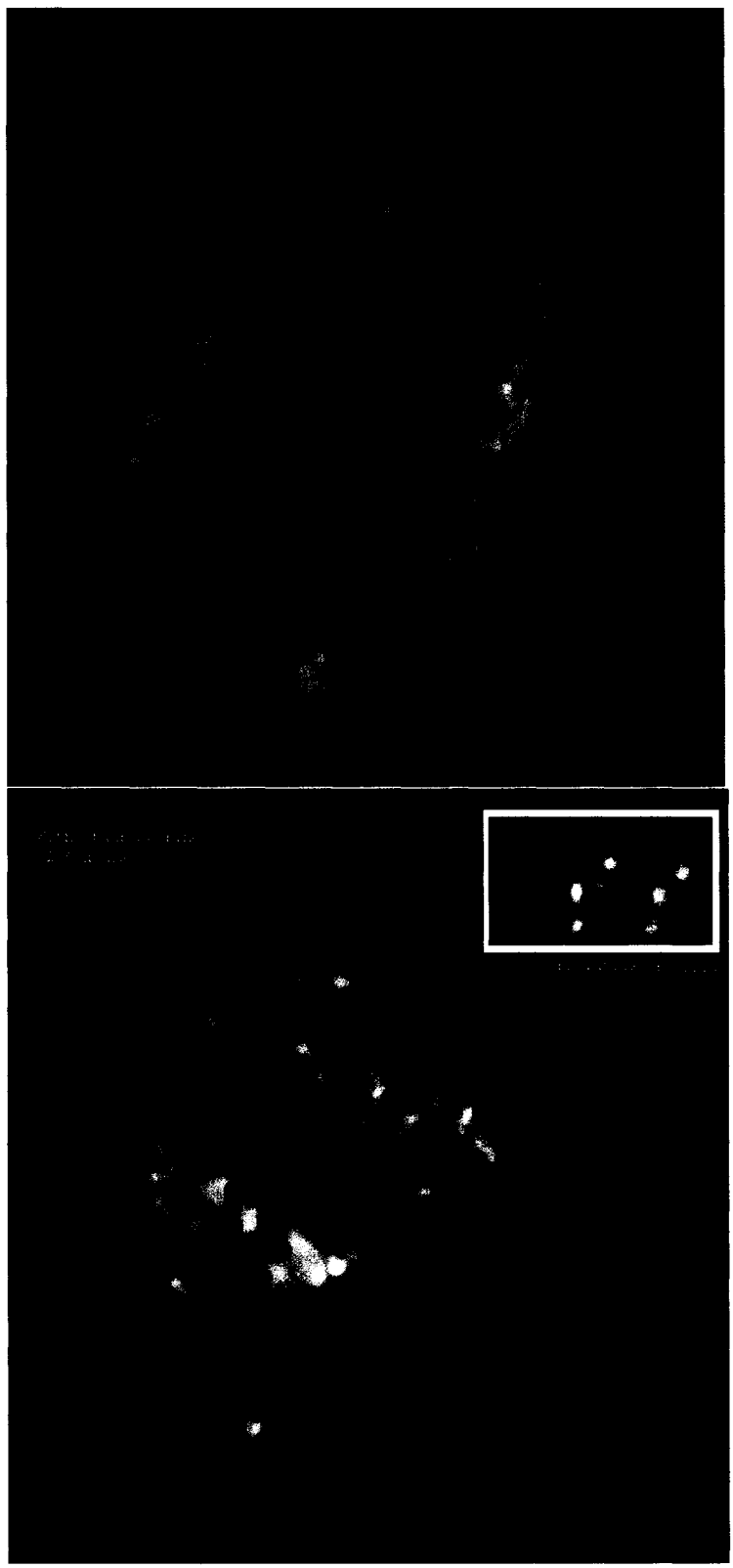

previous reports (1) (**Figure 10**, panel A). However, upon induction of apoptosis with staurosporine (STS), a general protein kinase inhibitor, the majority of cytosolic DRP1 CFP is recruited to mitochondria and subsequently, most of the mitochondria appear fragmented. As seen in panel A of **Figure 11**, DRP1 is oligomerized around most mitochondrial tubules shortly after the induction of apoptosis. The same cell 2.5 hours later has significantly fragmented mitochondria (**Figure 11**, panel B). The insert highlights the localization of DRP1 CFP to the point of fission, indicating that the increased fragmentation is due to increased DRP1 recruitment. Since this experiment confirmed that apoptosis stimulates DRP1 recruitment to mitochondria, we next sought to determine if apoptosis could be blocked by inhibiting DRP1 recruitment and, consequently, inhibiting mitochondrial fission.

3.1.2. Over-expression of dominant negative DRP1(K38E) inhibits apoptosis

DRP1 (K38E) is an analogous mutation to the Dynamin 1 (K44A) dominant negative mutation that inhibits clathrin-mediated endocytosis. Over-expression of DRP1 (K38E) also results in a dominant negative phenotype where mitochondrial fission is blocked. **Figure 10** illustrates the differences in protein staining and mitochondrial phenotype seen by over-expression of DRP1 CFP and dominant negative DRP1 (K38E) CFP. Notably, the DRP1 (K38E) CFP protein forms large cytosolic aggregates incapable of recruitment to the mitochondria. This is in contrast to the cytosolic staining of DRP1 CFP (**Figure 10**, compare Ai and Bi). In addition, the mitochondria in DRP1 (K38E) CFP over-expressing cells are significantly interconnected (**Figure 10**, compare Aii and Bii) and eventually collapse into a perinuclear region (see **Supplementary Movie 3**). To determine if blocking mitochondrial fission affects the progression of programmed cell

death, apoptosis assays were performed on Cos7 cells transfected with wild-type DRP1 CFP and DRP1 (K38E) CFP. The activation of Caspase-3, a final effector of the apoptotic pathway, was used to quantify cell death. **Figure 12** compares the relative level of Caspase-3 activation after incubation with STS under conditions of normal or blocked mitochondrial fission. Under normal conditions, basal levels of Caspase-3 activation in both DRP1 CFP and DRP1 (K38E) CFP over-expressing cells are low. When apoptosis is triggered, Caspase-3 activation increases approximately 10-fold in DRP1 CFP over-expressing cells. However, such an increase is not seen in DRP1 (K38E) CFP overexpressing cells. Instead, DRP1 (K38E) overexpression appears to have a protective effect against apoptosis as shown by the partial inhibition of Caspase-3 activation. The activation that is seen is likely due to untransfected cells in the sample. These two experiments suggest that recruitment of functional fission machinery to mitochondria is required for the progression of programmed cell death. To understand how this recruitment is regulated, a yeast-two-hybrid screen was performed to identify DRP1 interacting proteins that may play a role in mediating DRP1 localization to mitochondria.

3.2 Yeast two-hybrid screen

3.2.1. Identification of DRP1 interacting clones.

Transformation of the L40 yeast strain with the pLEXA2:DRP1 bait was successful, as demonstrated by yeast growth on SD agar (-Trp) plates. Introduction of DRP1 into the yeast did not result in auto-activation of reporter genes, as determined by lack of yeast growth on SD agar (-Leu, -His) plates. The LEXA2 DRP1 fusion protein

Figure 12. Overexpression of DRP1 (K38E) inhibits apoptosis. Cos7 cells were transiently transfected with either pECFP:DRP1 or pECFP:DRP1 (K38E). 36 hours post transfection, half of the cell samples were washed with 1XPBS and incubated with 1.2μM STS for 2.5 hours. All the cells were then collected by centrifugation, washed and lysed on ice (50 mM Tris-HCL pH 7.5, 1% NP-40, 0.25% sodium deoxycholate, 150 mM NaCl, 1mM EGTA) for 15 minutes. The protein concentrations of the lysates were equalized with lysis buffer and incubated, in triplicate, with 2mM DTT and 0.05μM of Caspase-3 fluorometric substrate for 10 minutes at room temperature. The fluorescence of the Caspase-3 substrate (excitation= 380nM and emission=460nm) was then determined as arbitrary units (AU) of Caspase-3 activity. Transfection efficiency of wild type and mutant DRP1 are comparable. Notably, overexpression of DRP1 (K38E) has a protective effect on the progression of apoptosis as shown by the 2-fold decrease in Caspase-3 activation upon apoptotic stimuli.

Figure 12.

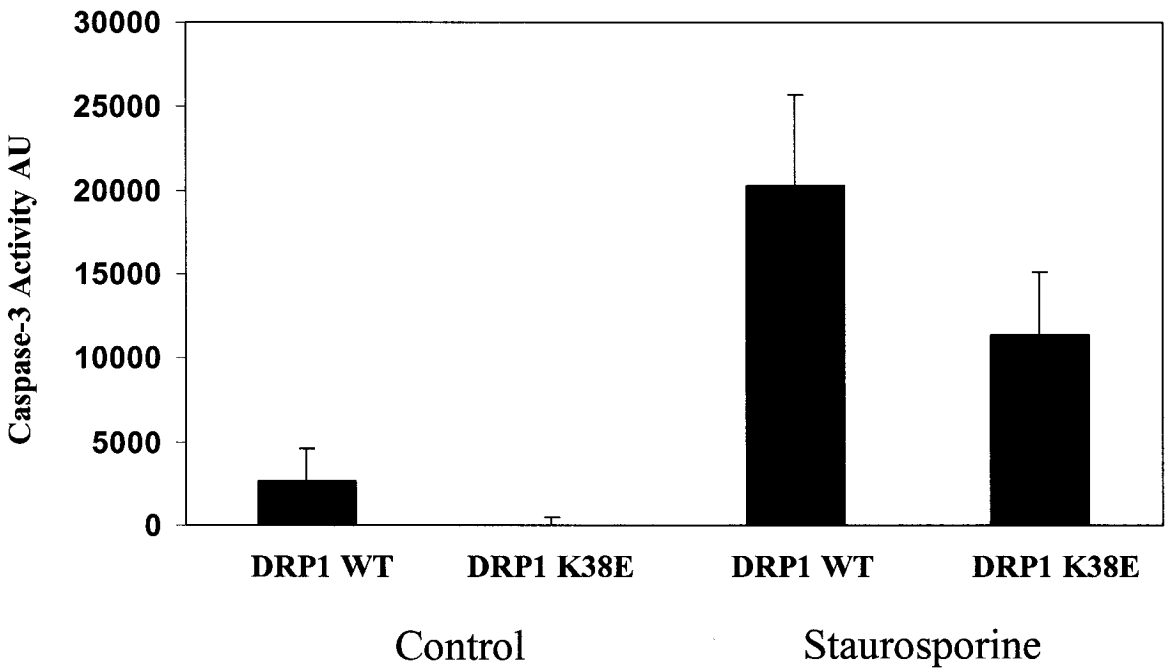
30000
25000
20000
15000
10000
5000
0
Caspase-3 Activity AU
DRP1 WT
DRP1 K38E
DRP1 WT
DRP1 K38E
Control
Staurosporine

Figure 13. LEXA2:DRP1 protein is highly expressed in L40 yeast. Yeast transformed with pLEXA2:DRP1 and pLEXA2 alone were grown to an OD_{600} of 0.6-0.8 in liquid SD (-Trp) media. The yeast were collected, washed and broken by snap freezing and thawing in liquid nitrogen and subsequent incubation at 60°C. The yeast were solubilized in cracking buffer (8M Urea, 5% w/v SDS, 40mM Tris-HCL pH 6.8, 0.1 mM EDTA, 0.4mg/ml bromophenol blue, deionized water) containing a protease inhibitor cocktail, heated at 70°C for 10 min, and vortexed in acid-washed glass beads. The supernatants were cleared by centrifugation, briefly boiled at 100°C, and run on a 10% SDS-PAGE. The proteins were transferred to nitrocellulose and probed with anti-LexA antibodies. The LEXA2:DRP1 fusion protein is expressed well in the yeast and runs at the expected molecular weight of ~105kDa.

Figure 13.

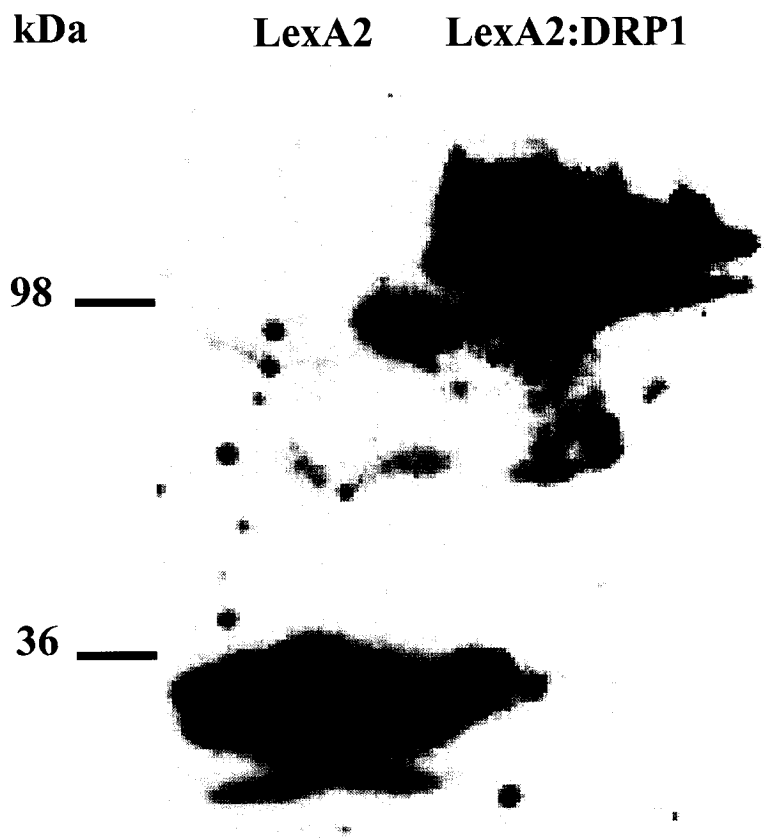

was expressed at high levels in the L40 yeast as shown by Western Blot analysis (**Figure 13**) using anti-LexA antibodies. The full fusion product was expressed and corresponded to the correct calculated molecular weight of 105 kDa. The LEXA2 control also shows a band at an appropriate molecular weight of 25 kDa. LEXA2 DRP1 transformed yeast were grown in large scale in order to screen the HeLa library. 1 x 10^6 transformants (of a 6 x 10^6 total clones) were isolated during the final yeast-two hybrid screen indicating that $1/6^{th}$ of the library was tested.

Positive yeast clones were detected by two reporter assays: yeast growth and both qualitative and quantitative β-galactosidase assays. Of the 1 x 10^6 transformants screened, 1050 yeast colonies grew on SD agar (-Trp, -Leu, -His) plates. These 1050 clones were then tested for β-galactosidase activity by filter-lift assay using yeast co-transformed with activated Rab5Q79L and its known effector, Rabaptin-5, as a positive control. This assay revealed that 51 of these clones were positive for the second reporter gene. Quantification by the β-galactosidase activity assay of these 51 clones enabled assessment of the relative strength of the yeast two-hybrid interaction (**Figure 14**). There was a broad range of β-galactosidase activity levels among the 51 clones. The values obtained were within a reasonable range for a positive yeast two-hybrid interaction when compared to the known interaction between Rab5Q79L and its effector Rabaptin-5 (**Figure 15**). Clones chosen for sequencing were mainly those with the highest β-galactosidase activity levels. Of these 51 positive clones, 16 clones were sequenced. The identities of these clones along with the general results of the yeast two-hybrid screen are shown in **Table 2**. 68% of the 16 clones sequenced were proteins known to be involved in the SUMOylation pathway (SUMO1 and Ubc9). Since proteins of the SUMOylation

Figure 14. Relative β-Galactosidase activity of the 51 positive yeast two-hybrid clones. Yeast clones positive for both reporter genes were grown in liquid SD (-Trp,-Leu) to an OD_{600} 0.5-0.8. The yeast were collected in triplicate by centrifugation and the cells were washed in Z buffer. The yeast pellet was resuspended in Z buffer and lysed by freeze/thaw cycles of liquid nitrogen/37°C. Once permeabilized, 4mg/ml of ONPG in Z buffer was added to the samples and the reaction was incubated at 30°C until the appearance of a yellow colour. The reaction was terminated with 1M Na_2CO_3. The yeast debris was cleared by centrifugation and the absorbance was read at 420nm. The strength of the protein-protein interaction is represented by the relative β-Galactosidase activity of the clones. The interaction between the positive control of activated Rab5Q79L and its effector Rabaptin-5 is generally found around 150-200 β-Gal units (see Figure 15) indicating that the majority of the yeast two-hybrid interactions found are significant. Samples were assayed in triplicate and results are shown with their standard error.

Figure 14.

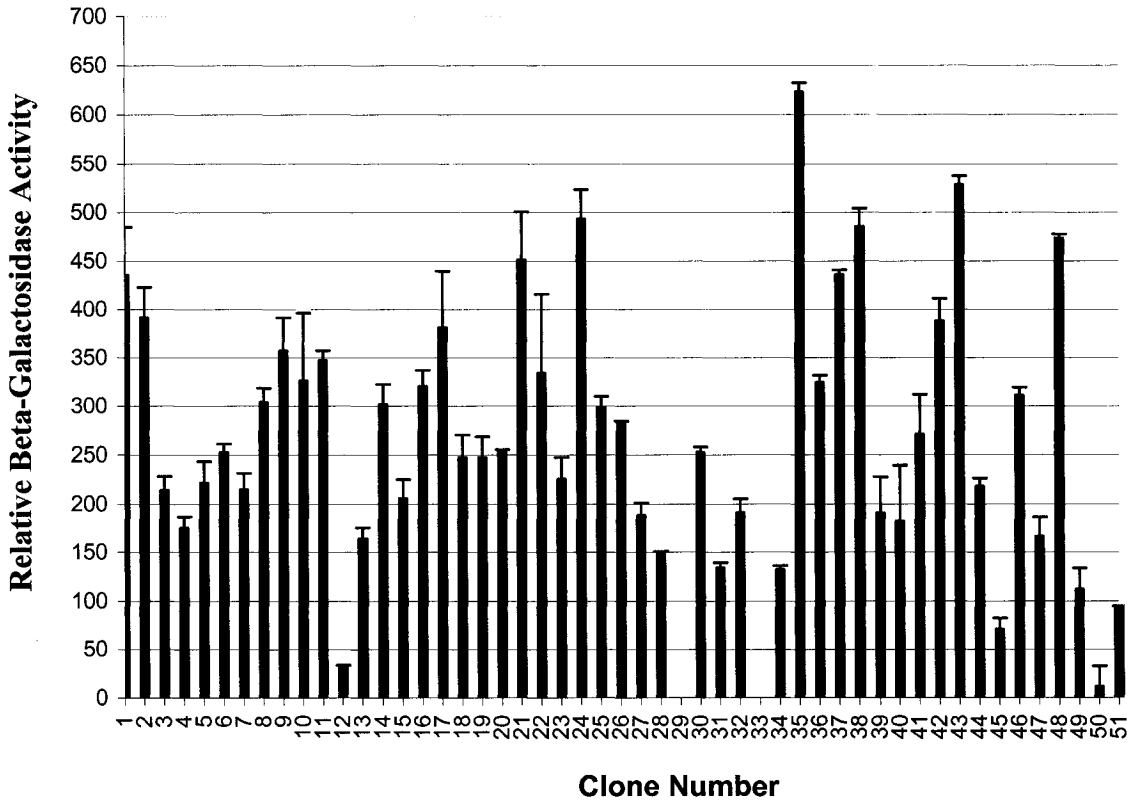
Relative Beta-Galactosidase Activity
700
650
600
550
500
450
400
350
300
250
200
150
100
50
0
1 2 3 4 5 6 7 8 9 10 11 12 13 14 15 16 17 18 19 20 21 22 23 24 25 26 27 28 29 30 31 32 33 34 35 36 37 38 39 40 41 42 43 44 45 46 47 48 49 50 51
Clone Number

Table 2. Results of the yeast two-hybrid screen. Listed are the results of the yeast two-hybrid screen including the efficiency of the screen, results of the reporter gene assays and identities of some of the positive clones with the number of times they were isolated from the screen and their NCBI accession numbers.

Table 2.

Full Library	**6 x 10^6 transformants**
Transformants screened	**1 x 10^6**
HIS positive clones	**1050**
HIS + *Lac* positive clones	**51**
Clone identities (number of times pulled out of screen) (NCBI accession number)	**Ubc9 (7) (BT006932)**
	SUMO1 (4) (BT006632)
	TOPORS, p53 RING finger binding protein (2) (AB045732)
	BRD7, bromodomain protein (2) (AF152604)
	Daxx (1) (AB015051)

Figure 15. Comparison of the relative strength of select DRP1 protein-protein interactions from the yeast two-hybrid screen. L40 yeast cotransformed with pLEXA2:DRP1 and each of pGAD:DRP1, pGAD:Ubc9, pGAD:SUMO1, pGAD:Topors, and pGAD:Rabaptin-5 (negative control) were quantitatively assayed for relative β-galactosidase activity (see section 2.4.5.3) along with yeast cotransformed with pLEXA:Rab5Q79L and pGAD:Rabaptin-5 (positive control). Samples were assayed in triplicate and results are shown with their standard error.

Figure 15.

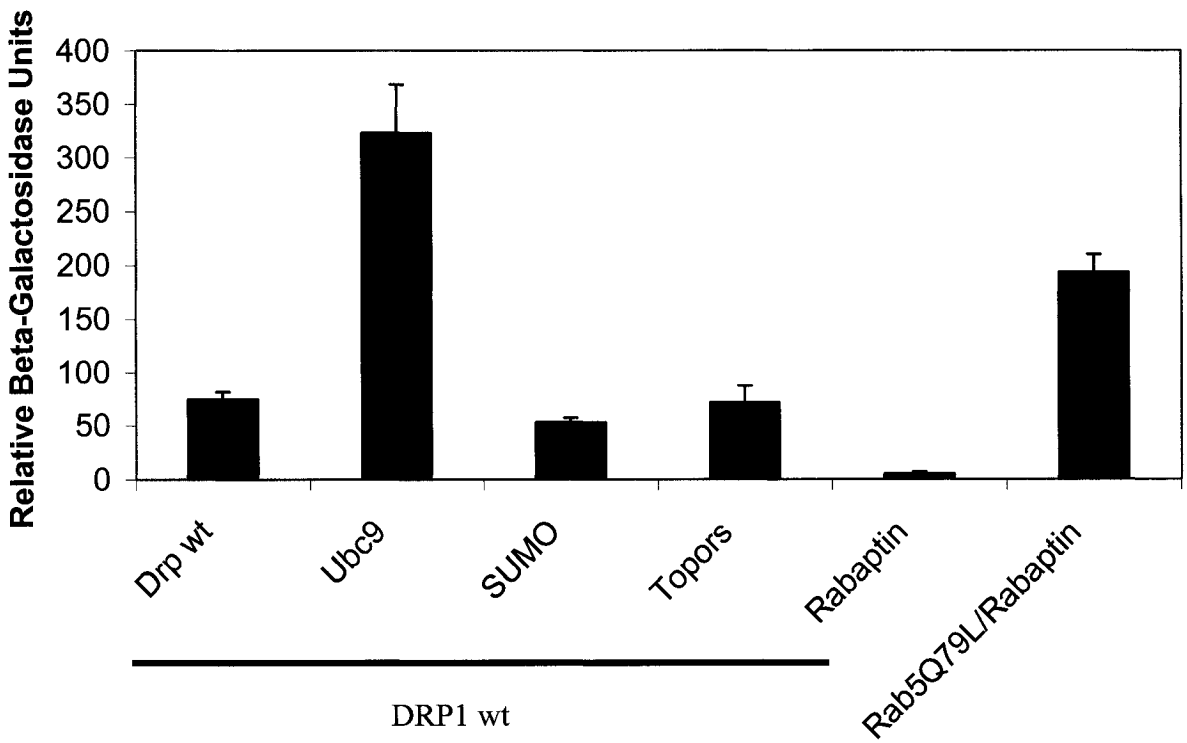
Relative Beta-Galactosidase Units
400
350
300
250
200
150
100
50
0
Drp wt
Ubc9
SUMO
Topors
Rabaptin
Rab5Q79L/Rabaptin
DRP1 wt
Cotransformed

pathway have been shown to interact with the Mx family of dynamin-like proteins (115) and since SUMOylation plays a key role in the yeast *S. Cerevisiae* bud neck formation by septin GTPases, the two-hybrid interactions between DRP1and the proteins of this pathway were further investigated. An additional clone chosen for further study was TOPORS, a p53-binding ring finger protein. The decision to pursue this clone was based on evidence indicating an interaction between TOPORS and Mx proteins in a yeast two-hybrid system (115), the existence of a strong relationship between p53 and apoptosis (thereby potentially explaining the link observed between apoptosis and mitochondrial fission machinery) and unpublished data indicating that TOPORS is a SUMO1 E3 ligase for p53 (personal communication Eric Ruben, New Jersey) (suggesting that it may also be a SUMO1 E3 ligase for DRP1).

3.3 Specificity of protein-protein interactions

3.3.1. Yeast two-hybrid testing and fluorescence microscopy

The specificity of the interactions between DRP1 and the selected proteins from the yeast two-hybrid screen were verified using a negative control, Rabaptin-5, and the positive controls of DRP1 itself and Rab5Q79L + Rabaptin-5. The results of the β-galactosidase quantification (**Figure 15**) reveal specificity of the interactions between DRP1 and each of Ubc9, SUMO1 and TOPORS. As expected, DRP1 interacts with itself but does not interact with the negative control Rabaptin-5. The relative strength of the interaction between DRP1 and Ubc9, in particular, is striking in comparison to the Rab5Q79L + Rabaptin-5 control. To determine if the interaction between DRP1 and SUMO1 depends on the ability of SUMO1 to be conjugated, the interaction between

DRP1 and SUMO1 was compared to the interaction between DRP1 and the non-conjugatable form of SUMO1, SUMO1ΔC5. To verify that SUMO1ΔC5 is incapable of conjugation, its cellular distribution was examined by transient transfection of Cos7 cells with SUMO1ΔC5 YFP. Indeed, this form of SUMO1 cannot be conjugated as indicated by diffuse cellular staining (**Figure 16A**). This is in contrast to the distinct punctate staining of SUMO1 YFP in the nucleus, cytosol and along the nuclear envelope, as it is conjugated to a variety of proteins at these sites. **Figure 16 B** shows that there is no interaction between DRP1 and SUMO1ΔC5 in the yeast two-hybrid system, indicating that the two terminal glycines of SUMO1 are required for this interaction. To further address the specificity of the interactions, experiments were performed to map out the regions of interaction between DRP1 and each of Ubc9, SUMO1 and TOPORS. The specific area of interaction was examined by testing various DRP1 domain constructs for interaction. The constructs used were DRP1 (1-260), which isolates the GTPase domain, DRP1 (254-525), which isolates the middle domain, DRP1 (254-579), which isolates the middle domain along with a variable region in the Insert B, and finally, DRP1 (579-736), which isolates the GED domain (**Figure 17Ai)**). **Figure 17Aii** shows that only full length DRP1 is capable of association with SUMO1, Ubc9 and TOPORS in the yeast two-hybrid system. Since experiments aimed at identifying domain interactions did not provide any information regarding the general areas of interaction, point mutations in DRP1 were made in an attempt to identify exact amino acids responsible for the interactions. As mentioned previously, SUMO1 is covalently attached to its substrate via a substrate lysine residue that may or may not be part of a consensus sequence (ψKXE, where ψ represents a large hydrophobic amino acid) (116). Therefore, lysine residues

Figure 16. SUMO1 conjugation is required for DRP1 interaction. A) Cos7 cells were transiently transfected with each of pEYFP:SUMO1 and pEYFP:SUMO1ΔC5. 24 hours post-transfection, cells were mounted in a live cell metal chamber in regular growth media supplemented with 20mM HEPES pH 7.4. Cellular distribution of SUMO1 YFP and SUMO1ΔC5 YFP were determined by excitation at 514 nm through a CFP/YFP dual pass filter at 100X magnification. Note the punctate SUMO1 YFP staining in the nucleus and cytosol in contrast to the diffuse cellular staining of SUMO1ΔC5 YFP. **B)** L40 yeast were cotransformed with pLEXA2:DRP1 and each of pGAD:SUMO1, pGAD:SUMO1ΔC5 and pGAD:Rabaptin-5. Quantitative β-Galactosidase assays were performed as described in section 2.4.5.3 and the relative strength of the protein-protein interaction were compared. Samples were assayed in triplicate and the results are shown with their standard error. Note the loss of DRP1 interaction with the non-conjugatable SUMO1ΔC5.

Figure 16.

A

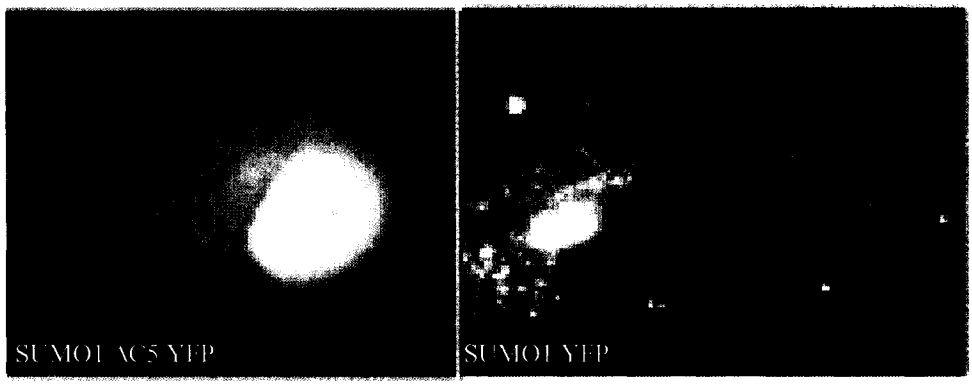
SUMO1 ΔC5 YFP
SUMO1 YFP

B

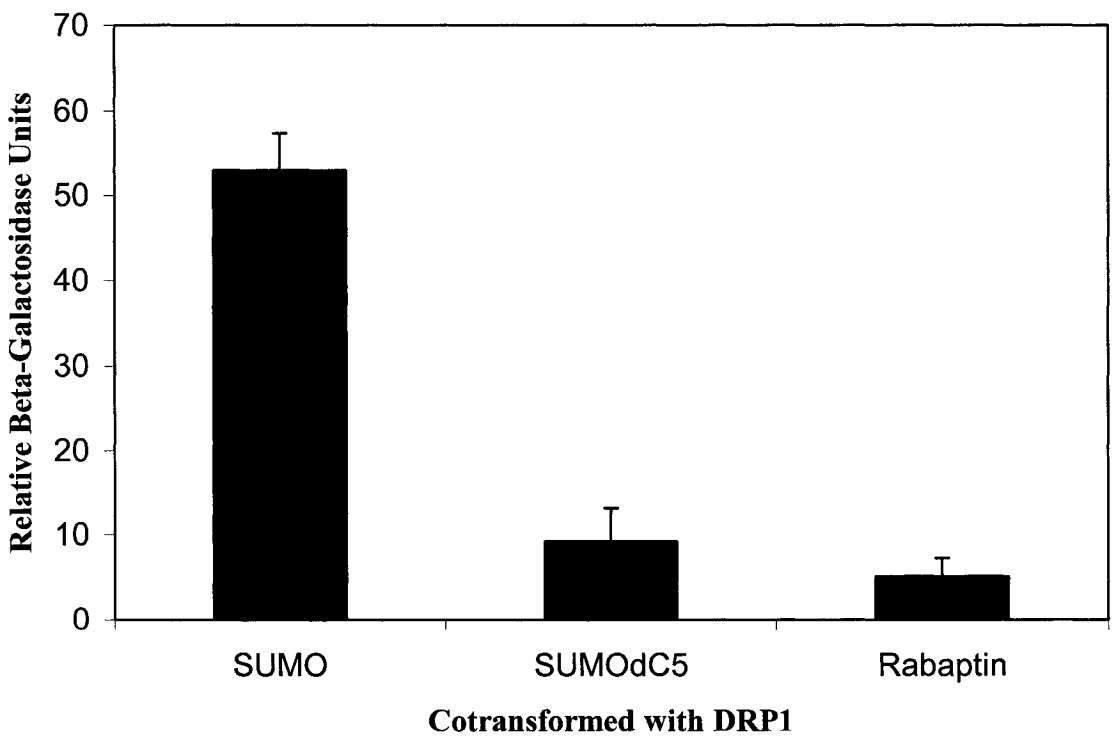
Relative Beta-Galactosidase Units
70
60
50
40
30
20
10
0
SUMO
SUMOdC5
Rabaptin
Cotransformed with DRP1

Figure 17. Specificity of DRP1 interactions. L40 yeast were cotransformed with combinations of constructs encoding GAL4 fusion products of Ubc9, SUMO1, SUMO1ΔC5, TOPORS and Rabaptin-5 and LEXA2 fusion products of **A)** DRP1, various DRP1 domain constructs (i) tested with the above proteins from the screen (ii) and Rab5Q79L + Rabaptin-5 (positive control) **B) (i)** DRP1, various DRP1 point mutants and Rab5Q79L + Rabaptin-5 (positive control) **(ii)** Overexpression of **(a)** DRP1 (K497V) CFP **(b)** and DRP1 (K597A) CFP in Cos 7 cells **C)** DRP1, the dominant negative GTPase deficient mutant DRP1 K38E and Rab5Q79L **D)** DRP1, Ubc9, SUMO1, TOPORS and Rab5Q79L + Rabaptin-5 (positive control). All cotransformed yeast were grown in liquid SD media (-Trp, -Leu) to log phase, quantitative β-galactosidase assays were performed and the results were compared.

Figure 17A.

i) **DRP1**

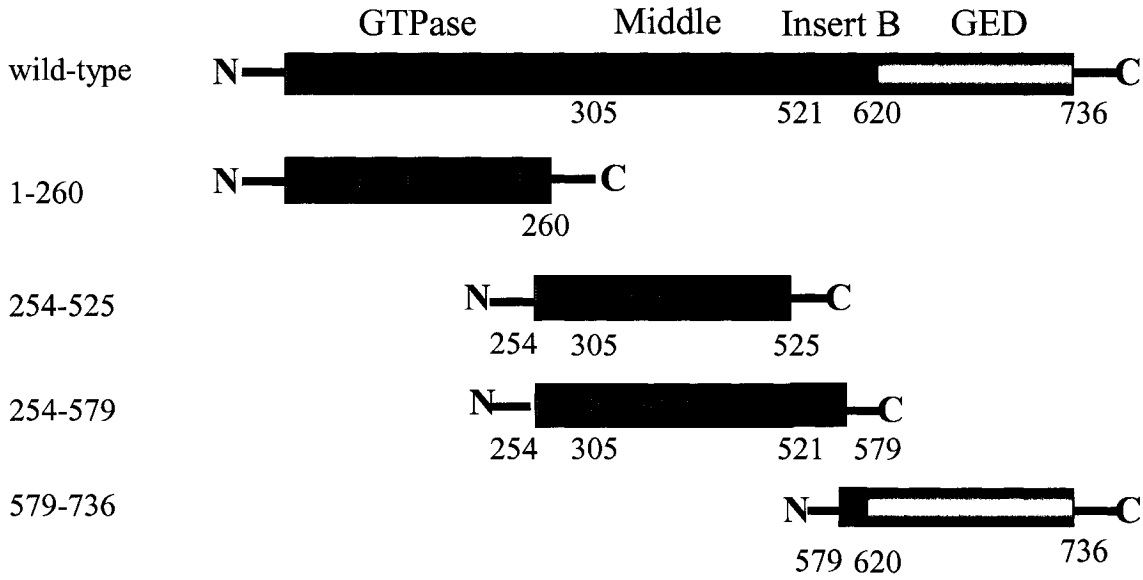

ii)

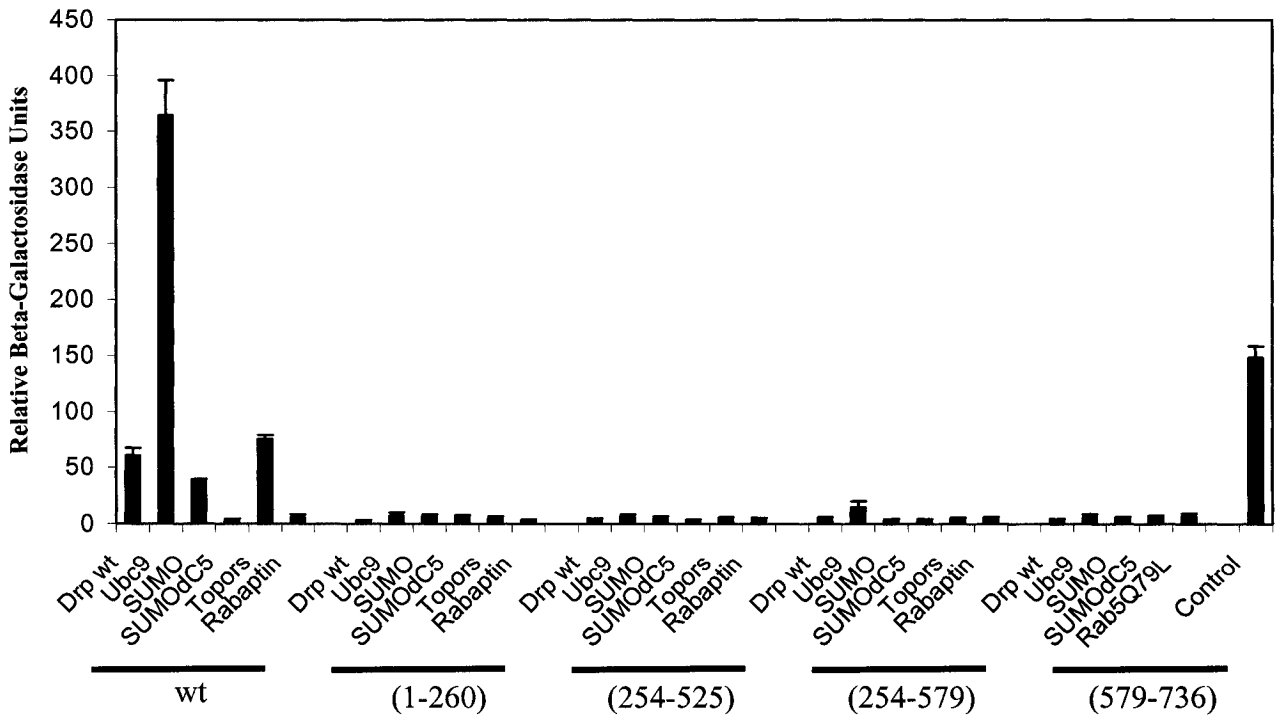

Figure 17B.

i)

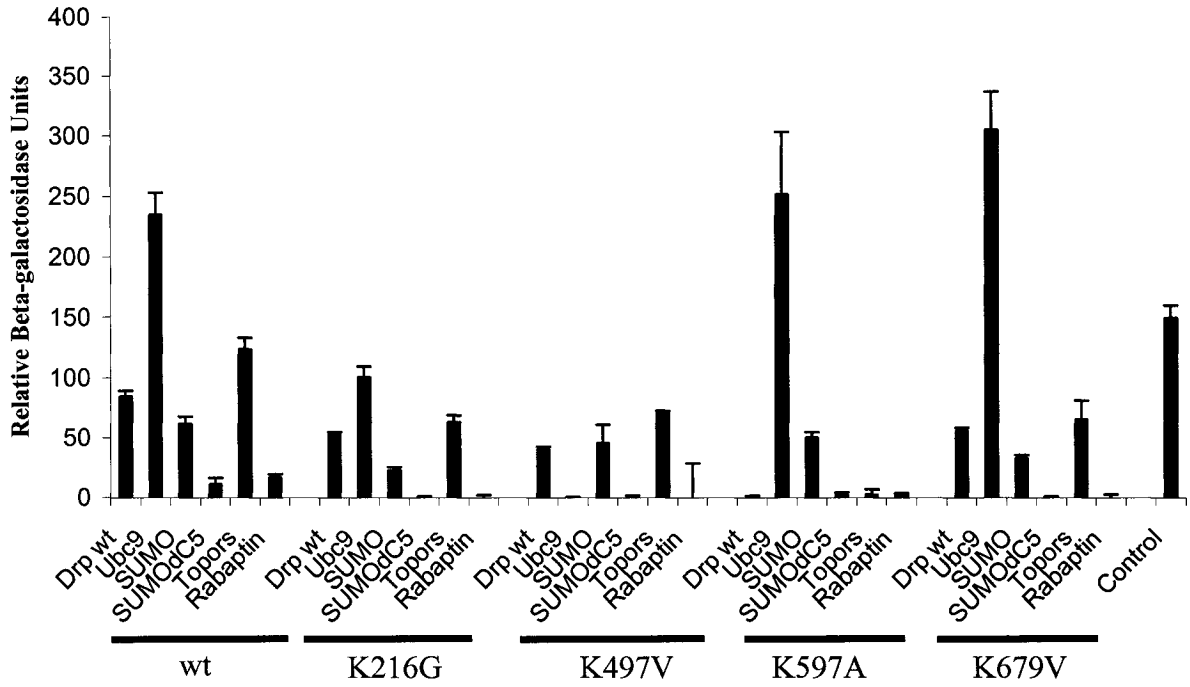

ii)

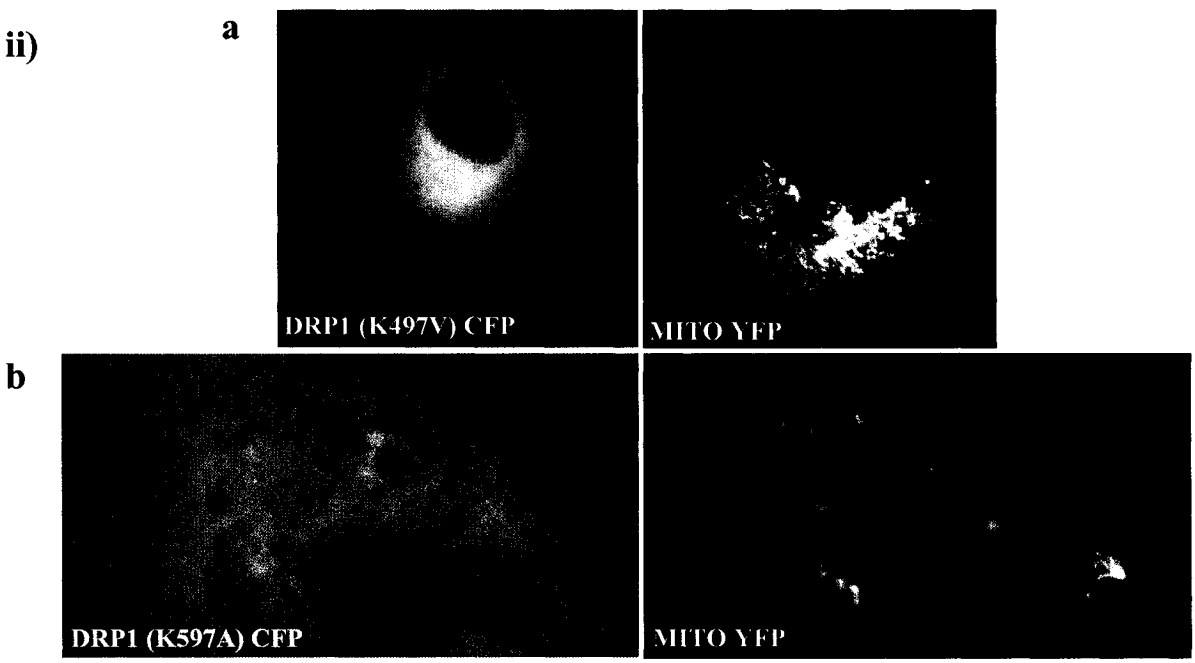

that most closely matched a consensus sequence were mutated (**Table 1C**) and the mutant DRP1 protein was again tested for its interaction with Ubc9, SUMO1 and TOPORS. Of all the mutations tested, two specific DRP1 mutants appeared to significantly affect interactions (**Figure 17B i)**). The K497V mutation in the middle domain abolishes the interaction with Ubc9, and decreases the interaction with TOPORS 2-fold, while maintaining the interaction with wild-type DRP1 and SUMO1. When DRP1 (K497V) CFP is overexpressed in Cos 7 cells, the protein is diffusely distributed throughout the cell and the mitochondria have a normal phenotype (**Figure 17B ii a**). The K597A mutation in the unique Insert B domain of DRP1 abolishes the interaction with TOPORS and wild-type DRP1, while maintaining the interactions with SUMO1 and Ubc9. When DRP1 (K597A) YFP is overexpressed in Cos 7 cells, the protein is also diffusely distributed. However, the mitochondria are interconnected, suggesting that this mutant is dominant interfering (**Figure 17B ii b**). Finally, experiments addressing whether the interactions between DRP1 and each of SUMO1, Ubc9 and TOPORS were dependent on GTPase activity were performed using the dominant interfering mutant DRP1 (K38E). **Figure 17C** shows that, in comparison to interactions seen with DRP1, the interaction between DRP1 (K38E) and Ubc9 is decreased 3-fold and its interaction with SUMO1 is abolished to almost control levels, while the interactions with DRP1 and TOPORS are maintained. These results suggest that the nucleotide state of DRP1 may be important for its interactions with these proteins. Various control experiments (**Figure 17D**), were performed to verify specificity of the experimental system.

Figure 17C.

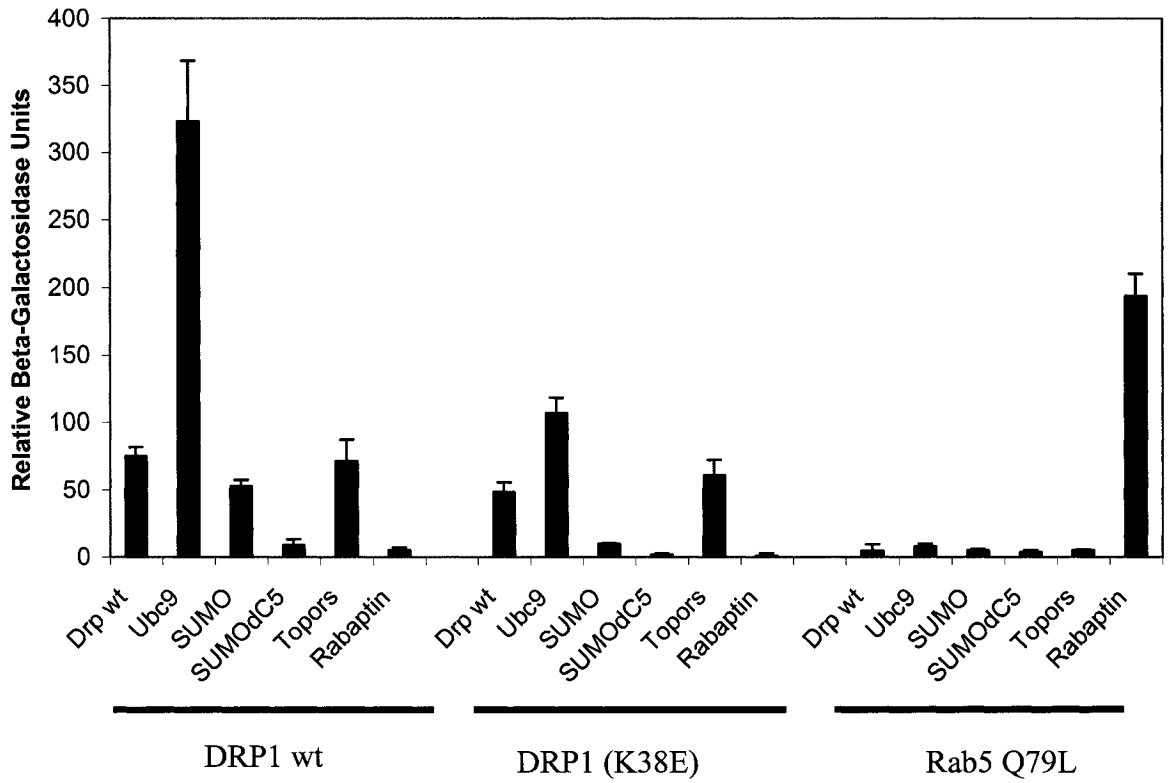
Relative Beta-Galactosidase Units
400
350
300
250
200
150
100
50
0
Drp wt
Ubc9
SUMO
SUMOdC5
Topors
Rabaptin
Drp wt
Ubc9
SUMO
SUMOdC5
Topors
Rabaptin
Drp wt
Ubc9
SUMO
SUMOdC5
Topors
Rabaptin
DRP1 wt
DRP1 (K38E)
Rab5 Q79L

Figure 17D.

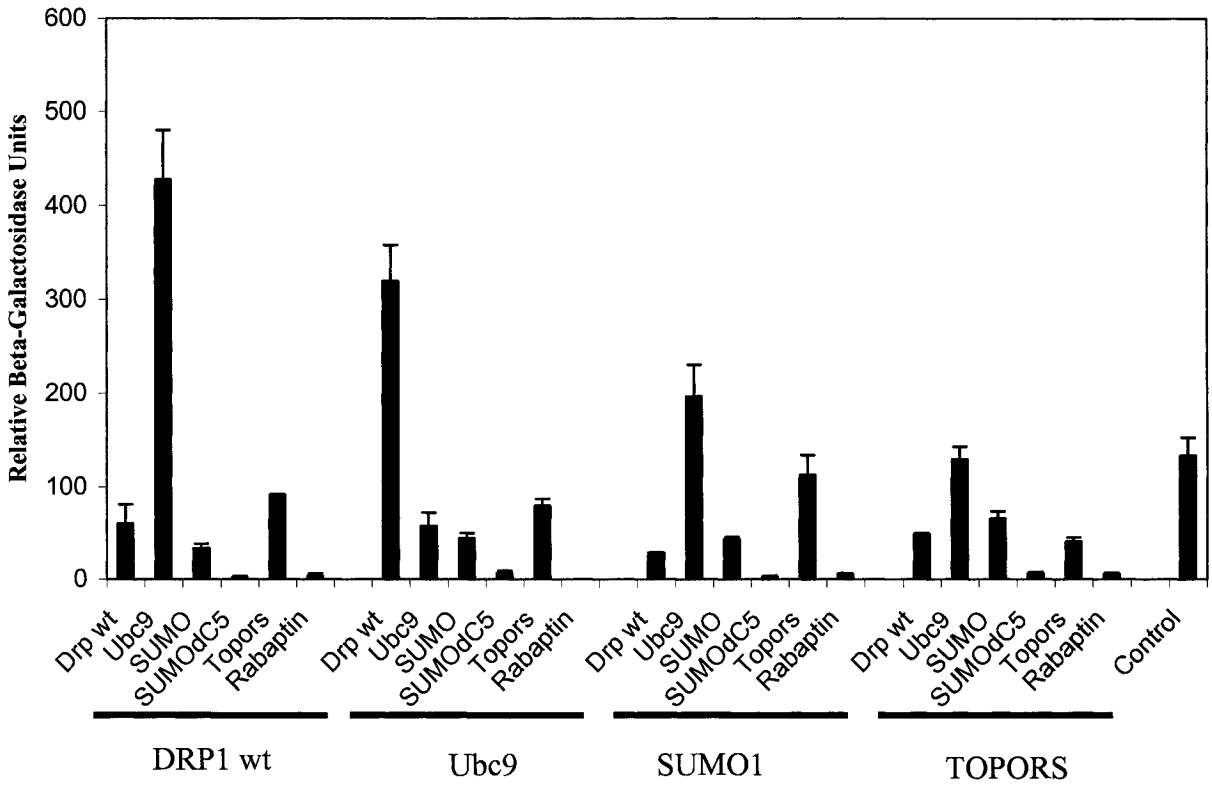
Relative Beta-Galactosidase Units
600
500
400
300
200
100
0
Drp wt
Ubc9
SUMO
SUMOdC5
Topors
Rabaptin
Control
DRP1 wt
Ubc9
SUMO1
TOPORS

3.3.2. Recombinant GST:DRP1 and GST:DRP1(K38E) pull down endogenous Ubc9 and SUMO1 from cytosol

The interaction between DRP1 and each of SUMO1 and Ubc9 were verified biochemically using GST pull down assays. Recombinant GST alone, GST:DRP1 and GST:DRP1 (K38E) purified from *E.Coli* were incubated with either bovine heart or rat liver cytosol (see 2.5.2.3). As shown in **Figure 18**, when the GST pull-down was probed with monoclonal anti-Ubc9 and anti-SUMO1 antibodies, both GST:DRP1 and GST:DRP1(K38E) but not GST alone were able to isolate endogenous Ubc9 and SUMO1. Both the Ubc9 and SUMO1 antibodies recognized endogenous SUMO1 and Ubc9 at approximate molecular weights of 40 kDa, which is not the predicted molecular weight of Ubc9 or unconjugated SUMO1. Furthermore, in contrast to the yeast two-hybrid data, DRP1 (K38E) appears to pull down an equivalent amount of Ubc9 as wild-type DRP1 and significantly more SUMO1 than wild-type DRP1. Due to poor antibodies for TOPORS, similar pull-down experiments could not be performed for this protein.

3.3.3. DRP1 is a SUMO1 substrate.

Since the cytosol was unable to support the potential SUMO1 conjugation of recombinant DRP1, we performed His6 pull down experiments from cell extracts cotransfected with DRP1 and SUMO1 to examine whether DRP1 was a true SUMO1 substrate. In **Figure 19**, His6:DRP1 was efficiently isolated from transfected cell extracts, and a second, higher molecular weight band appeared, which was also SUMO1 positive, and NEM sensitive (**Figure 19 B**, lane 8 open circles in top and bottom panels). NEM inhibits SUMO1 proteases, thereby stabilizing the generally labile SUMO1

Figure 18. Recombinant GST:DRP1 and GST:DRP1 K38E pull-down endogenous Ubc9 and SUMO1 from cytosol. Western blot of a GST pull-down of endogenous Ubc9 and SUMO1 by DRP1 and DRP1 K38E. Bacterially expressed GST, GST:DRP1 and GST:DRP1 K38E were purified on Glutathione Sepharose beads and incubated first overnight with 2mg of both bovine heart and rat liver cytosol and then for another 2 hours in the presence of 20mM NEM. Bound proteins were released by resuspending the beads in SDS loading buffer and boiling for 15 minutes. Samples were run on a 4-20% gradient SDS-PAGE, transferred onto nitrocellulose and probed with monoclonal DRP1, monoclonal Ubc9 (bovine heart cytosol) and monoclonal SUMO1 (rat liver cytosol) antibodies. Both DRP1 and DRP1 K38E but not GST alone pull down relatively equivalent amounts of an endogenous 40kDa Ubc9 reactive band. Both DRP1 and, to a much greater extent, DRP1 K38E but not GST alone, pull down an endogenous 40 kDa SUMO1 reactive band.

Figure 18.

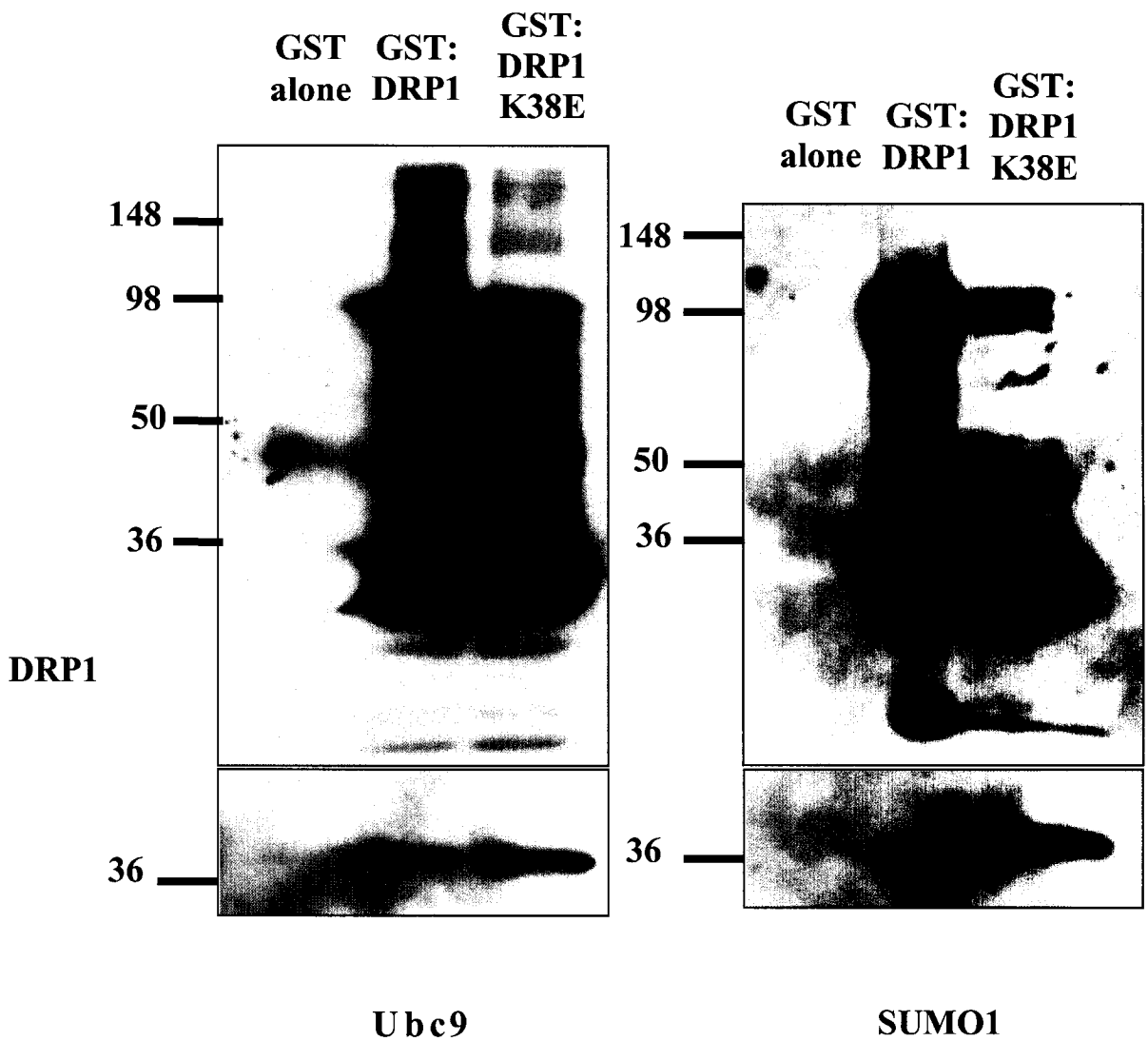
GST alone
GST: DRP1
GST: DRP1 K38E
148
98
50
36
DRP1
36
Ubc9
GST alone
GST: DRP1
GST: DRP1 K38E
148
98
50
36
36
SUMO1

Figure 19. DRP1 is SUMO1 modified. Cos7 cells cotransfected as indicated were solubilized in the presence or absence of 20 mM NEM. Shown is a Western Blot of total lysates **(A)** (lanes 1-6) cleared and incubated with Nickel agarose beads **(B)** (lanes 7-18). Half of the total eluates from the Nickel beads (Ni+) along with 50 μg of each flow through (FT) were loaded on a 4-20% gradient gel, transferred to nitrocellulose and blotted with anti-DRP1, anti-FP, or anti-SUMO1 antibodies, as indicated. The lower arrow in the top panel of **B** indicates endogenous DRP1 and the higher arrow represents DRP1:YFP. Open circles denote a 175 kDa SUMOylated species of DRP1.

Figure 19.

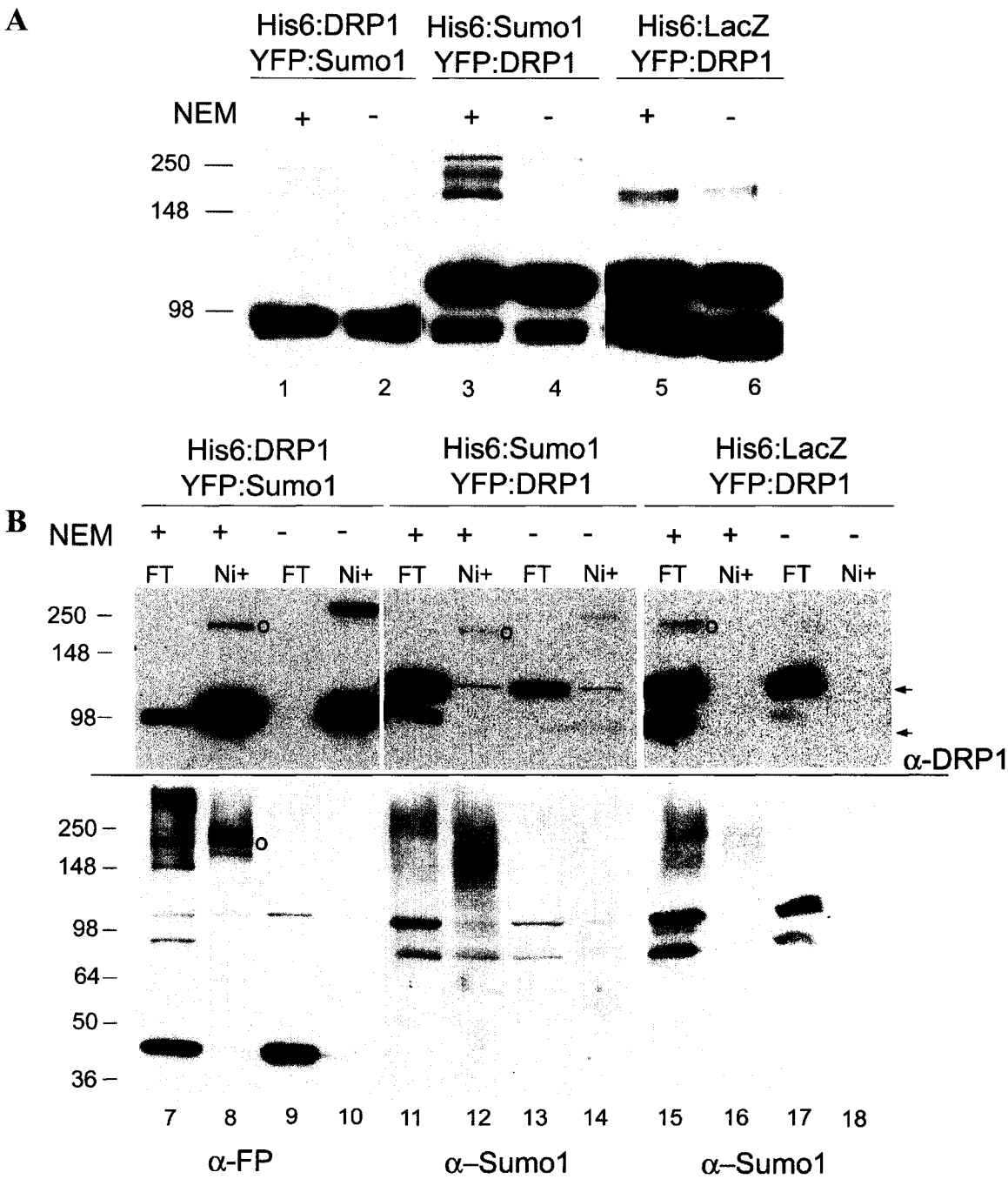
A
His6:DRP1
YFP:Sumo1
His6:Sumo1
YFP:DRP1
His6:LacZ
YFP:DRP1
NEM
+ - + - + -
250
148
98
1 2 3 4 5 6
B
His6:DRP1
YFP:Sumo1
His6:Sumo1
YFP:DRP1
His6:LacZ
YFP:DRP1
NEM
+ + - - + + - - + + - -
FT Ni+ FT Ni+ FT Ni+ FT Ni+ FT Ni+ FT Ni+
250
148
98
o
α-DRP1
250
148
98
64
50
36
o
7 8 9 10 11 12 13 14 15 16 17 18
α-FP
α–Sumo1
α–Sumo1

conjugated products during the experiment. The other two YFP:SUMO1 conjugates visible in the His6:DRP1 pull down do not represent specific interactions since they were not reproducible and sometimes appeared in the His6:LacZ/YFP:SUMO1 control (data not shown). A second high molecular weight DRP1 reactive product is visible in lane 10 top panel. However, this product is not SUMO1 modified (**Figure 19**, **B**, lane 10, bottom panel) and its origins are unknown. Importantly, the reciprocal experiment also shows that His6:SUMO1, but not His6:LacZ, is able to pull down DRP1:YFP (**Figure 19**, **B,** lanes 12 vs. 16, top panel). In lane 12 (**B**, top panel), the 175 kDa modified form of DRP1 is visible, along with the 100 kDa DRP:YFP monomer, suggesting either that SUMO1 is also able to interact with monomeric DRP:YFP in the absence of conjugation, or that the SUMOylated, 175 kDa form of DRP1 remains in a complex (dimer) with the unmodified form, thereby pulling both forms of DRP1 out of the lysate. Although the SUMO1 modified form of DRP1 (open circles) is NEM sensitive, the specific interaction between SUMO1 and DRP1:YFP (**Figure 19**, **B**, lane 8 vs. 12, top panel) also occurs whether or not DRP1:YFP is conjugated. Finally, it is important to note that the amount of endogenous DRP1 present in the total cell extracts declined over the duration of the experiment, and this apparent degradation was inhibited when the incubations were performed in the presence of NEM (**Figure 19**, **B,** lanes 7 vs. 9, 11 vs. 13 and 15 vs. 17, lower arrow, top panel).

3.4. Subcellular localization of SUMO1

3.4.1. Endogenous SUMO1 associates with purified mitochondria

Since SUMO1 and Ubc9 were shown to interact with DRP1, a protein that cycles on and off the mitochondria, it was imperative to test whether SUMO1 and Ubc9 were also found localized to mitochondria. To address this issue, endogenous DRP1, and SUMO1 protein levels from nuclear, cytosolic and mitochondrial fractions of Cos7 cells isolated with and without NEM were determined by Western Blot analysis (**Figure 20**). In the experiment without NEM, probing with anti-SUMO1 antibodies revealed the presence of varying levels of SUMO1 conjugates in the nuclear, cytosolic and mitochondrial fractions. The pattern and intensity of bands in the fractions were different, indicating that there is minimal cross-contamination between the fractions. Interestingly, there appeared to be higher protein levels of a 40kDa SUMO1 species in the cytosolic and mitochondrial fraction than in the nuclear fraction (**Figure 20**, lower arrow), perhaps consistent with the 40 kDa SUMO1 immunoreactive band isolated in the GST:DRP1 affinity column. When the fractions were purified in the presence of NEM, the amount of SUMO1 conjugates in all fractions, particularity the nuclear and mitochondrial fractions, significantly increased and the banding patterns changed, indicating greater stability of SUMO1 conjugates upon inhibition of deSUMOylating enzymes. To further verify the existence of SUMOylation on the mitochondria, Ubc9 staining revealed notable levels of this protein in all fractions examined with and without NEM (data not shown). Finally, probing the fractions with anti-DRP1 revealed the presence of two DRP1 molecular weight sizes: one at the predicted molecular weight of 80 kDa and the other one at approximately 160kDa. This additional band may represent a covalently

Figure 20. Endogenous SUMO1 and an NEM-sensitive high molecular weight species of DRP1 are found on purified mitochondria. Nuclear (Nuc)/unbroken cells (UC), cytosolic (Cyt) and mitochondrial (Mito) fractions were obtained from 10 10cm dishes of confluent Cos7 cells in the presence and absence of 20 mM NEM. Approximately 200 μg of the nuclear and mitochondrial fractions were loaded, and 100 μg of cytosol were loaded on a 4-20% gradient SDS-PAGE gel. The proteins were transferred onto nitrocellulose and probed with polyclonal SUMO1, monoclonal DRP1, and monoclonal TOM20 antibodies.

Figure 20.

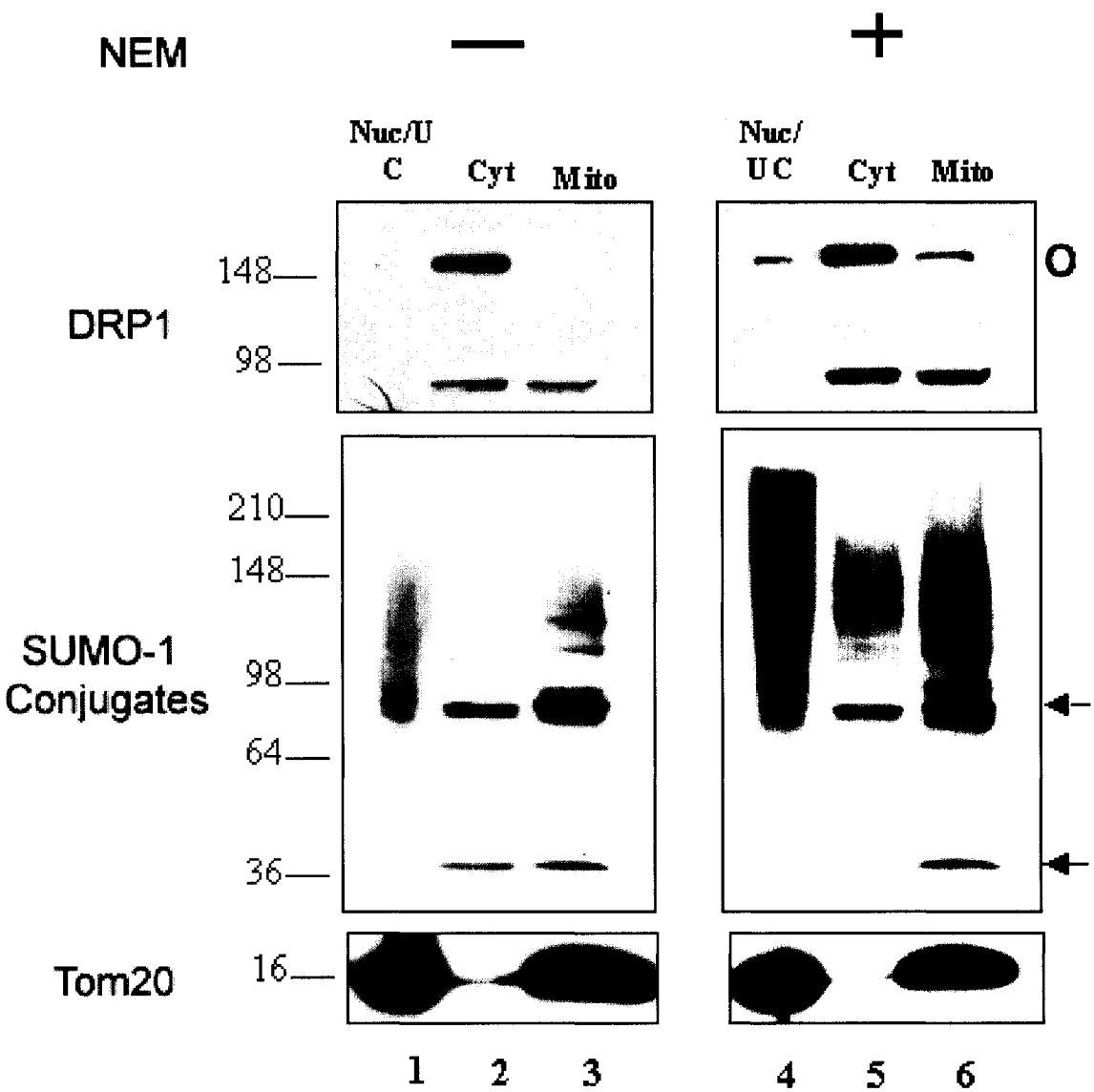
NEM
—
+
Nuc/U C
Cyt
Mito
Nuc/ UC
Cyt
Mito
DRP1
148
98
O
SUMO-1 Conjugates
210
148
98
64
36
Tom20
16
1
2
3
4
5
6

modified form of the protein or a DRP1 multimer. Interestingly, various combinations of these two forms are seen in specific fractions. In the experiment without NEM, only a very small amount of the high molecular weight form is seen in the nuclear/unbroken cells fraction. The cytosolic fraction contains large, but equivalent, amounts of both forms and the mitochondrial fraction contain only the low molecular weight form. In the experiment with NEM, DRP1 sizes in the nuclear and cytosolic fractions are unchanged. However, both the high and low molecular weight bands are present in the mitochondrial fraction, suggesting the existence of a potential NEM sensitive modification specific to mitochondria. The subcellular localization of TOPORS could not be determined due to poor antibodies.

3.4.2. Cytosolic SUMO1 YFP associates with dynamic mitochondria and localizes to the site of mitochondrial fission

Live cell fluorescence microscopy was used to visualize Ubc9, SUMO1 and TOPORS intracellular localization with respect to mitochondria. Overexpression of Ubc9 YFP in Cos 7 cells revealed intense Ubc9 YFP cytosolic staining (data not shown) making it difficult to distinguish if any fraction of this cytosolic Ubc9 YFP was associated with mitochondria. Overexpression of TOPORS GFP in Cos7 cells did not reveal any mitochondrial localization, as the protein was strictly nuclear where is was either evenly distributed or punctate (data not shown). Finally, overexpression of SUMO1 YFP also showed intense nuclear staining (**Figure 21, a**). As expected, SUMO1 staining in the nucleus was heterogenous. Cells displayed large puncta consistent with PML bodies and small punctate SUMO1 staining along the nuclear envelope consistent with SUMOylation of RanGAP and RanBP of the nuclear pore complex. At the initial

Figure 21. A fraction of SUMO1 YFP is found in the cytosol and often localizes to mitochondria. Cos 7 cells transiently co-transfected with pEYFP:SUMO1 and pOCT: CFP were visualized 24 hours post-transfection by live cell fluorescence microscopy using a 100X objective. Snapshots were taken after excitation of OCT CFP at 434 for 400ms and excitation of SUMO1 YFP at 514 nm for 400ms and 2000ms (high exposure). The mitochondrial and high exposure SUMO-snapshots were then overlayed. The bottom panels are high magnification images demonstrating localization of SUMO1 YFP to mitochondria. See Supplementary Movie 4 for additional evidence highlighting tight association of SUMO1 to mitochondria.

Figure 21.

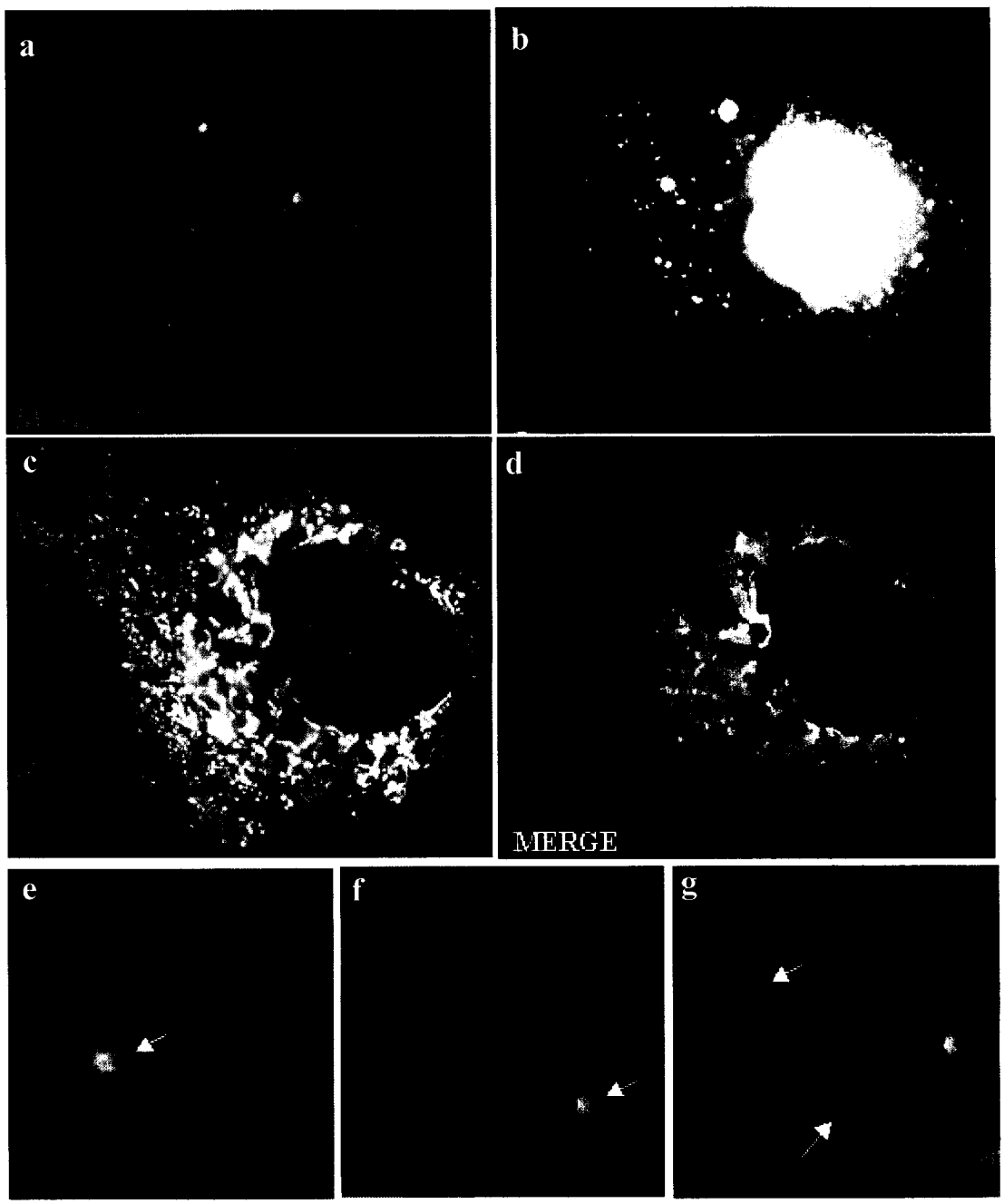

exposure used, minimal cytosolic SUMO1 staining is observed. However, when the exposure is increased, it is evident that there is a significant amount of SUMO1 puncta in the cytosol (**Figure 21, b**). At higher magnification, it is clear that a portion of cytosolic SUMO1 YFP is associated with mitochondria (**Figure 21**, e-g). This association is highlighted in **Supplementary Movie 4** where SUMO1 YFP appears tightly bound to the mitochondria as they move dynamically during the course of the movie. In addition to the apparent tethering of SUMO1 to the mitochondria, SUMO1 YFP localizes to the site of mitochondrial fission (**Figure 22 and Supplementary Movie 5**). After the fission event, SUMO-YFP is transferred to one of the two mitochondrial fragments.

3.4.2. Endogenous DRP1 partially colocalizes with SUMO1 YFP.

To examine whether the YFP:SUMO1 spots observed on the mitochondria co-localize with endogenous DRP1, we performed an immunofluorescence experiment with cells cotransfected with pEYFP:SUMO1 and pOCT:DsRed2 and labeled with anti DRP1 antibodies. As can be seen in **Figure 23A (b,d,** arrowheads), only a few of the SUMO1 spots observed on the mitochondria co-localize with DRP1. The mitochondrial associated SUMO1 and DRP1 spots are often positioned at the tips of mitochondria (**Figure 23A b**) or near the sites of apparent constriction (**Figure 23A d**). The large proportion of the YFP:SUMO1 spots do not colocalize with DRP1, which is consistent with the biochemical fractionation data indicating the existence of multiple mitochondrial SUMO1 substrates. We also examined the overlap between YFP:SUMO1 and CFP:DRP(K38E) (**Figure 24B**). It has been previously shown that, upon transient transfection, DRP1(K38E) is not recruited to the mitochondria, and instead assembles

Figure 22. SUMO1 YFP localizes to the site of mitochondrial fission. Cos 7 cells transiently co-transfected with pEYFP:SUMO1 and pOCT CFP were visualized 24 hours post-transfection by live cell video fluorescence microscopy using a 100X objective and a CFP/YFP dual pass filter. Movie protocol consisted of excitation of OCT CFP at 434 nm for 400 ms, excitation of SUMO1 YFP at 514 nm for only 150 ms (to prevent photobleaching of the YFP fluorescence), followed by a 4000 ms delay for each frame. A total of 100 frames were recorded for a single cell. Only selected frames of a cropped area of interest of the cell are shown. SUMO1 YFP fluorescence was manually intensified approximately 5-fold for better visualization prior to movie compilation. Arrow depicts SUMO1 YFP at the site of mitochondrial fission.

Figure 22.

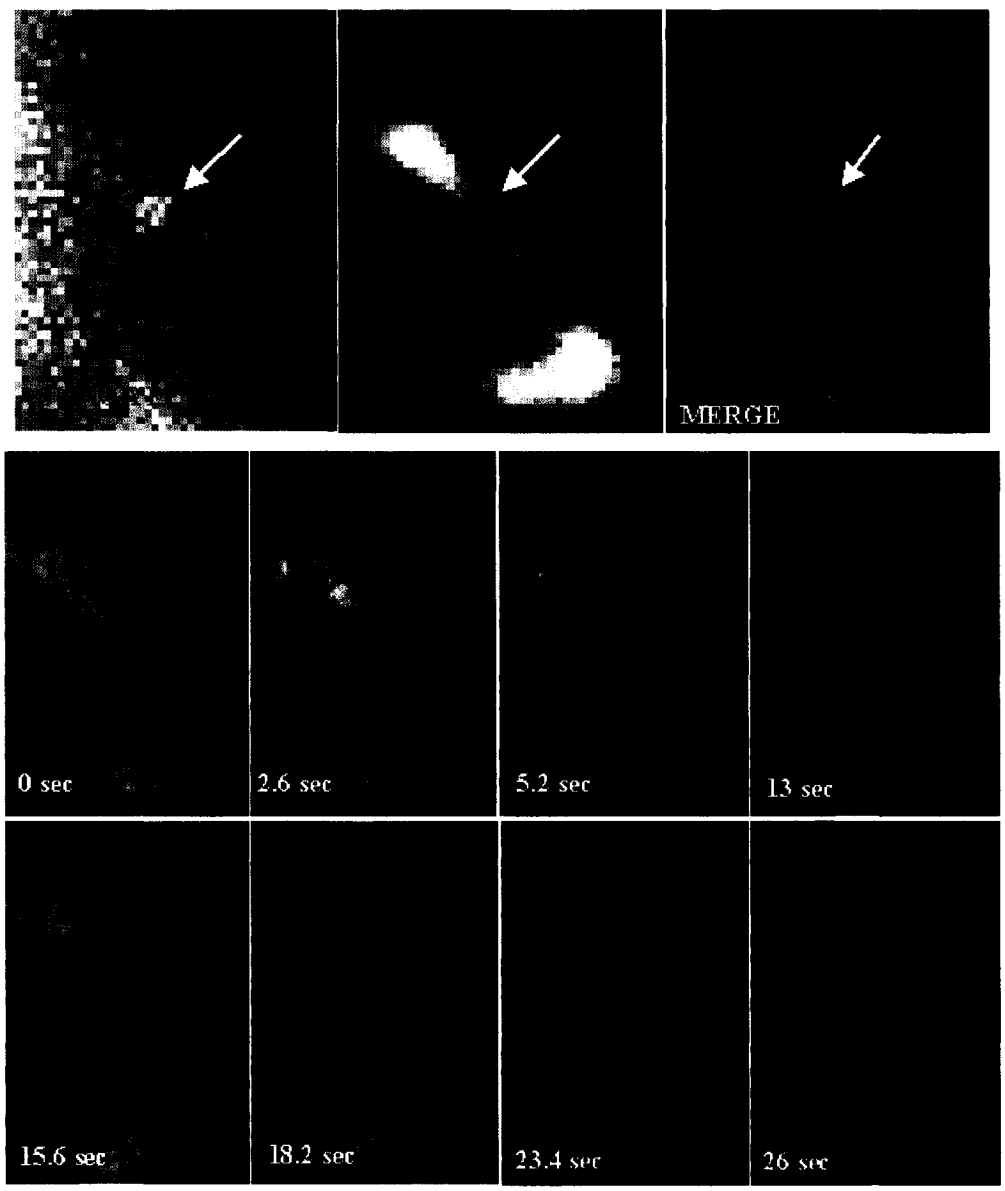

Figure 23. Endogenous DRP1 partially colocalizes with mitochondrial YFP SUMO1. **A.** Cos 7 cells were transiently cotransfected with pEYFP:SUMO1 (green) and pOCT:DsRed2 (shown blue) and immunolabeled for endogenous DRP1 (red) using Alexa 350 conjugated secondary antibodies. The white boxes in a and c indicate the areas that were enlarged (b,d). Arrowheads indicate the sites where YFP:SUMO1 co-localizes with DRP1. Also note the numerous YFP:SUMO1 spots decorating the mitochondrial that do not overlap with DRP1 (arrows). Scale bars = 1 μm. **B.** Cos7 cells were transiently cotransfected with pECFP:DRP1 (K38E) (red), pEYFP:SUMO1 (green), and stained with MitofluorRed 589 (shown blue). The DRP1 (K38E):CFP protein aggregates. However there is no YFP:SUMO1 found within these sites, consistent with the two-hybrid data . Scale bar = 500nm.

Figure 23.

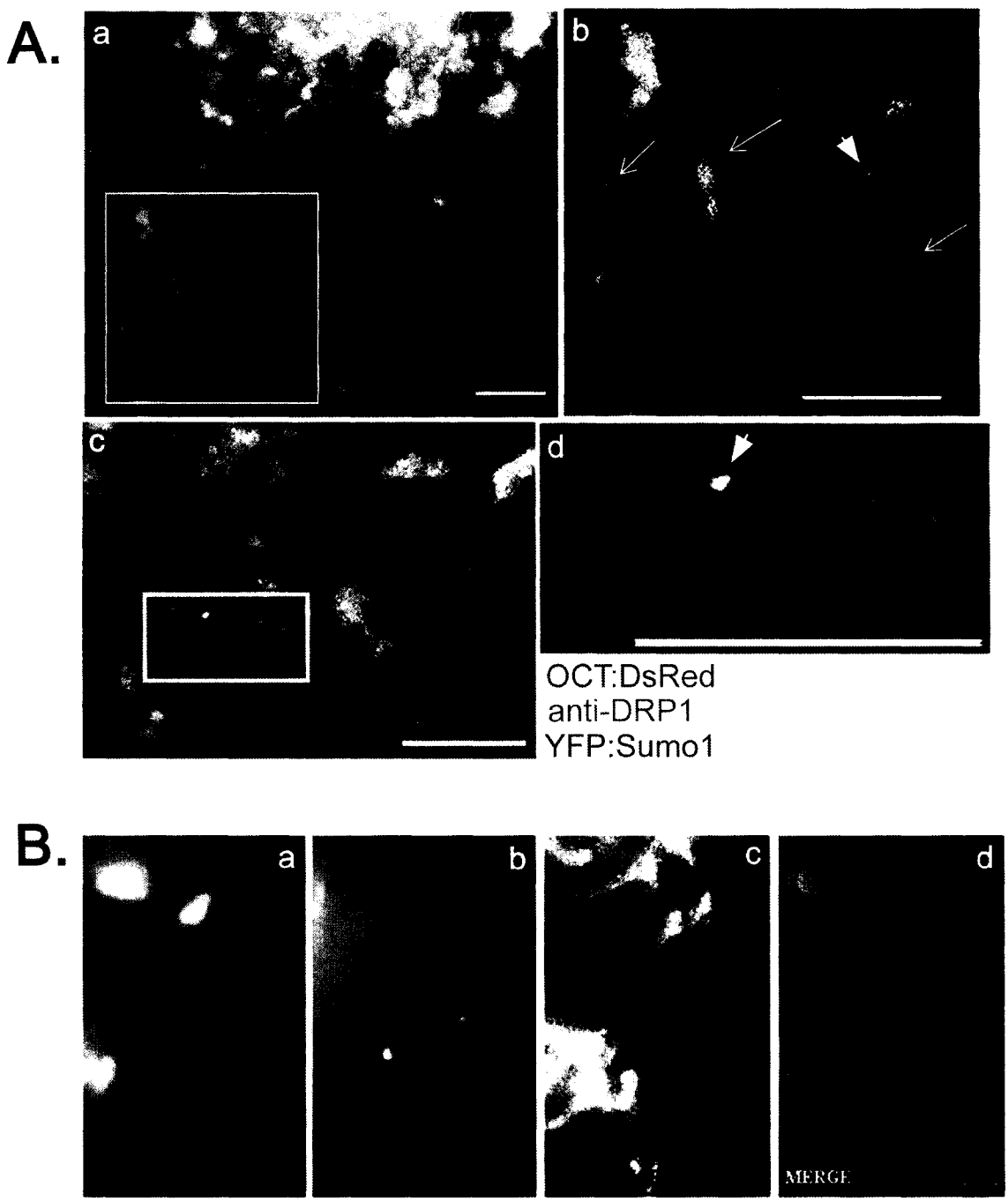

into oligomeric structures within the cytosol. These oligomeric DRP1 (K38E) containing structures do not co-localize with SUMO1 (**Figure 23B**) consistent with the yeast two-hybrid data indicating that lack of interaction between SUMO1 and DRP1(K38E).

3.5 Functional analysis of SUMOylation in mitochondrial fission

3.5.1. Overexpression of SUMO1 YFP causes increased mitochondrial fragmentation and protects DRP1 from degradation

The functional role of SUMO1 on the mitochondria was examined by overexpression studies. The mitochondrial phenotypes of Cos7 cells overexpressing YFP alone, SUMO1 YFP and SUMO1ΔC5 YFP were quantified. Three different mitochondrial phenotypes were generally observed (**Figure 24A**). Long and thin mitochondria were classified as tubular. Mitochondria that were shorter and wider were classified as rod-like, and small round mitochondria were considered fragmented. Under control conditions, the percentage of tubular: rod-like: fragmented mitochondria in a large population of cells was generally 50: 30: 20 (**Figure 24B**). Upon overexpression of SUMO1 YFP, the ratio of tubular: rod-like: fragmented mitochondria reversed to 20:25:55 indicating approximately a 2-fold decrease in tubular mitochondrial and a 2-fold increase in fragmented mitochondria. Overexpression of SUMO1ΔC5 YFP did not have significant changes on mitochondrial phenotype.

To further understand the reasons for the increase in mitochondrial fission observed with overexpression of SUMO1, the fate of endogenous DRP1 was examined in these cells. As previously seen in **Figure 19**, endogenous DRP1 protein levels are substantially decreased in the absence of NEM in the flowthrough material of the His6

Figure 24. Overexpression of SUMO1 causes increased mitochondrial fragmentation and protects DRP1 from degradation. (A) Cos 7 cells transiently co-transfected with pOCT CFP and either pEYFP alone, pEYFP:SUMO1 or pEYFP:SUMO1ΔC5 were quantified 24 hours post-transfection by live cell fluorescence microscopy using a 60X objective and a CFP/YFP dual pass filter. Cells expressing YFP were located first by excitation at 514 nm and then the mitochondrial phenotype was noted as tubular, rod-like or fragmented (shown in A) by excitation at 434 nm. A total of 552 cells were counted for vector alone, 576 cells were counted for SUMO1 YFP and 357 cells were counted for SUMOΔC5 YFP. Counts were done in triplicate and the results are shown as averages with their standard deviation **(B)** Quantification of mitochondrial phenotypes from (A). Experiment was performed in triplicate results are shown with SD. **(C)** Cos7 cells were transiently transfected with pEYFP alone, pEYFP:SUMO1 or pEYFP:SUMO1ΔC5. Cells were solubilized in the presence and absence of 20mM NEM and whole cell lysates were probed for DRP1. Ponceau Red staining was used to control for protein loading.

Figure 24.

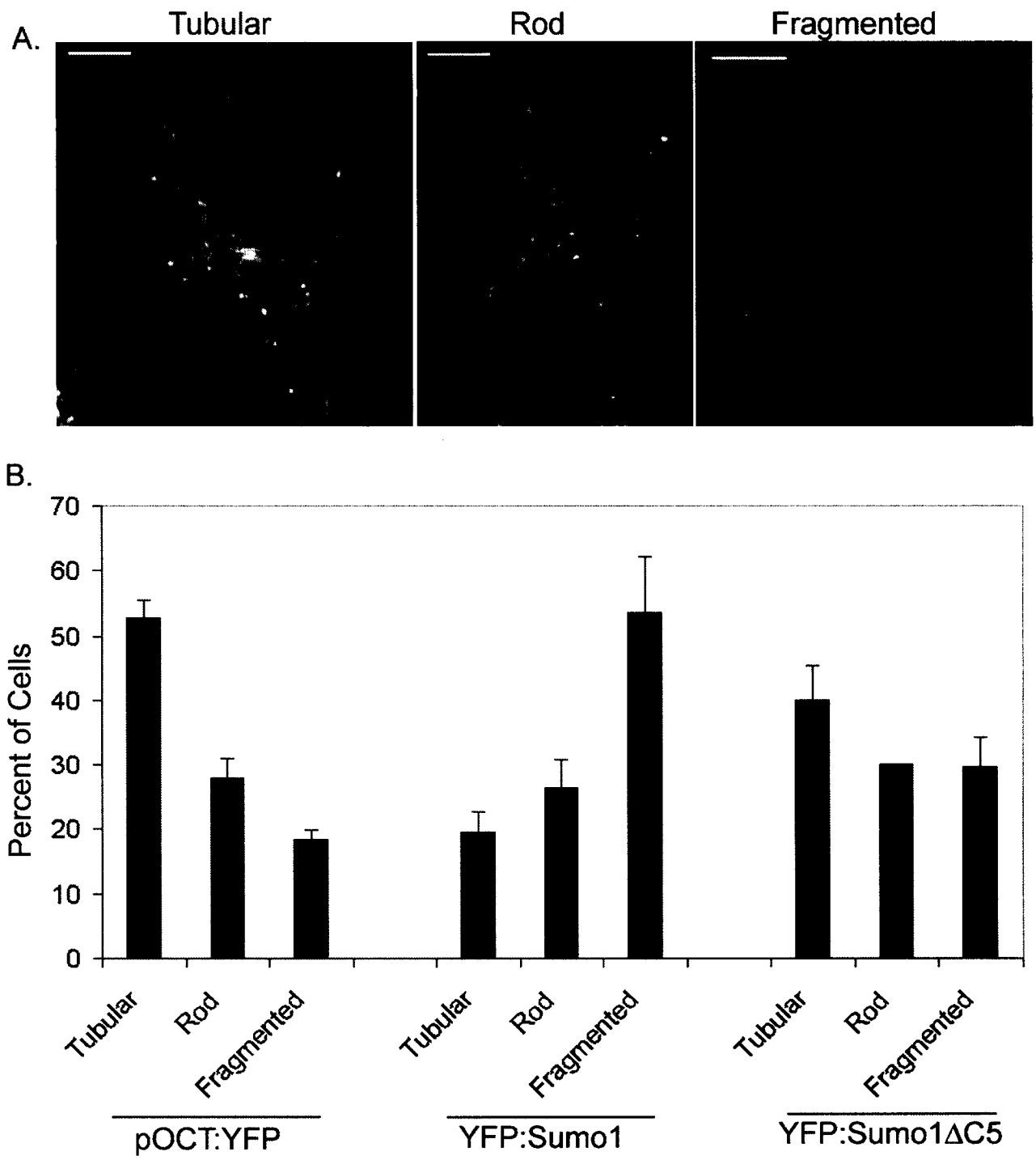
A.
Tubular
Rod
Fragmented
B.
Percent of Cells
70
60
50
40
30
20
10
0
Tubular
Rod
Fragmented
Tubular
Rod
Fragmented
Tubular
Rod
Fragmented
pOCT:YFP
YFP:Sumo1
YFP:Sumo1ΔC5

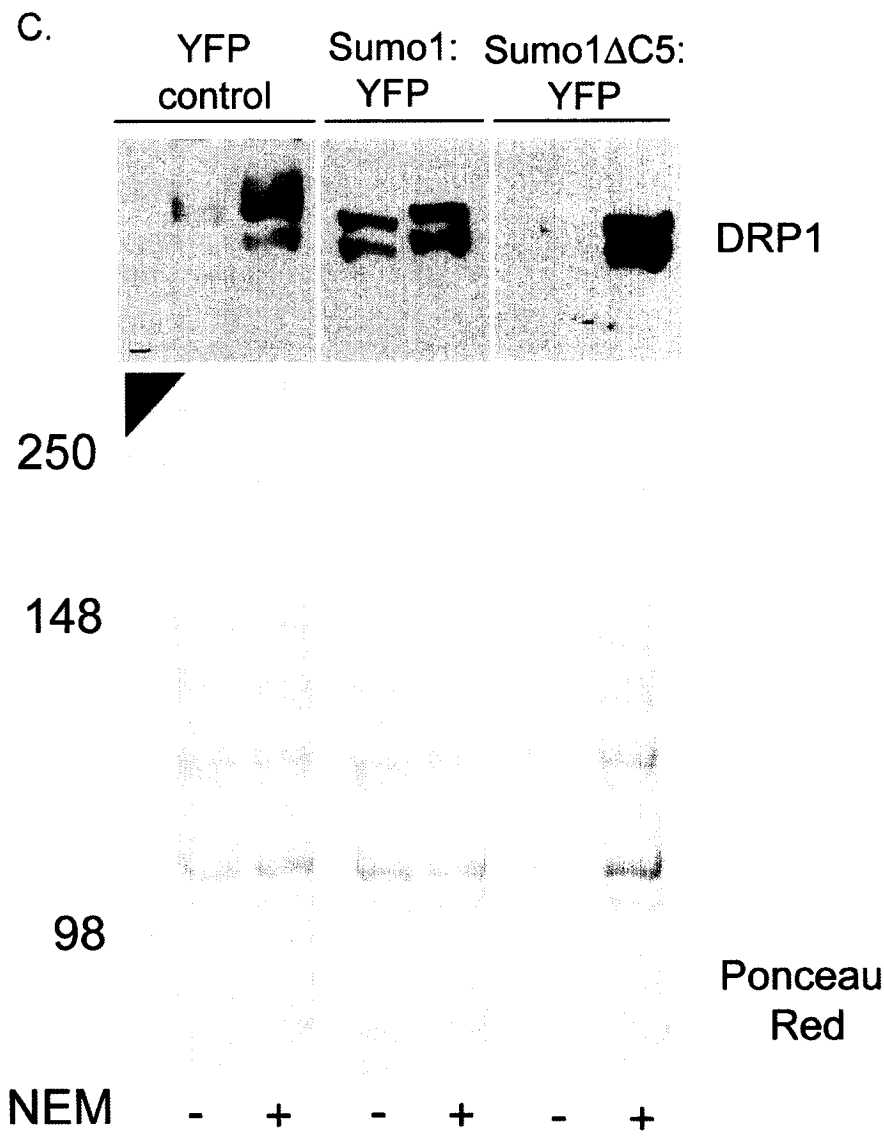
C.
YFP control
Sumo1: YFP
Sumo1ΔC5: YFP
DRP1
250
148
98
Ponceau Red
NEM - + - + - +

pull-down (**Figure 19**, lanes 7 vs. 9, 11 vs. 13, and 15 vs. 17), indicating that DRP1 is stabilized in the presence of NEM. These results suggest that maintaining increased levels of SUMOylation in the cell protects DRP1 from protein degradation. To confirm this, we overexpressed SUMO1 is Cos7 cells and examined the protein levels of DRP1. Notably, overexpression of YFP:SUMO1, but not YFP alone or YFP:SUMO1ΔC5, protects DRP1 against degradation, (**Figure 24C**, compare lanes 3 and 4). Interestingly, co-expression with exogenous DRP1 competes for the protection of the endogenous DRP1 protein, since endogenous DRP1 is still degraded even in the presence of SUMO1 (**Figure 19**, **B**, top panel, lane 13, bottom vs. top arrows).

4. Discussion

4.1 Mitochondrial fission is stimulated during apoptosis

In order to better understand the regulation of mitochondrial fission, our first experiments were aimed at determining the cellular signals that trigger this process. Previous unpublished data from our laboratory indicated that mitochondrial morphology and distribution change during the progression of apoptosis. Fluorescence video microscopy monitoring mitochondrial morphology during a 3-hour segment of Fas antigen stimulated apoptosis in KB cells, showed substantial mitochondrial fragmentation and migration to a specific region of the cell (data not shown). These observations suggested that mitochondrial fission was stimulated, or that mitochondrial fusion was inhibited, during the progression of programmed cell death. Importantly, it needed to be determined if fission or fusion were directly involved in the onset and/or progression of apoptosis, or if the change in mitochondrial morphology was simply a downstream effect. To address these questions, we first studied DRP1 recruitment to mitochondria. We used a construct consisting of cyan-fluorescent protein attached to the N-terminus of DRP1, transiently transfected Cos 7 cells and triggered apoptosis with the general protein kinase inhibitor staurosporine (STS). STS has been previously shown to be a potent apoptotic stimulus and is used to trigger caspase-dependent cell death (117). In our microscopy studies, we have observed that the duration of apoptosis triggered by STS is 5-6 hours until approximately >90% of cells have died. Even though the time-course for apoptosis ranges with cell lines, complete cell death by 8-10 hours using STS is typical for most cell culture lines. Initially, we observed stimulated DRP1 recruitment to mitochondria approximately 30 minutes after initiation of apoptosis with STS. This stimulation was characterized by the translocation of the majority of cytosolic DRP1 to the mitochondria.

CFP:DRP1 recruited to mitochondria appeared as spirals of protein around the tubules, reminiscent of electron microscopy images depicting GTPγS induced Dynamin 1 spirals around the neck of budding vesicles (36). Between 1.5- 2.5 hours of incubation with STS, the mitochondria were predominantly fragmented with CFP:DRP1 found at the tips of spherical fragmented mitochondria or at the site of constriction (**Figure 11 B,** insert). Therefore, mitochondrial fragmentation occurs early on in the apoptotic process, suggesting that it may play a role in the progression of apoptosis rather than occurring as a result of cell death. To further verify this, we tested if inhibition of mitochondrial fission affected the outcome of apoptosis. To do this, we utilized the dominant interfering GTPase deficient DRP1 mutant harboring a K38E substitution in the highly conserved P-Loop region of the GTPase domain. This mutation is analogous to the Dynamin 1 K44A that blocks clathrin-mediated endocytosis (118). DRP1 (K38E) has been previously shown to inhibit mitochondrial fission resulting in interconnection of mitochondrial tubules (42;119) and eventual collapse of the mitochondrial network into a perinuclear region (42), observations that we also note in our studies. To more accurately assess the extent of apoptosis in our experiment, we used a fluorescent caspase-3 substrate. Caspase activation marks the 'point of no return' in apoptosis. This family of proteases is responsible for the final stages of cell death and degrades a major proportion of cellular proteins (see review (120)). Use of the fluorescent Caspase-3 substrate enables better quantification of cell death and allows us to properly examine the role that mitochondrial fission plays in this process. Cos 7 cells were transiently transfected with wild-type pECFP:DRP1 and pECFP:DRP1(K38E). 24 hours post-transfection, cell death was triggered with STS. The degree of progression of apoptosis was determined with the

fluorescent Caspase-3 sensor after 3 hours of incubation with STS. Results revealed that when mitochondrial fission was inhibited by overexpression of DRP1(K38E), there was approximately 50% less STS-stimulated cell death than in those cells overexpressing wild-type DRP1 **(Figure 12)**. A similar trend was noted in those cells where apoptosis was not triggered **(Figure 12)**. There was a notable decrease in basal cell death with overexperssion of DRP1 (K38E) when compared to cells overexpressing wild-type DRP1 indicating that there is a protective effect on apoptosis by inhibition of mitochondrial fission. These results show that mitochondria fragment during apoptosis, and that mitochondrial fragmentation is required for apoptosis, suggesting that mitochondrial fission plays a distinct role in the apoptotic pathway. These conclusions are consistent with work published, during the course of our studies, by Richard Youle and collegues (121). His work also implicated mitochondrial fission as an important event during programmed cell death. During experiments where he treated cells with various apoptotic stimuli, he noted significant changes in mitochondrial morphology prior to the release of cytochrome c. He documented increased mitochondrial fragmentation during apoptosis and also an approximately 50% reduction in cell death and maintenance of mitochondrial membrane potential with overexpression of the dominant interfering DRP1 (K38A). The exact function of mitochondrial fission in the apoptotic pathway was not determined in his work. However, it is well known that mitochondria play a key role in the progression of programmed cell death by releasing cytochrome C (cyt C) from the intermembrane space. Cyt C then mediates the formation of a central apoptotic complex that triggers a cascade of events ultimately leading to degradation of the cell. The mode of cyt C release by the mitochondria is unclear. Since it is known that 85% of cyt C is

compartmentalized within enclosed folds of the cristae (122), it has been proposed that matrix remodeling, through involvement of the pro-apoptotic factor tBid, is required to attain complete cyt c redistribution and release from enclosures inside the mitochondria (122). Current data is consistent with a role for mitochondrial fragmentation in the release of cyt c, potentially through the reorganization of cristal membranes and consequent opening of cyt c storage depots.

After these studies, our focus was redirected at determining factors that mediate DRP1 recruitment to the mitochondria. Since a limited number of DRP1 interacting proteins are known to date, our goal was to identify additional DRP1 binding partners in hopes of uncovering novel proteins involved in the regulation of DRP1 mediated mitochondrial fission. This was accomplished by performing a yeast two-hybrid screen using DRP1 as bait.

4.2 Ubc9, SUMO1 and TOPORS interact with DRP1 in a yeast two-hybrid system

The yeast two-hybrid system is a powerful tool used for identification of protein-protein interactions. There are many advantages in using this system. First, it is an *in vivo* system that allows for the efficient and sensitive identification of novel protein interactions when screening a DNA library. It is also able to detect transient and weak interactions that are physiologically significant but that may not be strong enough to detect biochemically. The bait and interacting proteins are likely found in their native conformations in the yeast nucleus, thereby increasing the sensitivity and accuracy of the interactions identified. A particular pool of target proteins can also be selected through

choice of a cDNA library. The strength of the protein-protein interactions can be assessed, as can the specific regions of interaction through mutational studies. For successful yeast two-hybrid screening, it is advantageous to have a soluble bait protein so that it is accessible in the yeast nucleus and will not aggregate, potentially becoming toxic to the yeast. It is also helpful to use bait that is not a resident nuclear protein. This will enable better judgment in discerning possible false positive results. DRP1 is a cytosolic protein that is easily expressed and is quite soluble making it ideal to use as bait in the yeast two-hybrid screen. Furthermore, the DRP1 protein was expressed at high levels in the yeast **(Figure 13)** and was found to not be toxic (data not shown). Consequently, the yeast two-hybrid screen was successful in identifying a number of DRP1 interacting proteins.

The efficiency of the yeast two-hybrid screen was 16%, indicating that only $1/6^{th}$ of the full DNA library was screened. Of the 1050 clones found to interact with DRP1 using the first reporter of growth on media lacking Histidine, only 51 clones were found to also be positive for a second reporter of β-galactosidase expression **(Table 2)**. The strengths of the protein-protein interaction between DRP1 and each of the 51 clones varied significantly **(Figure 14)**. There was approximately a 25-fold difference between the weakest and strongest interactions. The identities of the clones that had the strongest protein interaction with DRP1 by quantitative β-galactosidase activity were determined first. 11 out of 16 clones identified were found to be components of the SUMOylation pathway of post-translational protein modification, namely Ubc9 and SUMO1 **(Table 2)**. As indicated in **Table 2**, other proteins identified included the transcriptional co-repressor Daxx, a bromodomain containing protein (BRD7) and a p53 RING-finger binding protein

TOPORS. Even though the majority of SUMOylated proteins are nuclear and SUMO1 is primarily found in the nucleus as well, we still decided to pursue studies with Ubc9 and SUMO1. This decision was based on the fact that these two proteins were consistently pulled out of the screen. The interaction between DRP1 and Ubc9 was particularly strong when compared to the positive control of Rab5 (Q79L) and Rabaptin-5 (2-fold greater than positive control) **(Figure 15)** and the strength of the interaction between DRP1 and SUMO1 was also deemed significant ($1/4^{th}$ of positive control). In addition, previous studies indicated that the majority of SUMOylated proteins were originally found as proteins that interacted with Ubc9 and SUMO1 in a yeast two-hybrid screen (for example (78;80;115;123;124)). The decision to study TOPORS was based on the possibility that if DRP1 did prove to be a SUMO1 substrate, TOPORS may potentially be the specific DRP1 E3 ligase since the RING finger domain is common to these proteins (see review (125)). The ability of TOPORS to bind p53, a protein involved in apoptosis, also made it a potential candidate as a link between DRP1 mediated mitochondrial fission and apoptosis.

The interaction between DRP1 and SUMO1 may indicate that DRP1 is covalently modified by SUMO1. To determine if this is the case, we created a mutant form of SUMO1 lacking the terminal glycines required for conjugation (SUMO1ΔC5) and tested its interaction with DRP1 by yeast two-hybrid. Overexpression of this construct in Cos7 cells confirms that, in contrast to the punctate nuclear and cytosolic staining of YFP:SUMO1, YFP:SUMO1ΔC5 staining is diffuse indicating that it does not conjugate to substrates and is, therefore, randomly distributed within the cell **(Figure 16A).** Other yeast studies have shown that this form of SUMO1 does not form conjugates *in vivo* (84).

Our results indicate that the interaction between DRP1 and SUMO1 is decreased to control levels upon deletion of the terminal glycine, suggesting that SUMO1 conjugation is required for its interaction with DRP1. This may indicate that DRP1 is SUMOylated directly or that DRP1 interacts indirectly with SUMO1 via another SUMOylated protein. The former possibility is more likely since the interaction between DRP1 and Ubc9 is so significant. However, before we confirmed this, we further tested the specificity of the DRP1 interactions with Ubc9, SUMO1, SUMO1ΔC5 and TOPORS by using the GTPase deficient dominant interfering form of DRP1, DRP1 (K38E), and a constitutively activated cytosolic regulatory GTPase, Rab5 (Q79L) (126). As positive and negative controls, we also confirmed that DRP1 is still able to self-associate in the yeast two-hybrid system and that it does not arbitrarily interact with another cytosolic protein, Rabaptin-5 (127). The DRP1 (K38E) mutant showed a 3-fold decrease in the interaction with Ubc9 and a 4-fold decrease in the interaction with SUMO1 while maintaining its ability self-associate (41). The interaction with TOPORS was relatively unaffected. The negative control, Rab5 (Q79L) did not interact with any of the tested proteins except its known binding partner Rabaptin-5 (128). These results provide additional evidence indicating that the interactions seen with DRP1 and proteins of the SUMOylation pathway are specific. Furthermore, the results obtained with DRP1 (K38E) suggest that nucleotide binding may play a role in regulating the association between DRP1 and proteins of the SUMOylation pathway.

We next sought to confirm if DRP1 is an authentic SUMO1 substrate. Our experiments focused on finding the exact site of SUMO1 conjugation. Initially, yeast two-hybrid testing was performed on domain constructs of DRP1 in an effort to narrow

down the region of interactions. These domain constructs isolated most of the GTPase domain (1-260), the middle domain (254-525), a small region within DRP1 that is not found in its homologs (254-579), and the GED domain (579-736) **(Figure 17Ai)**. These experiments indicated that only full-length DRP1 is capable of interaction with Ubc9, SUMO1, and TOPORS **(Figure 17Aii)**. These results were unexpected and suggested a number of things. First, it was possible that self-assembly of DRP1 was important for the interactions since they manifested only when DRP1 was able to self-associate. Or, the interactions were dependent on the co-presence of specific regions of DRP1 that were not included in the domain construct. For example, if the Ubc9, E3 ligase binding site and SUMO1 site of conjugation are found on different domains of the protein, SUMOylation will not occur if these domains are not all present. Therefore, we attempted to find the site of SUMO1 conjugation by mutational analysis. A SUMOylation consensus sequence (ψKXD/E/Sp, where ψ is a hydrophobic residue, X is any amino acid and the last residue is positively charged. This can also include a phosphorylated serine or threonine (Frauke Melchoir, personal communications)) has been identified for some substrates (129). The DRP1 amino acid sequence does not contain any exact SUMO1 consensus site matches. However, there are some sites where the sequences are similar. Single point mutations of these sites were created and the DRP1 mutants were again tested for their interaction with Ubc9, SUMO1 and TOPORS in a yeast two-hybrid system **(Figure 17B)**. The K216G mutation is located in the switch I region and the lysine is highly conserved. The mutation reduced the DRP1 interaction with Ubc9 and SUMO1 by half and the TOPORS interaction by $1/4^{th}$. Since the interaction with SUMO1 was not completely abolished with this mutation, it suggests that, a most, this site may be one of multiple potential sites

of SUMOylation. This can be tested if the K216G mutation is combined with mutations of other potential sites. The K497V mutation is found near the end of the middle domain and the lysine is not conserved. The interaction with Ubc9 was completely abolished with this mutation **(Figure 17Bi)**. Interestingly, however, the interaction with SUMO1 was relatively unaffected. By fluorescence microscopy, transfection of a N-terminal CFP-tagged DRP1 (K497V) fusion construct into Cos 7 cells did not reveal any significant changes in mitochondria morphology **(Figure 17Biia)**, suggesting that the interaction with SUMO1 is sufficient to maintain DRP1 function. The K597A mutation, found in the unique Insert B domain, also contains a non-conserved lysine. This mutation abolished the interaction with TOPORS as well as the interaction with wild-type DRP1 **(Figure 17Bi)**. Transient transfection of an N-terminal CFP-tagged DRP1 (K597A) into Cos 7 cells caused a striking interconnected mitochondrial phenotype similar to the one produced by the dominant interfering DRP1 (K38E) **(Figure 17Biib)**. This phenotype may reflect the loss of interaction with TOPORS. The reasons for which are yet unknown. If TOPORS were the DRP1 E3 ligase, it might suggest that SUMOylation of DRP1 is required for its function at the mitochondria. However, it is also probable that the inability of DRP1 to assemble with this mutant may be responsible for the block in mitochondrial fission. This mutant may be binding to and sequestering DRP1 effectors, thereby interfering with the function of endogenous DRP1. The final mutated lysine, K679V, is located in the GED domain. This mutation is analogous to a mutation in yeast DRP1 (Dnm1p) that reportedly stimulates mitochondrial fission (47). This DRP1 mutant did not appear to have any significant effect on the interactions with Ubc9, SUMO1 or TOPORS **(Figure 17Bi)**. Analysis of this mutant by fluorescence microscopy also did

not indicate any striking changes in mitochondrial morphology (data not shown). Overall, the mutational analysis of DRP1 did not pinpoint any obvious sites of SUMOylation. This may be due to the possibility that DRP1 has multiple sites of SUMOylation. This would be consistent with the size of the DRP1 conjugate seen in the His6 pull down experiment (**Figure 19B**, open circle) and cellular fractionation **(Figure 20,** open circle). Consequently, mutation of a single site would not be expected to abolish the interaction with SUMO1. Creation of multiple mutations in combination would be required to determine which sites are SUMOylated. In addition, it is also possible that SUMO1 conjugation occurs on a lysine that is neither part of a consensus nor conserved. This has been previously observed with other substrates (for example (130)). Since DRP1 has a large number of lysines, this type of mutational analysis, especially if there are numerous sites of SUMOylation, would be experimentally laborous. Instead, we attempted to address the SUMOylation status of DRP1 biochemically.

4.3 DRP1 is reversibly modified by SUMO1.

The interactions seen between DRP1, Ubc9 and SUMO1 were confirmed biochemically by GST pull-down **(Figure 18)** and His-tagged pull-down **(Figure 19)**. Either of two possible outcomes of these experiments was expected. If DRP1 were not conjugated by SUMO1 but the interaction was simply transient, the pull down would result in isolation of the SUMO1 monomer at approximately 18kDa. On the other hand, if DRP1 were covalently modified by SUMO1, the pull-down would result in isolation of a product with a molecular weight (MW) greater than 100 kDa (80kDa for DRP1 + approximately 20kDa for MW of tag + n (18kDa) for number (n) of SUMO1 molecules).

As a source of SUMO1 and Ubc9 in the GST pull-down, we used rat liver and bovine heart cytosol. Due to species specificity of the antibodies, rat liver cytosol was used for the Ubc9 pull-down and bovine heart cytosol was used for the SUMO1 pull-down. Bacterially expressed recombinant DRP1 and DRP1(K38E) recruited a 40kDa Ubc9 immunoreactive band and a 40kDa SUMO1 immunoreactive band to the GST column from their respective cytosolic sources. These results were surprising since the molecular weight of both Ubc9 and SUMO1 is approximately 18kDa. The products pulled out are not likely Ubc9:SUMO1 complexes since the reducing agent DTT was added to the cytosol and would have broken thiol bonds that complex the two proteins together. A similar 40 kDa SUMO1 immunoreactive product is present in cytosolic and mitochondrial subcellular fractions **(Figure 20,** bottom arrow), probed with anti-SUMO1 antibodies and may represent a small 20 kDa SUMOylated protein. It is possible that DRP1 is recruiting this protein from cytosol. A high molecular weight band that would represent a SUMOylated DRP1 product was not found in this experiment. It is likely that the cytosol preparations used do not contain the necessary components to support the SUMOylation of DRP1, for example, a specific E3 ligase. Surprisingly, DRP1(K38E) appeared to recruit significantly more of these two products than wild-type DRP1. This is in contrast to the yeast two-hybrid data. The discrepancy in the results seen may be explained by potential differences in nucleotide state of DRP1(K38E). Since previous studies indicate that DRP1(K38E) is defective in GTP hydrolysis and remains predominantly GTP loaded (41), it is likely found in this form in the yeast nucleus during the two-hybrid screen. However, the GST pull-down was performed in the excess of GDP, thereby maintaining DRP1(K38E) GDP bound. Considering that Ubc9 and

SUMO1 appear to bind more strongly to this GDP loaded DRP1(K38E) in the GST pull-down, this may suggest that Ubc9 and SUMO1 preferentially interact with GDP bound DRP1.

Additional His6 pulldown experiments were performed to determine the SUMOylation of DRP1 by cotransfection of Cos 7 cells with combinations DRP1 and SUMO1 tagged with either His6 or YFP. Cells were solubilized in the presence or absence of N-ethyl maleimide (NEM). Solubilization of cells can result in the rapid deSUMOylation of substrates by Ubiquitin-like proteases ULPs. The addition of NEM to the experiment inhibits the action of ULPs and maintains substrates in their SUMOylated forms. Total cells lysates of cotransfected cells probed with monoclonal anti-DRP1 antibodies revealed the presence of NEM-sensitive high molecular weight DRP1 products (**Figure 19A**, lanes 1 and 3). The 80 kDa bands represent endogenous DRP1 and the 100kDa bands represent YFP:DRP1. When the cleared lysate of His6:DRP1 and YFP:SUMO1 transfected cells was passed over Nickel agarose beads, a high molecular weight 175kDa DRP1 immunoreactive product was recruited to the beads (**Figure 19B**, lane 8, top panel, o) along with unmodified His6:DRP1. Importantly, this 175kDa band was SUMO1 immunoreactive (**Figure 19B**, lane 8, bottom panel, o) strongly indicating that it represents a SUMO1 conjugated form of DRP1. A second high molecular weight DRP1 reactive product is visible in lane 10, top panel of **Figure 19B**. However, this product is not SUMO1 modified and its origins are unknown. Furthermore, in the reciprocal experiment of His6:SUMO1 and YFP:DRP1 transfected cells, this same 175kDa DRP1 immunoreactive band was recruited by SUMO1, but not LacZ, to the beads (**Figure 19B**, compare lane 12 vs lane 16). Curiously, the 100 kDa DRP:YFP

monomer is also pulled down in the experiment, suggesting either that SUMO1 is able to interact with monomeric YFP:DRP1 in the absence of conjugation, or that the SUMOylated, 175 kDa form of DRP1 remains in a complex (dimer) with the unmodified form, thereby pulling both forms of DRP1 out of the lysate.

Since DRP1 is found in both the cytosol and on the mitochondria, we sought to determine which population of DRP1 is SUMOylated. To do this, Cos7 cells were broken in the presence and absence of NEM and fractionated by centrifugation to isolate the nuclear, cytosolic and mitochondrial fractions. These fractions were then probed with DRP1, SUMO1 and TOM20 (mitochondrial outer membrane marker used as a control) antibodies **(Figure 20)**. The cytosolic fractions isolated contained two endogenous SDS-resistant forms of DRP1 in relatively equal proportions: an 80 kDa species consistent with the predicted molecular weight of the DRP1 monomer, and an additional 150 kDa high molecular weight species (**Figure 20**, open circle), which is ~25 kDa smaller than the DRP1:YFP conjugate observed in **Figure 19**, (open circles), consistent with the molecular weight of YFP. Both cytosolic DRP1 forms were isolated in the presence and absence of NEM indicating that SUMO1 modified DRP1 is stable in cytosol and not readily deconjugated. The mitochondrial fraction also contained both monomeric DRP1 and SUMOylated DRP1 in proportional amounts also indicating that only a fraction of mitochondrial DRP1 is SUMOylated (**Figure 20**, lane 6). This is consistent with our immunofluorescence data demonstrating only partial colocalization of endogenous DRP1 with YFP:SUMO1 on mitochondria **(Figure 23A)**. These sites of colocalization are often found at the tips of mitochondria **(Figure 23Ab)** or near the sites of apparent constriction **(Figure 23Ad)**. Interestingly, though, the mitochondrial fraction of SUMOylated DRP1

is NEM sensitive, implying that DRP1 deSUMOylation occurs only on the mitochondria. This is suggestive of the presence of a DRP1 specific ULP on mitochondria. To date, there has not been any mitochondrial ULP identified. However, potential candidate mitochondrial ULPs will be discussed later. Overall, these results indicate that there are two pools of DRP1, an unmodified DRP1 pool and a SUMO1 modified DRP1 pool both in cytosol and at the mitochondria, and that the SUMO1 modified DRP1 is only deSUMOylated at the mitochondria.

4.4 SUMO1 is found at the mitochondria and localizes to the site of mitochondrial fission.

To better understand the role of SUMO1 at the mitochondria, YFP:SUMO1 was transiently co-transfected into Cos7 cells along with the mitochondrial matrix marker OCT:CFP. As expected, the majority of YFP:SUMO1 localized to the nucleus. YFP:SUMO1 primarily stained the nuclear envelope **(Figure 21a)**, consistent with the distribution of SUMOylated proteins such as RanGAP1 and RanBP2 at the nuclear pore complex and was found as large puncta inside the nucleus consistent with distribution of PML bodies. However, upon increasing the exposure, a notable amount of punctate YFP:SUMO1 is also visualized in the cytosol **(Figure 21b)**, a fraction of which clearly localizes to the mitochondria **(Figure 21d)**. This SUMO1 is found along the length of mitochondrial tubules **(Figure22e**, arrow) as well as at the tips of fragmented mitochondria (**Figure 21 f and g**, arrows). Immunofluorescence experiments revealed that not all of the mitochondrial SUMO1 colocalizes with endogenous DRP1 **(Figure 23A,** open end arrows) suggesting that a number of other mitochondrial proteins interact

transiently with SUMO1 or are covalently modified by SUMO1. This is consistent with cellular fractionation experiments indicating that, in addition to the numerous expected nuclear SUMO1 conjugates, there are many unique NEM-sensitive SUMO1 conjugates present in the mitochondrial fraction (**Figure 20,** arrows). Next, live cell video fluorescence microscopy was used to assess the dynamics of SUMO1 association with the mitochondria. The studies revealed that SUMO1 is tightly associated with dynamic mitochondria **(Supplementary movie 3)** and is also found at the site of mitochondrial fission **(Figure 22, and Supplementary movie 4).** As indicated in the series of panels in **Figure 22**, SUMO1 initially localizes to the center of the mitochondrial tubule (**Figure 22**, arrow). As the mitochondrion begins to divide and finally separates completely, the SUMO1 spot remains associated with the site of fission **(Figure 22,** 0 -15.6 sec) and then eventually translocates to the tip of one of the fragmented mitochondria **(Figure 22,** 26 sec). The transfer of fission machinery to only one side of the fragmented mitochondria has been previously observed in *C.elegans* (2) and yeast (131) and suggests that at least a part of the fission machinery is SUMO1 associated.

4.5 SUMO1 over-expression stimulates mitochondrial fission and protects DRP1 against degradation

Since our experiments clearly indicate the presence of SUMO1 on the mitochondria, we wanted to better understand its functional role there. Therefore, we overexpressed YFP:SUMO1 and YFP:SUMO1ΔC5 in Cos7 cells and monitored changes in mitochondrial phenotype. In control cells overexpressing YFP alone, three predominant mitochondrial phenotypes were observed: tubular, rod-shaped and

fragmented. The phenotypes presented in the overall proportions of 53%, 28% and 18% respectively. However, overexpression of YFP:SUMO1 caused a substantial increase in the level of mitochondrial fragmentation and the ratio of mitochondrial phenotypes reversed to 20%, 26% and 54% respectively. This notable change in mitochondrial morphology is directly due to an increase in SUMO1 conjugation since overexpression of conjugation deficient YFP:SUMO1ΔC5 did not significantly change the ratio of mitochondrial phenotypes. The overexpression of SUMO1 resulting in stimulated mitochondrial fragmentation can be explained by a number of possibilities. First, the change in mitochondrial phenotype can be due to stimulation of apoptosis. One study has demonstrated that co-expression of SUMO1 (but not SUMO1 lacking the terminal glycine) with a mutant atrophin-1 containing expanded polyglutamine stretches accelerated nuclear aggregate formation and consequent apoptosis of PC12 cells (132). Furthermore, SUMO1 is known to conjugate and alter the activity of some proteins that are directly or indirectly involved in apoptosis including p53 (103;133;134), Daxx (135) Smad4 (136;137), and Topo1(138). On the contrary, overexpression of SUMO1 has also been shown to provide protection against both anti-Fas/APO-1 and TNF-induced cell death (78;139). An alternative explanation for the increase in mitochondrial fragmentation seen with SUMO1 overexpression is that there is an increase in SUMOylation of proteins directly participating in mitochondrial fission, such as DRP1. There are a number of possible functions for SUMOylation of DRP1. The interaction between DRP1 and SUMO1 could play a role in recruiting DRP1 to the mitochondria where it might interact with its specific E3 ligase, in a situation analogous to that of RanGAP1 and RanBP2. Or, SUMOylation of DRP1 may resemble the SUMOylation of

the yeast septins where it regulates the oligomerization of DRP1 around mitochondria, either mediating DRP1 oligomer assembly of disassembly. Finally, SUMOylation of DRP1 may regulate DRP1 degradation and maintain an active DRP1 pool available for recruitment to the mitochondria. Our results suggest that the latter function may indeed be the case. In the His6 pull-down, it is notable that the total DRP1 present in the total solubilized extracts (samples immediately suspended in SDS loading buffer) was equivalent in the +/- NEM conditions (**Figure19A**, lanes 1-6). However, following the additional 1.5 hour incubation with the Nickel agarose beads, endogenous DRP1 appeared to be degraded in an NEM sensitive manner (**Figure19B**, lanes 7 vs. 9, 11 vs. 13 and 15 vs. 17, lower arrow, top panel). Furthermore, DRP1 appeared to be protected from degradation in the absence of NEM by over-expression of YFP:SUMO1 but not YFP:SUMO1ΔC5 or YFP alone (**Figure 24C**, DRP1 blot). This protection may result in stabilization of a pool of DRP1 making it available for mitochondrial fission. This is consistent with the increase in mitochondrial fission observed with over-expression of SUMO1. In this case, SUMOylation of DRP1 is reminiscent of SUMOylation of IκBα where SUMO1 competes for the site of ubiquitination and prevents the proteosomal degradation of IκBα. It is tempting to speculate that DRP1 degradation is also mediated by the ubiquitin/proteosomal system. However, this hypothesis remains to be tested.

5. Conclusions and Future Directions

This study highlights the importance of mitochondrial dynamics as a phenomenon occurring under normal steady state cellular conditions, and examines, in particular, the regulation of mitochondrial fission. Dynamin-related protein 1 (DRP1) is a fundamental component of the core mitochondrial fission machinery that is recruited to the mitochondria from the cytosol, where it is thought to oligomerize and mediate outer membrane scission through GTP hydrolysis. The signals or factors that recruit DRP1 from cytosol have remained elusive. The results documented in this study indicate that apoptosis is one of the signals that stimulates DRP1 function. Since our studies were initiated, work done by others has confirmed that DRP1 is an essential player in the progression of apoptosis and this has lead to the formulation of a promising hypothesis for the function of mitochondrial fission in reorganization of cristal membranes enabling the release of cytochrome c from storage depots.

The actual mechanism of DRP1 mediated mitochondrial fission still remains poorly understood. The majority of the work presented herein was aimed at uncovering other factors, in addition to apoptotic signals, that control DRP1 function at the mitochondria. Yeast two-hybrid screening revealed that Ubc9 and SUMO1 proteins of the SUMOylation pathway interact with DRP1 in a nucleotide dependent manner. Biochemical studies confirmed that DRP1 is an authentic SUMO1 substrate (addition of approximately 3-4 SUMO1 molecules) consistent with the yeast two-hybrid data demonstrating a loss of the interaction between DRP1 and conjugation-defective form of SUMO1, SUMO1ΔC5. SUMOylated DRP1 and non-modified DRP1 are found in both the cytosol and on the mitochondria in relatively equivalent quantities. Furthermore,

strictly the mitochondrial SUMOylated DRP1 appears sensitive to NEM, suggesting the presence of SUMO1:DRP1 deSUMOylating enzymes specific to the mitochondria.

Live cell video fluorescence microscopy revealed that a fraction of the punctate cytosolic YFP:SUMO1 overlapped with mitochondrial staining and often localized to the site of mitochondrial fission as well as to the tips of newly divided mitochondria. In line with this, there is colocalization of endogenous DRP1 with YFP:SUMO1 primarily at the site of mitochondrial constriction and at mitochondrial tips. Interestingly, the presence of numerous non-DRP1 containing YFP:SUMO1 puncta on the mitochondria suggests the existence of mitochondrial SUMO1 substrates consistent with biochemical fractionation studies indicating a number of SUMOylated products unique to the mitochondria. These results suggest that SUMOylation may be a prominent means of regulation of a number of mitochondrial proteins.

Functionally, SUMO1 may directly participate in mitochondrial fission since mitochondrial fragmentation is substantially stimulated upon overexpression of SUMO1 but not SUMO1ΔC5. Its particular role may be in the stabilization of active DRP1 pools as suggested by the sensitivity of DRP1 protein levels to NEM and overexpression of SUMO1 (but not SUMO1ΔC5). Given these results, it appears that the purpose of SUMO1 conjugation to DRP1 appears to be in regulation of DRP1 degradation.

The findings in this study provide the basis for extensive future work that will focus on a number of novel aspects of DRP1 regulation. First, the SUMOylation of DRP1 will be further characterized by identification of the exact sites of SUMO1 conjugation. This will require complex mutational analysis of DRP1 but it will ultimately enable definitive assessment of the function of DRP1 SUMOylation. Second, work will be

performed to identify both the novel DRP1 specific SUMO E3 ligase as well as the DRP1 specific mitochondrial ULP. Currently, two candidate ULPs, Axam (140;141) and SenP5, are being investigated. These proteins both contain clear mitochondrial targeting signals, and so far, there has been some evidence indicating that Axam is at least partially localized to the mitochondria. Identification of these additional components of the SUMOylation pathway will enable proper delineation of how DRP1 function is regulated through SUMO modification.

Work will also focus on discerning the mode of SUMO1-regulated DRP1 protein stabilization. It will be imperative to determine if DRP1 protein degradation is mediated through the ubiquitin-proteosomal system or by specific protease. If DRP1 is ubiquitinated, SUMOylation and ubiquitination may act antagonistically to regulate DRP1 function in a manner resembling the regulation of NF-κB function. This would also require the identification of a DRP1 and mitochondrial specific ubiquitin E3 ligase. An intriguing candidate ubiquitin E3 ligase for DRP1 is Parkin, a key protein in the development of Parkinson's disease (the neurodegenerative disorder is characterized by apoptotic loss of dopaminergic neurons in the substantia nigrais (see (142) for review)). Studies in *Drosophila melanogaster* parkin null mutants reveal mitochondrial pathology and dysfunction that leads to muscle degeneration (143). Also, induction of Parkin expression in PC12 cells delays mitochondrial swelling, cytochrome c release and caspase-3 activation in ceramide-mediated cell death (144), suggesting that Parkin promotes the degradation of mitochondrial substrates that are involved in apoptosis. This is consistent with a potential role for Parkin in the selective ubiquitination and degeneration of DRP1. Therefore, the potential regulation of DRP1 protein levels by

ubiquitination by Parkin may regulate susceptibility to apoptosis and muscle degeneration seen in Parkinson's disease. Substantial in depth work will be required to confirm this hypothesis.

Furthermore, studies will be aimed at identifying some of the other SUMOylated mitochondrial substrates as well as the remaining 30 other DRP1 interacting proteins isolated from the yeast two-hybrid screen. These studies may lead to the identification and characterization of more novel proteins directly or indirectly involved in mitochondrial fission and may provide clues as to additional means of DRP1 regulation and control of mitochondrial fission.

Overall, work presented in this thesis is the first to implicate a function for SUMO1 at the mitochondria and suggest a role for SUMO1 in mitochondrial fission. It provides novel insight into the control of DRP1 and offers new directions for future studies of mitochondrial dynamics.

6. Supplementary Movies

Supplementary movie 1. Mitochondrial fission and fusion are at equilibrium in mammalian cells. Cos7 cells were transiently transfected with pOCT:YFP to label the mitochondrial matrix, and mitochondrial dynamics were monitored (see section 2.3.1 for methods of movie acquisition and compilation). Shown is both a fission event (bottom right) and fusion event (center) of two mitochondria.

Supplementary movie 2. Mitochondrial fission is a rapid process and occurs under steady state condirions in mammalian cells. Cos7 cells were transiently transfected with pOCT:YFP and mitochondrial fission was monitored (see section 2.3.1 for methods of movie acquisition and compilation). Shown is a fission event of a single mitochondrion.

Supplementary movie 3. Overexpression of DRP1(K38E) inhibits mitochondrial fission resulting in collapse of interconnected mitochondria into a perinuclear region. Cos7 cells were transiently cotransfefcted with pOCT:YFP and pECFP:DRP1(K38E) and mitochondrial fission was monitored (see section 2.3.1 for methods of movie acquisition and compilation). Shown are two cells (top and bottom) with interconnected mitochondria collapsed around the nucleus.

Supplementary movie 4. YFP:SUMO1 is tightly associated with the tips of fragmented mitochondria. Cos7 cells were transiently cotransfected with pOCT:CFP and pEYFP:SUMO1 and mitochondrial dynamics were monitored (see section 2.3.1 for methods of movie acquisition and compilation). Shown is a single cell with YFP:SUMO1 puncta (shown red) associated with fragmented mitochondia (shown green).

Supplementary movie 5. YFP:SUMO1 localizes to the site of mitochondrial fission. Cos7 cells were transiently cotransfected with pOCT:CFP and pEYFP:SUMO1 and mitochondrial fission was monitored (see section 2.3.1 for methods of movie acquisition and compilation). Shown is a single cell with a YFP:SUMO1 puncta (shown red) localized to the site of mitochondrial fission (shown green) at the start of the movie, which then eventually transfers to the tip of one of the mitochondrial fragments.

7. Reference List

1. Smirnova, E., Griparic, L., Shurland, D. L., and van der Bliek, A. M. (2001) *Mol.Biol.Cell* **12,** 2245-2256

2. Labrousse, A. M., Zappaterra, M. D., Rube, D. A., and van der Bliek, A. M. (1999) *Mol.Cell* **4,** 815-826

3. Bleazard, W., McCaffery, J. M., King, E. J., Bale, S., Mozdy, A., Tieu, Q., Nunnari, J., and Shaw, J. M. (1999) *Nat.Cell Biol.* **1,** 298-304

4. Shaw, J. M. and Nunnari, J. (2002) *Trends Cell Biol.* **12,** 178-184

5. Saraste, M. (1999) *Science* **283,** 1488-1493

6. Stocco, D. M. (2001) *Annu.Rev.Physiol* **63:193-213.,** 193-213

7. Wu, G. and Morris, S. M., Jr. (1998) *Biochem.J.* **336,** 1-17

8. Jordan, J., Cena, V., and Prehn, J. H. (2003) *J.Physiol Biochem.* **59,** 129-141

9. Nangaku, M., Sato-Yoshitake, R., Okada, Y., Noda, Y., Takemura, R., Yamazaki, H., and Hirokawa, N. (1994) *Cell* **79,** 1209-1220

10. Tanaka, Y., Kanai, Y., Okada, Y., Nonaka, S., Takeda, S., Harada, A., and Hirokawa, N. (1998) *Cell* **93,** 1147-1158

11. Schroer, T. A., Steuer, E. R., and Sheetz, M. P. (1989) *Cell* **56,** 937-946

12. Boldogh, I., Vojtov, N., Karmon, S., and Pon, L. A. (1998) *J.Cell Biol.* **141,** 1371-1381

13. Simon, V. R., Karmon, S. L., and Pon, L. A. (1997) *Cell Motil.Cytoskeleton* **37,** 199-210

14. Hermann, G. J., Thatcher, J. W., Mills, J. P., Hales, K. G., Fuller, M. T., Nunnari, J., and Shaw, J. M. (1998) *J.Cell Biol.* **%19;143,** 359-373

15. Hales, K. G. and Fuller, M. T. (1997) *Cell* **90,** 121-129

16. Santel, A. and Fuller, M. T. (2001) *J.Cell Sci.* **114,** 867-874

17. Chen, H., Detmer, S. A., Ewald, A. J., Griffin, E. E., Fraser, S. E., and Chan, D. C. (2003) *J.Cell Biol.* **%20;160,** 189-200

18. Rojo, M., Legros, F., Chateau, D., and Lombes, A. (2002) *J.Cell Sci.* **115,** 1663-1674

19. Gammie, A. E., Kurihara, L. J., Vallee, R. B., and Rose, M. D. (1995) *J.Cell Biol.* **130,** 553-566

20. Otsuga, D., Keegan, B. R., Brisch, E., Thatcher, J. W., Hermann, G. J., Bleazard, W., and Shaw, J. M. (1998) *J.Cell Biol.* **%19;143,** 333-349

21. Pitts, K. R., Yoon, Y., Krueger, E. W., and McNiven, M. A. (1999) *Mol.Biol.Cell* **10,** 4403-4417

22. Kamimoto, T., Nagai, Y., Onogi, H., Muro, Y., Wakabayashi, T., and Hagiwara, M. (1998) *J.Biol.Chem.* **273,** 1044-1051

23. Shin, H. W., Shinotsuka, C., Torii, S., Murakami, K., and Nakayama, K. (1997) *J.Biochem.(Tokyo)* **122,** 525-530

24. Sesaki, H. and Jensen, R. E. (1999) *J.Cell Biol.* **147,** 699-706

25. Danino, D. and Hinshaw, J. E. (2001) *Curr.Opin.Cell Biol.* **13,** 454-460

26. van der Bliek, A. M. (1999) *Trends Cell Biol.* **9,** 96-102

27. Grigliatti, T. A., Hall, L., Rosenbluth, R., and Suzuki, D. T. (1973) *Mol.Gen.Genet.* **120,** 107-114

28. Hinshaw, J. E. (2000) *Annu.Rev.Cell Dev.Biol.* **16:483-519.,** 483-519

29. Powell, K. A., Valova, V. A., Malladi, C. S., Jensen, O. N., Larsen, M. R., and Robinson, P. J. (2000) *J.Biol.Chem.* **275,** 11610-11617

30. Muhlberg, A. B. and Schmid, S. L. (2000) *Methods* **20,** 475-483

31. Okamoto, P. M., Tripet, B., Litowski, J., Hodges, R. S., and Vallee, R. B. (1999) *J.Biol.Chem.* **274,** 10277-10286

32. Slepnev, V. I., Ochoa, G. C., Butler, M. H., Grabs, D., and Camilli, P. D. (1998) *Science* **281,** 821-824

33. Lai, M. M., Hong, J. J., Ruggiero, A. M., Burnett, P. E., Slepnev, V. I., De Camilli, P., and Snyder, S. H. (1999) *J.Biol.Chem.* **274,** 25963-25966

34. Liu, J. P., Sim, A. T., and Robinson, P. J. (1994) *Science* **265,** 970-973

35. Krishnan, K. S., Rikhy, R., Rao, S., Shivalkar, M., Mosko, M., Narayanan, R., Etter, P., Estes, P. S., and Ramaswami, M. (2001) *Neuron* **30,** 197-210

36. Takei, K., McPherson, P. S., Schmid, S. L., and De Camilli, P. (1995) *Nature* **374,** 186-190

37. Stowell, M. H., Marks, B., Wigge, P., and McMahon, H. T. (1999) *Nat.Cell Biol.* **1,** 27-32

38. Marks, B., Stowell, M. H., Vallis, Y., Mills, I. G., Gibson, A., Hopkins, C. R., and McMahon, H. T. (2001) *Nature* **410,** 231-235

39. Tomizawa, K., Sunada, S., Lu, Y. F., Oda, Y., Kinuta, M., Ohshima, T., Saito, T., Wei, F. Y., Matsushita, M., Li, S. T., Tsutsui, K., Hisanaga, S., Mikoshiba, K., Takei, K., and Matsui, H. (2003) *J.Cell Biol.* **163,** 813-824

40. Shin, H. W., Takatsu, H., Mukai, H., Munekata, E., Murakami, K., and Nakayama, K. (1999) *J.Biol.Chem.* **274,** 2780-2785

41. Yoon, Y., Pitts, K. R., and McNiven, M. A. (2001) *Mol.Biol.Cell* **12,** 2894-2905

42. Smirnova, E., Shurland, D. L., Ryazantsev, S. N., and van der Bliek, A. M. (1998) *J.Cell Biol.* **%19;143,** 351-358

43. Niemann, H. H., Knetsch, M. L., Scherer, A., Manstein, D. J., and Kull, F. J. (2001) *EMBO J.* **20,** 5813-5821

44. Vallis, Y., Wigge, P., Marks, B., Evans, P. R., and McMahon, H. T. (1999) *Curr.Biol.* **9,** 257-260

45. Klein, D. E., Lee, A., Frank, D. W., Marks, M. S., and Lemmon, M. A. (1998) *J.Biol.Chem.* **273,** 27725-27733

46. Warnock, D. E., Hinshaw, J. E., and Schmid, S. L. (1996) *J.Biol.Chem.* **271,** 22310-22314

47. Fukushima, N. H., Brisch, E., Keegan, B. R., Bleazard, W., and Shaw, J. M. (2001) *Mol.Biol.Cell* **12,** 2756-2766

48. Warnock, D. E., Baba, T., and Schmid, S. L. (1997) *Mol.Biol.Cell* **8,** 2553-2562

49. Zhang, P. and Hinshaw, J. E. (2001) *Nat.Cell Biol.* **3,** 922-926

50. Warnock, D. E., Terlecky, L. J., and Schmid, S. L. (1995) *EMBO J.* **14,** 1322-1328

51. Song, B. D. and Schmid, S. L. (2003) *Biochemistry* **42,** 1369-1376

52. Thompson, H. M. and McNiven, M. A. (2001) *Curr.Biol.* **11,** R850

53. Sever, S., Muhlberg, A. B., and Schmid, S. L. (1999) *Nature* **398,** 481-486

54. Sever, S., Damke, H., and Schmid, S. L. (2000) *J.Cell Biol.* **150,** 1137-1148

55. Lichte, B., Veh, R. W., Meyer, H. E., and Kilimann, M. W. (1992) *EMBO J.* **11,** 2521-2530

56. David, C., McPherson, P. S., Mundigl, O., and De Camilli, P. (1996) *Proc.Natl.Acad.Sci.U.S.A* **93,** 331-335

57. Grabs, D., Slepnev, V. I., Songyang, Z., David, C., Lynch, M., Cantley, L. C., and De Camilli, P. (1997) *J.Biol.Chem.* **272,** 13419-13425

58. Wigge, P., Vallis, Y., and McMahon, H. T. (1997) *Curr.Biol.* **7,** 554-560

59. Shupliakov, O., Low, P., Grabs, D., Gad, H., Chen, H., David, C., Takei, K., De Camilli, P., and Brodin, L. (1997) *Science* **276,** 259-263

60. Marks, B. and McMahon, H. T. (1998) *Curr.Biol.* **8,** 740-749

61. Salim, K., Bottomley, M. J., Querfurth, E., Zvelebil, M. J., Gout, I., Scaife, R., Margolis, R. L., Gigg, R., Smith, C. I., Driscoll, P. C., Waterfield, M. D., and Panayotou, G. (1996) *EMBO J.* **15,** 6241-6250

62. Achiriloaie, M., Barylko, B., and Albanesi, J. P. (1999) *Mol.Cell Biol.* **19,** 1410-1415

63. McPherson, P. S., Garcia, E. P., Slepnev, V. I., David, C., Zhang, X., Grabs, D., Sossin, W. S., Bauerfeind, R., Nemoto, Y., and De Camilli, P. (1996) *Nature* **379,** 353-357

64. Cremona, O., Di Paolo, G., Wenk, M. R., Luthi, A., Kim, W. T., Takei, K., Daniell, L., Nemoto, Y., Shears, S. B., Flavell, R. A., McCormick, D. A., and De Camilli, P. (1999) *Cell* **99,** 179-188

65. Cestra, G., Castagnoli, L., Dente, L., Minenkova, O., Petrelli, A., Migone, N., Hoffmuller, U., Schneider-Mergener, J., and Cesareni, G. (1999) *J.Biol.Chem.* **274,** 32001-32007

66. de Heuvel, E., Bell, A. W., Ramjaun, A. R., Wong, K., Sossin, W. S., and McPherson, P. S. (1997) *J.Biol.Chem.* **272,** 8710-8716

67. Schuske, K. R., Richmond, J. E., Matthies, D. S., Davis, W. S., Runz, S., Rube, D. A., van der Bliek, A. M., and Jorgensen, E. M. (2003) *Neuron* **40,** 749-762

68. Verstreken, P., Koh, T. W., Schulze, K. L., Zhai, R. G., Hiesinger, P. R., Zhou, Y., Mehta, S. Q., Cao, Y., Roos, J., and Bellen, H. J. (2003) *Neuron* **40,** 733-748

69. Lee, S. Y., Wenk, M. R., Kim, Y., Nairn, A. C., and De Camilli, P. (2004) *Proc.Natl.Acad.Sci.U.S.A* **101,** 546-551

70. Schmidt, A., Wolde, M., Thiele, C., Fest, W., Kratzin, H., Podtelejnikov, A. V., Witke, W., Huttner, W. B., and Soling, H. D. (1999) *Nature* **401,** 133-141

71. Nemoto, Y. and De Camilli, P. (1999) *EMBO J.* **18,** 2991-3006

72. Mozdy, A. D., McCaffery, J. M., and Shaw, J. M. (2000) *J.Cell Biol.* **151,** 367-380

73. Tieu, Q. and Nunnari, J. (2000) *J.Cell Biol.* **151,** 353-366

74. Jakobs, S., Martini, N., Schauss, A. C., Egner, A., Westermann, B., and Hell, S. W. (2003) *J.Cell Sci.* **116,** 2005-2014

75. James, D. I., Parone, P. A., Mattenberger, Y., and Martinou, J. C. (2003) *J.Biol.Chem.* **%19;278,** 36373-36379

76. Yoon, Y., Krueger, E. W., Oswald, B. J., and McNiven, M. A. (2003) *Mol.Cell Biol.* **23,** 5409-5420

77. Tieu, Q., Okreglak, V., Naylor, K., and Nunnari, J. (2002) *J.Cell Biol.* **158,** 445-452

78. Okura, T., Gong, L., Kamitani, T., Wada, T., Okura, I., Wei, C. F., Chang, H. M., and Yeh, E. T. (1996) *J.Immunol.* **157,** 4277-4281

79. Muller, S., Hoege, C., Pyrowolakis, G., and Jentsch, S. (2001) *Nat.Rev.Mol.Cell Biol.* **2,** 202-210

80. Boddy, M. N., Howe, K., Etkin, L. D., Solomon, E., and Freemont, P. S. (1996) *Oncogene* **13,** 971-982

81. Matunis, M. J., Coutavas, E., and Blobel, G. (1996) *J.Cell Biol.* **135,** 1457-1470

82. Kamitani, T., Kito, K., Nguyen, H. P., Fukuda-Kamitani, T., and Yeh, E. T. (1998) *J.Biol.Chem.* **273,** 11349-11353

83. Gong, L., Li, B., Millas, S., and Yeh, E. T. (1999) *FEBS Lett.* **448,** 185-189

84. Johnson, E. S., Schwienhorst, I., Dohmen, R. J., and Blobel, G. (1997) *EMBO J.* **16,** 5509-5519

85. Schwarz, S. E., Matuschewski, K., Liakopoulos, D., Scheffner, M., and Jentsch, S. (1998) *Proc.Natl.Acad.Sci.U.S.A* **%20;95,** 560-564

86. Desterro, J. M., Thomson, J., and Hay, R. T. (1997) *FEBS Lett.* **417,** 297-300

87. Gong, L., Kamitani, T., Fujise, K., Caskey, L. S., and Yeh, E. T. (1997) *J.Biol.Chem.* **272,** 28198-28201

88. Melchior, F., Schergaut, M., and Pichler, A. (2003) *Trends Biochem.Sci.* **28,** 612-618

89. Kamitani, T., Kito, K., Nguyen, H. P., Wada, H., Fukuda-Kamitani, T., and Yeh, E. T. (1998) *J.Biol.Chem.* **273,** 26675-26682

90. Tatham, M. H., Jaffray, E., Vaughan, O. A., Desterro, J. M., Botting, C. H., Naismith, J. H., and Hay, R. T. (2001) *J.Biol.Chem.* **276,** 35368-35374

91. Desterro, J. M., Rodriguez, M. S., and Hay, R. T. (1998) *Mol.Cell* **2,** 233-239

92. Hay, R. T., Vuillard, L., Desterro, J. M., and Rodriguez, M. S. (1999) *Philos.Trans.R.Soc.Lond B Biol.Sci.* **354,** 1601-1609

93. Wilson, V. G. and Rangasamy, D. (2001) *Exp.Cell Res.* **271,** 57-65

94. Johnson, E. S. and Blobel, G. (1999) *J.Cell Biol.* **147,** 981-994

95. Mahajan, R., Delphin, C., Guan, T., Gerace, L., and Melchior, F. (1997) *Cell* **88,** 97-107

96. Cole, C. N. and Hammell, C. M. (1998) *Curr.Biol.* **8,** R368-R372

97. Pichler, A., Gast, A., Seeler, J. S., Dejean, A., and Melchior, F. (2002) *Cell* **108,** 109-120

98. Maul, G. G., Negorev, D., Bell, P., and Ishov, A. M. (2000) *J.Struct.Biol.* **129,** 278-287

99. Zhong, S., Muller, S., Ronchetti, S., Freemont, P. S., Dejean, A., and Pandolfi, P. P. (2000) *Blood* **95,** 2748-2752

100. Sternsdorf, T., Jensen, K., Reich, B., and Will, H. (1999) *J.Biol.Chem.* **274,** 12555-12566

101. Li, H., Leo, C., Zhu, J., Wu, X., O'Neil, J., Park, E. J., and Chen, J. D. (2000) *Mol.Cell Biol.* **20,** 1784-1796

102. Kwek, S. S., Derry, J., Tyner, A. L., Shen, Z., and Gudkov, A. V. (2001) *Oncogene* **20,** 2587-2599

103. Gostissa, M., Hengstermann, A., Fogal, V., Sandy, P., Schwarz, S. E., Scheffner, M., and Del Sal, G. (1999) *EMBO J.* **18,** 6462-6471

104. Jang, M. S., Ryu, S. W., and Kim, E. (2002) *Biochem.Biophys.Res.Commun.* **295,** 495-500

105. Finger, F. P. (2002) *Dev.Cell* **3,** 761-763

106. Schwienhorst, I., Johnson, E. S., and Dohmen, R. J. (2000) *Mol.Gen.Genet.* **263,** 771-786

107. Li, S. J. and Hochstrasser, M. (2000) *Mol.Cell Biol.* **20,** 2367-2377

108. Li, S. J. and Hochstrasser, M. (1999) *Nature* **398,** 246-251

109. Hang, J. and Dasso, M. (2002) *J.Biol.Chem.* **277,** 19961-19966

110. Nishida, T., Tanaka, H., and Yasuda, H. (2000) *Eur.J.Biochem.* **267,** 6423-6427

111. Bailey, D. and O'Hare, P. (2004) *J.Biol.Chem.* **279,** 692-703

112. Kruman, I., Guo, Q., and Mattson, M. P. (1998) *J.Neurosci.Res.* **51,** 293-308

113. Fields, S. and Song, O. (1989) *Nature* **%20;340,** 245-246

114. Toby, G. G. and Golemis, E. A. (2001) *Methods* **24,** 201-217

115. Engelhardt, O. G., Ullrich, E., Kochs, G., and Haller, O. (2001) *Exp.Cell Res.* **271,** 286-295

116. Rodriguez, M. S., Dargemont, C., and Hay, R. T. (2001) *J.Biol.Chem.* **%20;276,** 12654-12659

117. Zhang, G., Yan, G., Gurtu, V., Spencer, C., and Kain, S. R. (1998) *Apoptosis.* **3,** 27-33

118. Damke, H., Binns, D. D., Ueda, H., Schmid, S. L., and Baba, T. (2001) *Mol.Biol.Cell* **12,** 2578-2589

119. Karbowski, M., Lee, Y. J., Gaume, B., Jeong, S. Y., Frank, S., Nechushtan, A., Santel, A., Fuller, M., Smith, C. L., and Youle, R. J. (2002) *J.Cell Biol.* **159,** 931-938

120. Degterev, A., Boyce, M., and Yuan, J. (2003) *Oncogene* **22,** 8543-8567

121. Frank, S., Gaume, B., Bergmann-Leitner, E. S., Leitner, W. W., Robert, E. G., Catez, F., Smith, C. L., and Youle, R. J. (2001) *Dev.Cell* **1,** 515-525

122. Scorrano, L., Ashiya, M., Buttle, K., Weiler, S., Oakes, S. A., Mannella, C. A., and Korsmeyer, S. J. (2002) *Dev.Cell* **2,** 55-67

123. Shen, Z., Pardington-Purtymun, P. E., Comeaux, J. C., Moyzis, R. K., and Chen, D. J. (1996) *Genomics* **36,** 271-279

124. Shen, Z., Pardington-Purtymun, P. E., Comeaux, J. C., Moyzis, R. K., and Chen, D. J. (1996) *Genomics* **37,** 183-186

125. Reed, S. I. (2003) *Nat.Rev.Mol.Cell Biol.* **4,** 855-864

126. Jones, A. T., Mills, I. G., Scheidig, A. J., Alexandrov, K., and Clague, M. J. (1998) *Mol.Biol.Cell* **9,** 323-332

127. Cosulich, S. C., Horiuchi, H., Zerial, M., Clarke, P. R., and Woodman, P. G. (1997) *EMBO J.* **16,** 6182-6191

128. Stenmark, H., Vitale, G., Ullrich, O., and Zerial, M. (1995) *Cell* **83,** 423-432

129. Sampson, D. A., Wang, M., and Matunis, M. J. (2001) *J.Biol.Chem.* **276,** 21664-21669

130. Hoege, C., Pfander, B., Moldovan, G. L., Pyrowolakis, G., and Jentsch, S. (2002) *Nature* **419,** 135-141

131. Legesse-Miller, A., Massol, R. H., and Kirchhausen, T. (2003) *Mol.Biol.Cell* **14,** 1953-1963

132. Terashima, T., Kawai, H., Fujitani, M., Maeda, K., and Yasuda, H. (2002) *Neuroreport* **13,** 2359-2364

133. Muller, S., Berger, M., Lehembre, F., Seeler, J. S., Haupt, Y., and Dejean, A. (2000) *J.Biol.Chem.* **275,** 13321-13329

134. Rodriguez, M. S., Desterro, J. M., Lain, S., Midgley, C. A., Lane, D. P., and Hay, R. T. (1999) *EMBO J.* **18,** 6455-6461

135. Ryu, S. W., Chae, S. K., and Kim, E. (2000) *Biochem.Biophys.Res.Commun.* **279,** 6-10

136. Lee, P. S., Chang, C., Liu, D., and Derynck, R. (2003) *J.Biol.Chem.* **278,** 27853-27863

137. Lin, X., Liang, M., Liang, Y. Y., Brunicardi, F. C., Melchior, F., and Feng, X. H. (2003) *J.Biol.Chem.* **278,** 18714-18719

138. Horie, K., Tomida, A., Sugimoto, Y., Yasugi, T., Yoshikawa, H., Taketani, Y., and Tsuruo, T. (2002) *Oncogene* **21,** 7913-7922

139. Franz, J. K., Pap, T., Hummel, K. M., Nawrath, M., Aicher, W. K., Shigeyama, Y., Muller-Ladner, U., Gay, R. E., and Gay, S. (2000) *Arthritis Rheum.* **43,** 599-607

140. Kadoya, T., Yamamoto, H., Suzuki, T., Yukita, A., Fukui, A., Michiue, T., Asahara, T., Tanaka, K., Asashima, M., and Kikuchi, A. (2002) *Mol.Cell Biol.* **22,** 3803-3819

141. Nishida, T., Kaneko, F., Kitagawa, M., and Yasuda, H. (2001) *J.Biol.Chem.* **%19;276,** 39060-39066

142. Michotte, A. (2003) *Acta Neurol.Belg.* **103,** 155-158

143. Greene, J. C., Whitworth, A. J., Kuo, I., Andrews, L. A., Feany, M. B., and Pallanck, L. J. (2003) *Proc.Natl.Acad.Sci.U.S.A* **100,** 4078-4083

144. Darios, F., Corti, O., Lucking, C. B., Hampe, C., Muriel, M. P., Abbas, N., Gu, W. J., Hirsch, E. C., Rooney, T., Ruberg, M., and Brice, A. (2003) *Hum.Mol.Genet.* **12,** 517-526